2016

Optimum Hydraulic Fracture Conductivity for Shale/Tight Reservoirs

Ye, Xiaoduan Jr

UNIVERSITY OF CALGARY

Optimum Hydraulic Fracture Conductivity for Shale/Tight Reservoirs

by

Xiaoduan Ye

A THESIS

SUBMITTED TO THE FACULTY OF GRADUATE STUDIES

IN PARTIAL FULFILMENT OF THE REQUIREMENTS FOR THE

DEGREE OF MASTER OF SCIENCE

GRADUATE PROGRAM IN CHEMICAL AND PETROLEUM ENGINEERING

CALGARY, ALBERTA

JUNE, 2016

Abstract

Slick-water fracturing has become the common hydraulic fracturing technique for shale plays. There is a thought that fracture conductivity is not important in shale plays, and one design applies to different property of shale plays. Many publications pointed out the improved fracture conductivity increases well production of tight reservoirs.

The objective of this study is to present a workflow for determining the optimum fracture conductivity requirements for shale/tight gas plays with different characteristics. Two hydraulic fracture models are explicitly established in a reservoir simulator, including planar fractures and a complex fracture network. The results of optimum fracture conductivity are compared and analyzed.

The simulation results show that fracture conductivity is very important in productivity of shale/tight gas plays. The optimum fracture conductivity is a function of reservoir and treatment parameters such as matrix permeability, reservoir geomechanics, natural fracture properties, hydraulic fracture length and spacing, production time, and fracture geometry.

Acknowledgements

First I would like to express my sincere gratitude to my supervisor Dr. Zhangxing (John) Chen not only for his time and guidance during my research work, also for giving me this opportunity to pursue my master degree at the University of Calgary and for his support and encouragement throughout my MSc studies in the Department of Chemical and Petroleum Engineering.

I also thank my committee members Dr. Roberto Aguilera and Dr. Ayodeji Jeje for their valuable comments.

I would like to thank Guoxuan Ren, Wanqiang Xiong, and Menglu Lin for their advices and helps on my research works.

Last but not least, I would like to thank my family for supporting me to pursue my dreams and always standing by during my good and bad times.

Table of Contents

List of Tables

List of Figures and Illustrations

List of Symbols, Abbreviations and Nomenclature

Symbol	Definition
k_f	permeability of propped fracture (L^2)
w	propped fracture width (L)
A	the cross-sectional area to flow (L^2)
L	flow length (L)
Q	flow rate (L^3/T)
k	matrix permeability (L^2)
Δp	pressure drop (M/LT^2)
μ	fluid viscosity (M/LT)
x_f	propped fracture half-length (L)
F_{CD}	dimensionless fracture conductivity
k_{rg}	gas relative permeability (fraction)
k_{rwg}	water relative permeability to gas (fraction)
∇p	pressure gradient vector (M/L^2T^2)
v	velocity (L/T)
β	non-Darcy flow coefficient (1/L)
ρ	phase density (M/L^3)
ω_i	moles of adsorbed gas per unit mass of rock (MN/M)
V_L	langmuir volume (MN/M)
p	pressure (M/LT^2)

p_L	langmuir pressure (M/LT^2)
E	young's modulus (M/LT^2)
I	coordinate direction
J	coordinate direction
K	coordinate direction
Δh	hydraulic head gradient (L)
W	the width of fracture face (L)
e	fracture aperture (L)

Abbreviation	**Definition**
SRV	stimulated reservoir volume
CMG	Computer Modelling Group LTD.
GIP	gas in place
Tcf	trillion cubic feet
OPAAT	one parameter at a time
RSM	response surface methodology
DECE	designed evolution and controlled exploration
WCSB	Western Canadian Sedimentary Basin
NFS	natural fracture spacing
NFC	natural fracture conductivity
HFS	hydraulic fracture spacing
RCS	resin-coated sand
RCC	resin-coated ceramic
ISO	International Organization for Standardization

Chapter 1: Introduction

Unconventional resources such as shale gas plays and tight oil reservoirs are playing an important role and have a tremendous potential for future reserves and production growth when conventional resources become depleted. The hydraulic fracturing technology has been employed widely to optimize the productivity of shale gas and tight gas/oil reservoirs due to their low and ultra-low permeability. A hydraulic fracturing treatment is a process of pumping a large volume of special fluids into a reservoir at a high injection rate to create fractures. Then the proppant particles are pumped down into the fractures with a fracturing fluid to hold them apart in case the fractures are closed by the closure pressure, after the pumps are stopped. The propped fractures form highly permeable flow paths through which oil and gas can easily flow into a wellbore. Thus, a key determinant of the scale of the expected productivity increase is the final conductivity of the propped fractures (Awoleke et al., 2012).

1.1 Fracture Conductivity

Fracture conductivity is defined as $k_f w$, where k_f is the permeability of proppants in the fractures and w is the propped fracture width. Hydraulic fracturing exposes a large flow area of low permeability formations, which actually changes the flow condition $\frac{A}{L}$ in terms of Darcy's flow$Q = \frac{kA\Delta p}{\mu L}$. The changed flow area is represented by a certain length of fractures with high conductivity. Thus the post-fracture productivity is governed by a combination of the fracture conductivity $k_f w$ and fracture half-length x_f. These variables are controlled by fracturing, and, therefore, they are the goals of a fracturing treatment design (Economides et al., 2000). The ability of low-permeability reservoirs to supply oil and gas flow to propped hydraulic fractures is limited. Even a fracture with narrow width and relatively low permeability can have high conductivity

compared to a low permeability matrix. Therefore, it is not necessary to have high conductivity fractures (wide and short fractures) to carry poor flow. A long and narrow fracture (low fracture conductivity) is needed to penetrate deeply into a reservoir to get more oil and gas recovery. On the contrary, a high conductivity fracture can meet the requirement to carry abundant flow from higher permeability reservoirs. Thus, traditionally a fracturing treatment design tended to create a long fracture for low permeability reservoirs, and high fracture conductivity for high permeability reservoirs. Reservoirs can produce more oil and gas if a fracture is long, but the resistance to flow in a narrow fracture may be significant. In order to balance these two production characteristics, Prats (1961) first introduced the dimensionless fracture conductivity, and Agarwal et al. (1979) defined the dimensionless fracture conductivity (F_{CD}) below, where k is the reservoir permeability.

$$F_{CD} = \frac{k_f w}{k x_f} \tag{1-1}$$

The dimensionless fracture conductivity is the ratio of the ability of fractures to carry flow into a well divided by the ability of a formation to feed the fractures (Economides et al., 2000). When F_{CD} is equal to 1, the fractures are able to carry the flow from the reservoir as fast as the reservoir can supply it. This case is applicable to a steady-flow condition. For transient flow which means the reservoir may produce more fluid than its natural level, F_{CD} greater than 1 is desirable. Cinco-Ley and Samaniego (1981) presented a relationship of an effective well radius (defined in Figure 1-1), fracture half-length and dimensionless fracture conductivity for pseudo-radial flow in Figure 1-2. It is known that the larger effective well radius the more production. The Figure 1-2 indicates that the effective well radius approaches half of the fracture half-length and there are diminishing returns for an additional increase in conductivity as F_{CD} increases beyond 10, which means that the fracture conductivity of 10 is usually optimum beyond which the production would not increase dramatically (Economides et al., 2000). Prats (1961) found out by analyzing the pressure

distribution around a fracture that when the effective well radius is half of the fracture half-length, corresponding to the dimensionless fracture conductivity F_{CD} greater than 30 in Figure 1-2, the fracture conductivity $k_f w$ is infinite. For conventional fracturing, a dimensionless fracture conductivity (F_{CD}) of 10 to 30 has generally been considered optimum because it can be observed from Figure 1-3 that when F_{CD} is greater 10, the effects of various F_{CD} are eventually the same. Thus, F_{CD} of 10-30 has been chosen as a standard design factor based on the technical and economical consideration. What value of optimum F_{CD} in the range of 10-30 should be chosen is dependent on the hydraulic fracture length. Once the optimum F_{CD} is determined, it is used to determine what propped fracture conductivity is needed, and then the amount of proppants and concentration of proppants based on the propped fracture conductivity can be scheduled as well.

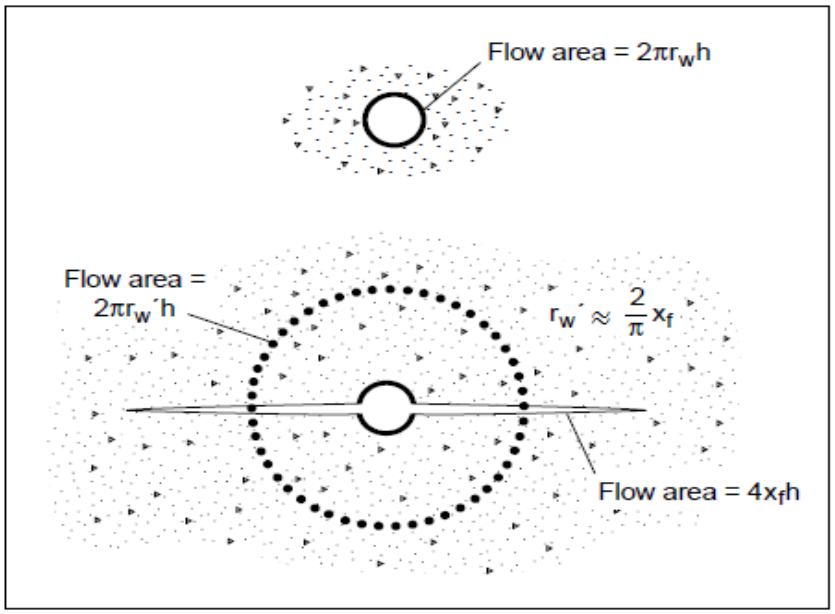

Figure 1-1: Effective well radius (Economides et al., 2000)

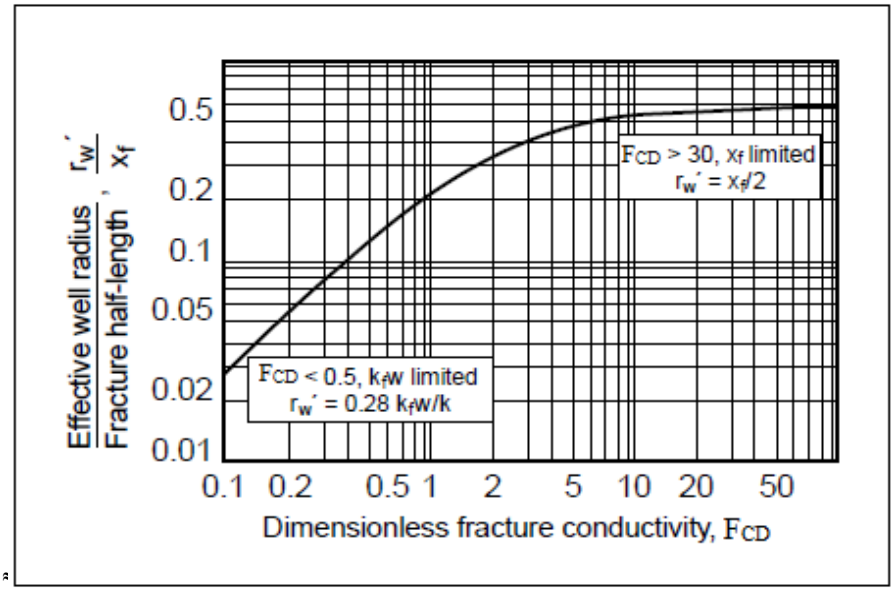

Figure 1-2: Effective well radius as a function of dimensionless fracture conductivity and fracture half-length (Economides et al., 2000)

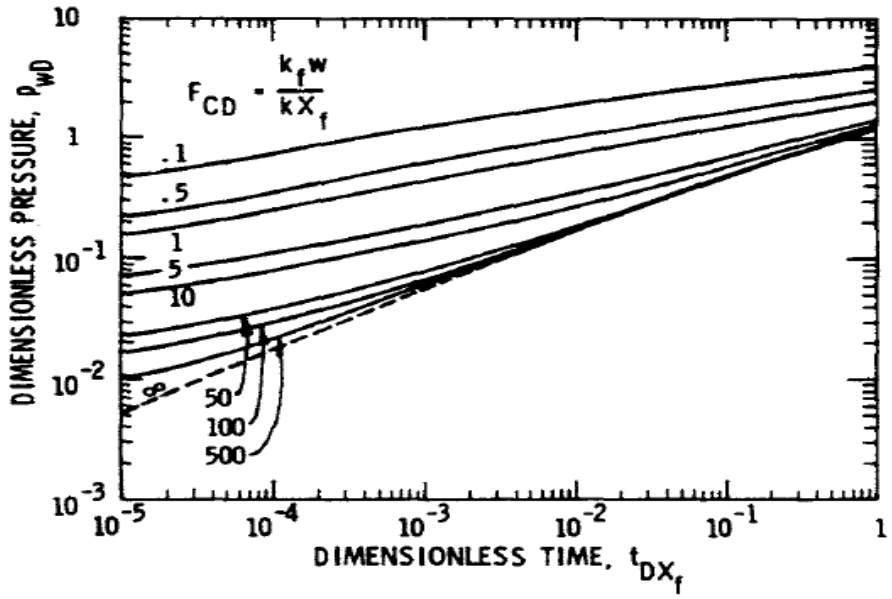

Figure 1-3: Dimensionless pressure drop vs. dimensionless time with different F_{CD} (Agarwal et al., 1979)

Factors that affect the propped fracture width and the proppant permeability in fractures can impact the final fracture conductivity since the fracture conductivity is the product of the fracture permeability and the fracture width. Researchers have found out that the fracture width is controlled by fracture geometry (i.e., fracture height and fracture length), Young's modulus and Poison's ratio of the rock, as well as the net pressure which is the difference between the pressure inside fractures and the minimum in-situ stress. Young's modulus is defined as the ratio of the stress to the strain, and it is a measure of the stiffness of the rock. If Young's modulus is large, the rock is stiff, which results in more narrow fractures in hydraulic fracturing. Poisson's ration is the ratio of transverse strain to axial strain. Both the two parameters can be measured by lab tests such as uniaxial and tri-axial tests or sonic logging. Moreover, the fracturing fluid viscosity and the pump rate affect the net pressure, and, therefore, impact the fracture width eventually. Additionally, the very important parameters that determine the final propped fracture width are the maximum in-situ proppant concentration at shut-in and proppant embedment due to high in-situ stress or soft formation.

Factors that decide the proppant permeability in fractures include the in-situ stress, residual damage from fluid additives, and proppant properties. The inadequate proppant strength under high closure pressure can deteriorate propped fracture permeability. Also, the proppant grain size and grain-size distribution can impact the proppant pack permeability. Last, proppant roundness, density and proppant impurities affect the proppant pack permeability as well. All in all, the formation parameters, hydraulic fracturing treatment parameters, and the selection of fracturing fluid and proppant affect the fracture conductivity.

On the other hand, the propped fracture conductivity is decreasing during production. Non-Darcy's flow for high-rate wells causes an additional pressure drop along the fracture and fines

migration, which can reduce the propped fracture conductivity (Economides et al., 2000). The pore pressure in fractures is reduced during production, which shifts overburden stress from the pore fluid to the rock matrix. This results in compaction and cause fracture permeability reduction (Fan et al., 2010). In addition, proppant crushing (in harder rock), proppant embedment (in softer rock), proppant diagenesis, and fines migration can contribute to the reduction of propped fracture conductivity during production.

1.2 Statement of Problems

One of the most significant beliefs before is "Fracture Conductivity is King" (McDaniel, 2011). In order to pursue the high fracture conductivity, a gelled fracturing fluid has been used to deliver more proppant and produce high proppant concentration. The fractures generated by using the gelled fracturing fluid are generally regarded as bi-wing planar fractures due to a high viscosity of the gelled fluid which cannot penetrate natural fractures to produce fracture complexity. A greatest disadvantage of a gelled fluid system is the damage caused by the gel residue to the fracture conductivity. Also, the cost of using a gelled fluid system is very high.

With a great success of Barnett shale development, the horizontal multi-stage, water fracking and low sand concentration fracturing technology has become the primary means to stimulate shale plays. McDaniel (2012) listed three advantages of water-fracking treatments: lower cost, lower fracture height and reduced damage to proppant packs compared with using a gelled fluid. However, the water fracking and low sand concentration result in low propped fracture conductivity, which seems to violate the traditional belief "Fracture Conductivity is King". Therefore, why this technology can still make a success in Barnett shale? Micro-seismic monitoring helps us to understand that the success of the fracturing technology in Barnett shale is because an extensive fracture network has been created, which provides an extreme amount of a

surface area producing into the fractures and lowers the fracture conductivity requirement. In addition, conductivity experiments (Fredd et al., 2001) and reservoir modeling in the Barnett Shale (Cipola et al., 2008) indicated that the produced displaced fractures without proppants in a very brittle formation can still have a certain conductivity to deliver gas. Barnett shale is brittle (Figure 1-4), and can easily generate displaced fractures with conductivity. Also, it has a natural network of natural fracturing, has an unusually small difference in the minimum and maximum horizontal stress values, and has ultra-low permeability (5 to 50 Nano-Darcy). All these properties, making complex fractures more easily achieved, have not been fully found elsewhere (McDaniel, 2012). Due to the low fracture conductivity requirement for hydraulic fracture treatments in Barnett shale, some engineers thought the fracture conductivity was not important in shale gas plays. However, if the fracture conductivity which transmits the fluids to a wellbore is inadequate, a stimulated reservoir volume (SRV) does not have to equate better stimulation (Bazan et al., 2013). Although any fracture provides infinite flow capacity compared to a tight formation, the immense surface area of propped fractures requires fluids to move away faster within the propped fractures than within the matrix. So propped fracture conductivity remains critical both for cleanup of fracking fluid and subsequent gas production (Warpinski et al., 2008). Maximizing fracture conductivity is still a concern for shale and tight plays.

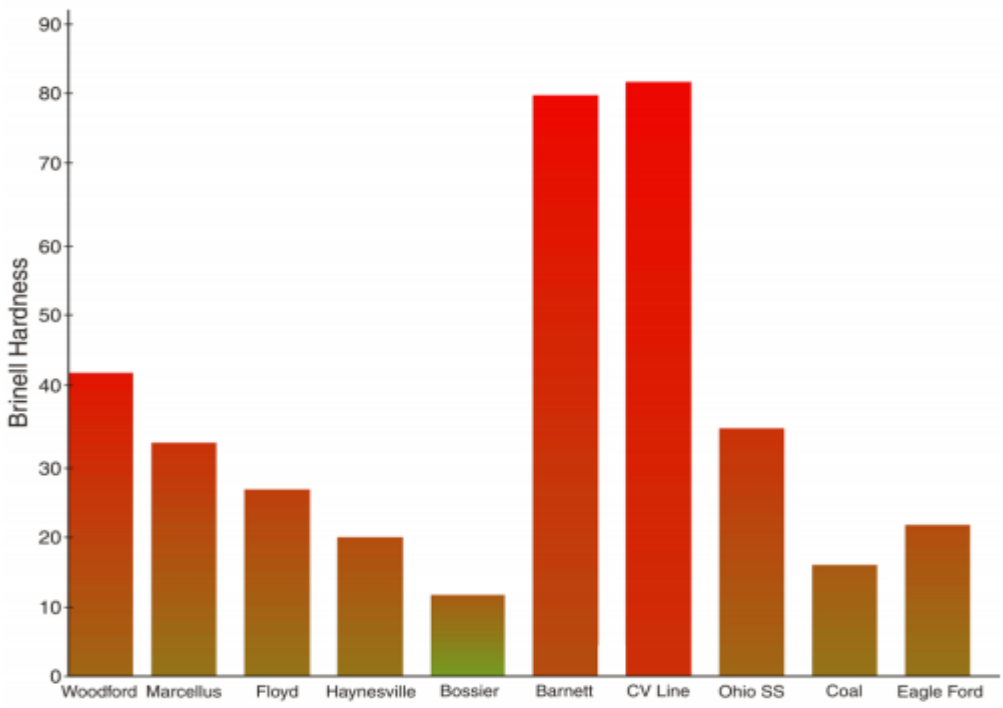

Figure 1-4: Brinnel hardness number (BHN) for various unconventional /tight gas plays across the USA (Mullen et al., 2010)

On the other hand, hydraulic fracture modeling in resource plays is challenging and often reduced to rules of thumb, and design concepts are taken from other shale plays (Bazan et al., 2013). In fact, no two shales are alike (King, 2010). Not all the shales have the properties which can cause a complex fracture network easily with water fracking and only need low fracture conductivity. Many shales are much more ductile, giving less complexity. Many shales have higher permeability than Barnett shale, in which it is more difficult to produce complex fractures due to fluid loss into the matrix. Slick water fracking plus low sand concentration were unsuccessful when applying to some other shale and tight reservoirs. Different properties of shale/ tight plays have different fracture conductivity requirements. A fracking fluid type, proppant type and their amount should be based on an optimum propped fracture conductivity. Some reservoirs which

have a higher fracture conductivity requirement may need a gelled fracking fluid system or hybrid fracking fluid (water + gelled fluid).

Moreover, using an optimum F_{CD} of 10 to 30 as a design guide may not apply to horizontal wells because F_{CD} does not consider the intersection between a wellbore and fractures and the associated flow convergence (Warpinski et al., 2008). Cipola et al. (2008) and Gu et al. (2014) illustrated by their simulation results the limitation of conventional F_{CD} to very tight reservoirs when applying optimum F_{CD} to estimate the propped fracture conductivity. As software and hardware advance, direct numerical simulation using a finite difference reservoir flow model to estimate the optimum propped fracture conductivity for shale/tight plays has gained increasing attentions (Gu et al., 2014). Cipolla et al. (2008) used reservoir simulation to determine the optimal fracture conductivity for different permeability reservoirs and different cases of fracture complexity. They built two kinds of reservoir models: One is with uniform fracture conductivity throughout fracture networks and the other one assumes an infinite fracture conductivity in the primary fractures, which are defined as the major cracks created by high fracturing treatment pressure and also mean hydraulic fractures. The assumption of uniform conductivity is inadequate due to the proppant settling through the hydraulic fractures, and the hydraulic fractures having higher conductivity than secondary or natural fractures. Relative to primary fractures, secondary fractures are pre-existing natural fractures that are opened due to the penetration of high rate of fracturing fluid and normally have higher conductivity than natural fractures. Furthermore, as stated earlier, many factors can cause a conductivity reduction such as proppant embedment, proppant crushing, and gel residual damage. Therefore, the assumption about infinite conductivity in primary fractures is inadequate as well. Gu et al. (2014) evaluated the effect of propped fracture length, production time, natural fractures, and water production on optimum fracture conductivity

by reservoir simulations. They considered the finite conductivity in hydraulic fractures (primary fractures), but their fracture models only embodied the interaction between a bi-wing planar fracture and natural fractures, and did not cover a complex fracture network. Last, both studies above assumed that the propped fracture conductivity was constant with time, and did not take into account a decrease in the propped fracture conductivity with production.

1.3 Objectives of the Study

The objective of this study is to determine the optimum hydraulic fracture conductivity for different property of shale/tight plays by reservoir simulations in order to maximize the production. The simulation results not only quantitatively give the values of optimum fracture conductivity, but also qualitatively describe the relationship between the optimum fracture conductivity and reservoir and fracturing treatment parameters such as matrix permeability, reservoir geomechanics, natural fracture spacing and conductivity, hydraulic fracture spacing and length, production time, and fracture geometry. Meanwhile, the requirements of optimum fracture conductivity for planar and complex fractures are compared. Once the optimum fracture conductivity is known, a procedure is provided to determine a fracking fluid type, proppants type and their amount in terms of the optimum fracture conductivity.

This study improves the reservoir models and relevant assumptions related to the fracture models compared to the previous work. First, the reservoir models include planar and complex fracture models. Also, the fracture models consider finite conductivity in the primary fractures, varied fracture conductivity through the primary fracture length and with production time, and different conductivity between primary and natural fractures. This workflow and the range of optimum propped fracture conductivity provided by this study can be useful to optimize a hydraulic fracturing treatment design for shale/tight plays.

1.4 Structure of the Thesis

This thesis is composed of four chapters. The first chapter is an introduction, which describes the definition of fracture conductivity, factors that affect fracture conductivity, and the development of optimizing the fracture conductivity. Meanwhile, the statement of problems, objectives of this study and a literature review about the development history of an understanding of the fracture conductivity are presented as well.

The second chapter illustrates a workflow to predict the optimum fracture conductivity, and describes the methodology used in this workflow in detail. First, how the reservoir model is built is demonstrated. Then, a sensitivity analysis and history match are presented to ensure the reliability of the reservoir model. Last, a detailed description about how to predict the optimum fracture conductivity by reservoir simulations, including the building of planar fracture and complex fracture models and a couple of reservoir properties that affect the optimum fracture conductivity, is given.

Chapter 3 contains the simulation results and discussions. This chapter summarizes the optimum fracture conductivity values for shale/tight gas reservoirs with various fracture length, production time, matrix permeability, Young's modulus, nature fracture conductivity and spacing, hydraulic fracture spacing, and a complex fracture network. Meanwhile, this chapter compares these conductivity values and analyzes what causes the different conductivity requirements for different situations. After the optimum fracture conductivity is determined, an example to choose proppants and fracture fluid based on the optimum fracture conductivity is presented.

Chapter 4 summarizes the conclusions from this study and future work recommendations.

1.5 Literature Review

As mentioned earlier, the primary design parameters for conventional hydraulic fracturing are fracture half-length and fracture conductivity (Economides et al., 2000). Since dimensionless fracture conductivity F_{CD} combines these two critical parameters, engineers often used F_{CD} as a principal parameter in fracturing design optimization. McGuire and Sikora (1960) summarized their research result (Figure1-5) about the effect of vertical fracture conductivity on well productivity in a semi-steady state. This result shows that the ratio of a productivity index for fractured to un-fractured cases increases with the relative conductivity. Also, it implies that the productivity can be augmented by increasing the relative conductivity from 10^3 to 10^4 regardless of the fracture length, which explained some failure of long fracture operations due to the lack of certain fracture conductivity. On the other hand, little benefit is gained by increasing relative conductivity of short fractures above 10^4. The Mcguire and Sikora curves were the primary reservoir tool for fracturing design and evaluation until the late 1970s (Economides et al. 2000). Prats (1961) first introduced the concepts of the fracture capacity, i.e., fracture conductivity, and dimensionless fracture conductivity. He showed that the effect of vertical fractures in a cylindrical reservoir can be represented by the production response of an effective well radius in steady-state conditions. The effective well radius is a half of the fracture half-length for an infinite-conductive fracture (also explained as a pressure drop in a fracture is negligible), decreasing with the fracture conductivity. He also found that for a given fracture volume (proppant volume), if there is no damage to a formation during the fracturing operations, the maximum production could be reached when F_{CD} was about 1.26. Later on, engineers gave the optimum F_{CD} values under various conditions. Elbel (1988) used a finite-difference reservoir simulator to model the productivity of a well containing a fracture with different conductivity in various fracture length scenarios. The

simulation results confirmed the validity of Prats' conclusion about the optimum F_{CD} value of 1.26 for a constant fracture volume after a pseudo-steady period was reached for the formation permeability in the range of 1md or greater, but the optimum F_{CD} equaled 3 or greater for the formation permeability of 0.1 to 0.001md. For low-permeability formations (k<0.01md), Elbel (1988) pointed out that higher values of F_{CD} should be more economical for a long period of time in transient production. For a constant fracture length, Economides et al. (2000) summarized from Holditch's work (1979a) that a F_{CD} of 10 and 30 has generally been accepted as an optimum range.

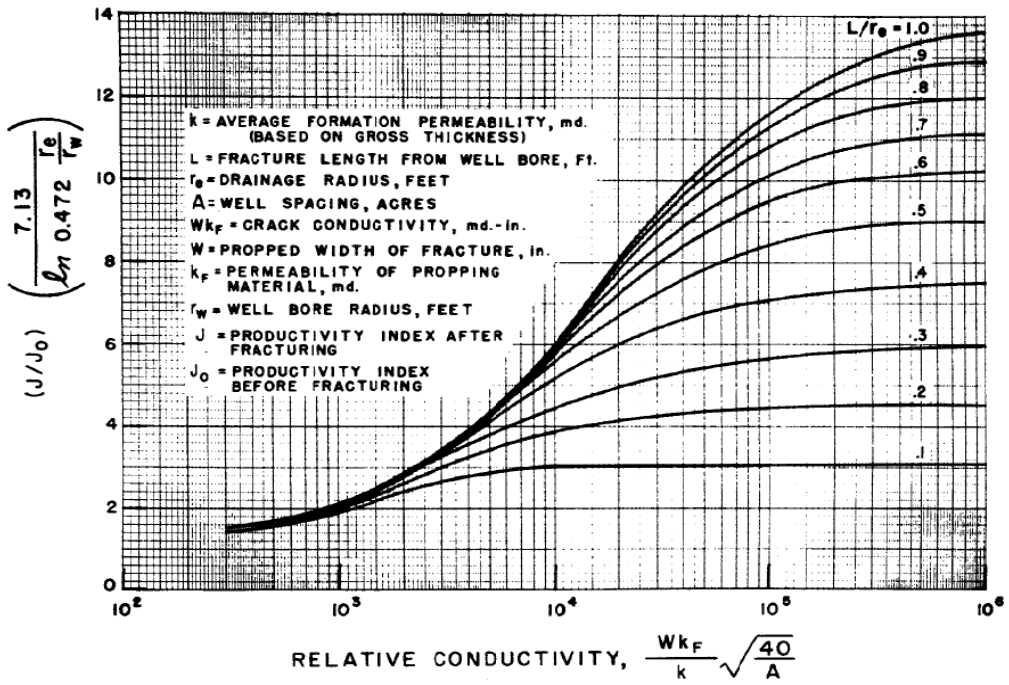

Figure 1-5: Relationship of productivity and relative conductivity (McGuire and Sikora 1960)

Most of the work above has considered a steady or semi-steady flow regime. In addition, engineers built type curves by using a pressure transient analysis to estimate reservoir and fracture characteristics, which is useful for fracturing design optimization. Scott (1963) examined transient pressure behavior of vertically fractured wells by means of a heat flow analogy, and concluded that an effective well radius is about a half of the fracture half-length even under transient flow for

a high conductivity vertical fracture. Based on the infinite conductivity concept from Prats (1961), Russell and Truitt (1964), Gringarten et al. (1974), and Gringarten et al. (1975) explored transient pressure behavior of a reservoir with a single infinite-conductivity vertical fracture by building the type cures of dimensionless pressure drop vs. dimensionless time with different fracture penetration ratio, demonstrated how to use the pressure build up data or flow test data to match the type curves, and obtained reservoir and fracture characteristics such as the formation permeability and fracture length. Thus, the effectiveness of fractures can be evaluated. The above methods to examine the transient pressure behavior of infinite conductive fractures and then evaluate the effectiveness of the fractures are useful for a small-volume fracturing treatment. With the later trend to develop tight gas reservoirs by massive hydraulic fracturing, these methods based on the concept of infinity fracture conductivity are inadequate for analyzing wells with finite-conductivity fractures resulted from the massive hydraulic fracturing (Agarwal et al., 1979). The assumption of infinity fracture conductivity is idealized. In reality, the operator's intention to an economical hydraulic fracturing resulted in finite-conductive fractures. A long fracture by using a massive hydraulic fracturing is a design target for low permeability reservoirs, which also resulted in finite-conductive fractures (Prats, 1961). Cinco L et al. (1978) first presented the pressure transient behavior for wells with finite-conductive vertical fractures. They used a semi-analytical approach to obtain constant-rate type curves for various values of F_{CD}, and the fracture characteristics can be evaluated by type curve matching. Agarwal et al (1979) extended Cinco L et al.'s work (1978). They used a finite-difference reservoir simulation model to build constant-rate and constant pressure type curves which showed the relationship of a production rate for various F_{CD} with time for massive hydraulic fracturing operations. However, Agarwal et al (1979) pointed out that the finite fracture conductivity type curves look alike and do not have distinct shapes. This is a

disadvantage when using type curve matching. Cinco-Ley and Samaniego (1981) developed new type curves for a transient pressure analysis of finite conductivity vertical fractures, considering the end of wellbore storage effects and overcoming the uniqueness problems exhibited by other type curves. They showed that F_{CD} must be 30 for a dimensionless time greater than 1 to maximize the transient production rate. They identified four flow periods for the transient flow behavior of a vertically fractured well: fracture linear flow, bilinear flow, formation linear flow, and pseudo-radial flow as shown in Figure 1-6. Their work has become the theoretical basis for many pressure transient analysis techniques for fractured wells (Economides et al., 2000). Wong et al. (1986) introduced the simultaneous use of the pressure behavior and pressure-derivative behavior for a fractured well to reduce the uniqueness problem in type-curve matching. The methods above using a type curve to predict the effect of fracture conductivity on the well productivity were based on homogeneous, isotropic reservoir models with uniform conductivity along fractures. In fact, reservoirs are heterogeneous and anisotropic, and may have natural fractures. Also, Bennett et al. (1983) pointed out the fracture conductivity was decreasing from a wellbore to a fracture tip. Poe et al. (1992) presented the variable fracture conductivity in a vertical direction. Therefore, type curve methods are not good candidates to deal with these kinds of reservoirs.

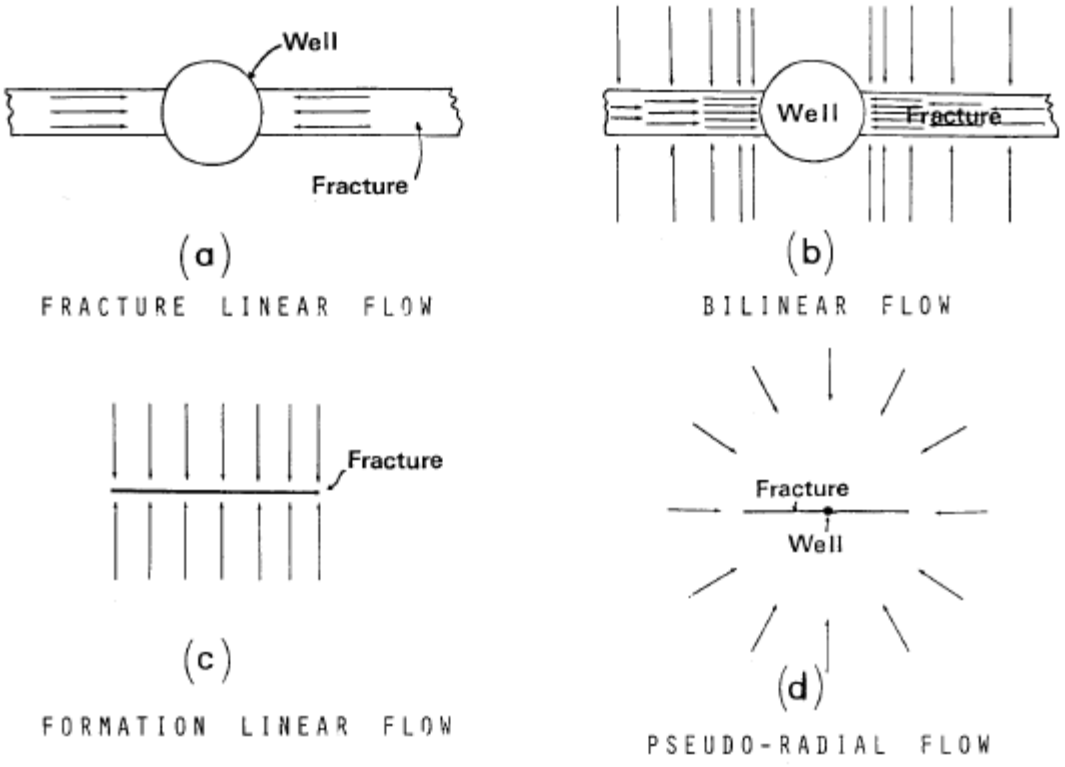

Figure 1-6: Four flow periods for a vertically fractured well (Cinco-Ley and Samaniego, 1981)

With the advent of fracturing horizontal wells in the 1990s, engineers devoted efforts to developing methods to predict or evaluate the performance of hydraulically fractured horizontal wells. Sollman et al. (1990) discussed some parameters to improve the productivity of hydraulically fractured horizontal wells. They concluded that the convergence of streamlines inside the transverse fractures toward a wellbore caused a higher pressure drop compared to a vertical well intercepting a vertical fracture, which required a very high F_{CD}, and a tail-in with high conductivity helped to reduce the observed pressure drop. Roberts et al. (1991) employed semi-analytical models and numerical simulation to evaluate the effects of fracture and reservoir properties on the productivity of tight gas horizontal wells which were multiply fractured. They found out that limited communication between a horizontal wellbore and a transverse hydraulic

fracture in a gas well resulted in a significant non-Darcy flow which reduced the well productivity. Raghavan and Joshi (1993) provided a procedure to evaluate the productivity of a horizontal well stimulated by vertical fractures. Raghavan et al (1997) used the pressure behavior to evaluate the effects of fracture properties, such as length, conductivity, location and orientation, for multiply fractured horizontal-wells. Besler et al. (2007) indicated that the micro-seismic technology showed the transverse fractures were more frequently created than longitudinal fractures in horizontal wells in North America, and they observed that production from transverse fractures was improved by increasing fracture conductivity. Stimulation of horizontal wells with transvers fractures was the best technique to touch formation; however, a near-wellbore region especially needed high conductivity since transverse fractures provided an extremely small area of intersection between the fractures and the wellbore (Vincent, 2012).

Engineers found out that the fracture conductivity values from well testing, production data analyses, and history matching were frequently smaller than the designed fracture conductivity. Some laboratory work has been performed to identify the discrepancies. Cooke (1973) did a series of experiments to test effects of the environment (fluid present, stress, and temperature) and non-Darcy's flow of gas on the fracture conductivity. He concluded that the non-Darcy flow of gas normally decreased the fracture conductivity, and the experiments to test the fracture conductivity should be under reservoir conditions. Later, Holditch and Morse (1976), Guppy et al. (1982), and Gidley (1991) respectively presented methods to correct F_{CD} used in a fracturing design and a pressure analysis due to non-Darcy's effect. Cooke (1975) did realistic experiments by using a polymer-based fluid flowing through a cell with rock and a proppant pack, and applying closure stress to test the effect of the fracturing fluid on the fracture conductivity. His experiments first concluded that the residue from guar polymer can cause a fracture conductivity reduction. Cooke's

experiments showed the factors that affect the fracture conductivity, and initiated the work to improve the proppant pack and breaker and reduce polymer concentration. Parker and McDaniel (1987) tested the fracture conductivity under in-situ conditions in the lab, and summarized that the effects of time, temperature, stress, and the presence of gel filter cakes were all important factors in the measurement of fracture conductivity. They also concluded that the conductivity of 20/40 Ottawa sand could not meet the requirement of many fracturing applications at that time due to the presence of gel filter cakes, and high proppant concentrations in fractures were necessary to alleviate the effect of gel filter cakes. Kim and Willingham (1987) and Holditch & Blakeley (1992) conducted experiments to demonstrate that stress cycles can significantly reduce the fracture conductivity in a gas well, and cyclic stress loading resulted in the additional proppant crushing. Penny and Jin (1995) summarized that the conductivity of a proppant pack could be reduced by a factor of 10 to 90% if the impact of time, temperature, proppant embedment, and gel residual damage were considered. In addition, they used their laboratory data to show that the multiphase, non-Darcy's flow could decrease the fracture conductivity as well, and high conductivity proppants could mitigate the negative impact. Palisch et al. (2007) analyzed the detrimental effects of non-Darcy's flow, multiphase flow, reduced proppant concentration, gel damage, fine migration and cyclic stress on effective fracture conductivity. They indicated the cumulative effects could be over 98% reduction from the baseline conductivity after accounting for these factors, and they also used field data and a combined type cure and decline curve analysis to validate this conclusion. McDaniel (1986), Cobb and Farrell (1986), and Handren and Palisch (2009) did long-term proppant conductivity testing under realistic in-situ conditions. All experimental results showed that the conductivity of a proppant pack reduced over time, proppants experienced particle breakage and compaction with the extended time testing, and some proppants were more durable

than others. Zhang et al. (2014) concluded from long-term fracture conductivity measurements with naturally fractured shale samples that the fracture conductivity could be reduced by as much as 20% within 20 hours. Their study also indicated that the propped fracture conductivity could increase by using a larger proppant size and higher proppant concentration.

Due to the success of water fracking and low sand concentration in the Barnett Shale, this technique has become the primary means to develop tight reservoirs currently. The success of the fracturing technique has different reasons. First, micro-seismic mapping helped engineers to realize a complex fracture network created by this technique so the network provided a much larger surface area of contact with a very tight reservoir. Second, the water fracking minimized the fracture conductivity damage caused by gel residue. Also, the water fracking and light sand or a smaller proppant size helped opening natural fractures and proppants entering the induced fractures (Fisher et al., 2002, Fisher et al., 2004, Coulter et al., 2004). In spite of the success of the water fracking with low sand concentration, it has a disadvantage which is the low carry capacity of the fluid resulting in the proppants settling, and therefore, leading to poor proppant placement and narrower fractures. However, Fredd et al. (2001) performed a series of laboratory conductivity experiments to demonstrate that fracture displacement can still provide sufficient conductivity in the absence of proppants, and concluded that the success of water fracking highly depended on the degree of fracture displacement, the size and distribution of asperities, and rock mechanical properties. Zhang et al. (2014) showed that poorly cemented natural fractures and un-propped displaced fractures could create conductivity of up to 0.5md-ft. Thus, un-propped conductivity could be a factor to contribute to the success of water fracking.

Beugelsdijk et al. (2000) used laboratory experiments to simulate the fractures propagation and the interaction of hydraulic fractures with natural fractures. They observed that the low

viscosity fluid and small horizontal stress difference could increase the fracture complexity. Weng et al. (2011) developed a new hydraulic fracture model to simulate complex fracture network propagation in a formation with pre-existing natural fractures. The simulation results showed that decreasing stress anisotropy or interfacial friction could change the induced fracture geometry from a bi-wing fracture to a complex fracture network. McDaniel (2012) pointed out that Barnett Shale has all the properties that seem to make it easy to achieve complex fractures: brittle rock, natural fractures, and small difference between the minimum and maximum horizontal stress values. The complex fractures reduced the fracture conductivity requirement due to the creation of an extreme amount of a surface area contacting with a tight reservoir. Many in the industry thought that fracture conductivity was unimportant with unconventional reservoirs because of their extremely low permeability (Pope et al., 2012), plus the reduced fracture conductivity requirements from complex fractures. However, Pope et al. (2012) pointed out that all the large reservoir contact produced by the complex fractures or long fractures would be useless if there was inadequate fracture conductivity. Most proppants could lose in excess of 90% of their effective conductivity under realistic conditions due to all kinds of factors affecting the conductivity as stated earlier. Mayerhofer et al. (2006) integrated the micro-seismic mapping results which defined a fracture network size with a reservoir simulator to investigate the impact of various fracture network parameters on production for Barnett Shale. They illustrated that higher conductivity could result in higher production, and pointed out that a fracture network in the Barnett shale was so large that fracture conductivity became important again in spite of ultra-low shale permeability, because very low fracture conductivity could result in the fracture inability to transport gas from the far reaching of the network. They also concluded more aggressive proppant pump schedules which could increase a network and near-wellbore conductivity should be considered if this action

could not sacrifice the fracture network size. Also, many other published studies have shown that well production even with tight reservoirs could be increased when the fracture conductivity was improved (Vincent, 2002; Palisch et al., 2007; Cipolla et al., 2010; Pope et al., 2012; Vincent, 2012; Sun and Schechter, 2015)

Due to the limitation of the previous type curve methods, Economides et al. (2000) pointed out that the finite difference reservoir simulation models were generally the preferred methods for estimating the performance of complex reservoirs with vertical fractures. Cipolla et al. (2010) also thought reservoir simulation was commonly the preferred method to predict and evaluate well performance given a complex fracture network and the ultra-low permeability in shale gas reservoirs combined with the predominance of horizontal completions. The distribution of proppants within fractures cannot be accurately predicted and neither can the fracture conductivity because of the complexity of fracture growth in many tight reservoirs. Bazan et al. (2013) pointed out that hydraulic fracture modeling was challenging and often reduced to rules of thumb, and fracture concepts were taken from other shale plays. No two shales were alike. There were no optimum, one-size-fits-all stimulation designs due to shale fabric differences (King, 2010). The fracture conductivity required to economically produce a horizontal well in unconventional reservoirs to improve hydrocarbon recovery would vary for the various shale plays (Bazan et al., 2013). For example, Cipolla et al. (2010) presented that the impact of stress dependent fracture conductivity in higher Young's modulus shale reservoirs may be small but great in lower Young's modulus shale reservoirs so the higher fracture conductivity was needed in lower Young's modulus shale reservoirs to improve production and gas recovery. On the other hand, McDaniel (2012) believed that the required fracture conductivity was dependent on the degree of enhanced "effective permeability", i.e., a fracture network size. Cipolla et al. (2008) used reservoir

simulation to investigate the fracture conductivity requirements in terms of various degrees and types of fracture complexity in different permeability tight gas reservoirs. They showed the limitation of dimensionless conductivity F_{CD} for estimating the optimum fracture conductivity in the low permeability reservoirs, and indicated that higher fracture conductivity requirements would be needed for low-permeability reservoirs by using reservoir simulation than by using the classical F_{CD} calculation. Gu et al. (2014) also applied three–dimensional finite difference reservoir simulation to examine the effects of hydraulic fracture length, production time, natural fractures, reservoir permeability, hydraulic fracture spacing, water production, and bottom flowing pressure on the optimum fracture conductivity for a planar fracture model. They showed the limitation of F_{CD} for shale gas reservoirs as well by comparing the optimum fracture conductivity from reservoir simulation and F_{CD}, respectively.

Chapter 2 : Hydraulic Fracture Conductivity Optimization

To execute the hydraulic fracture conductivity optimization, first, the typical Muskwa formation parameters in Horn River basin were chosen to build a reservoir model. Then, a sensitivity analysis was performed using CMG CMOST to verify the important effect of the hydraulic fracture conductivity on post-fracture productivity. Also a history match was used to ensure the reliability of the reservoir model; therefore, the optimum fracture conductivity can be forecasted. The workflow is shown as below:

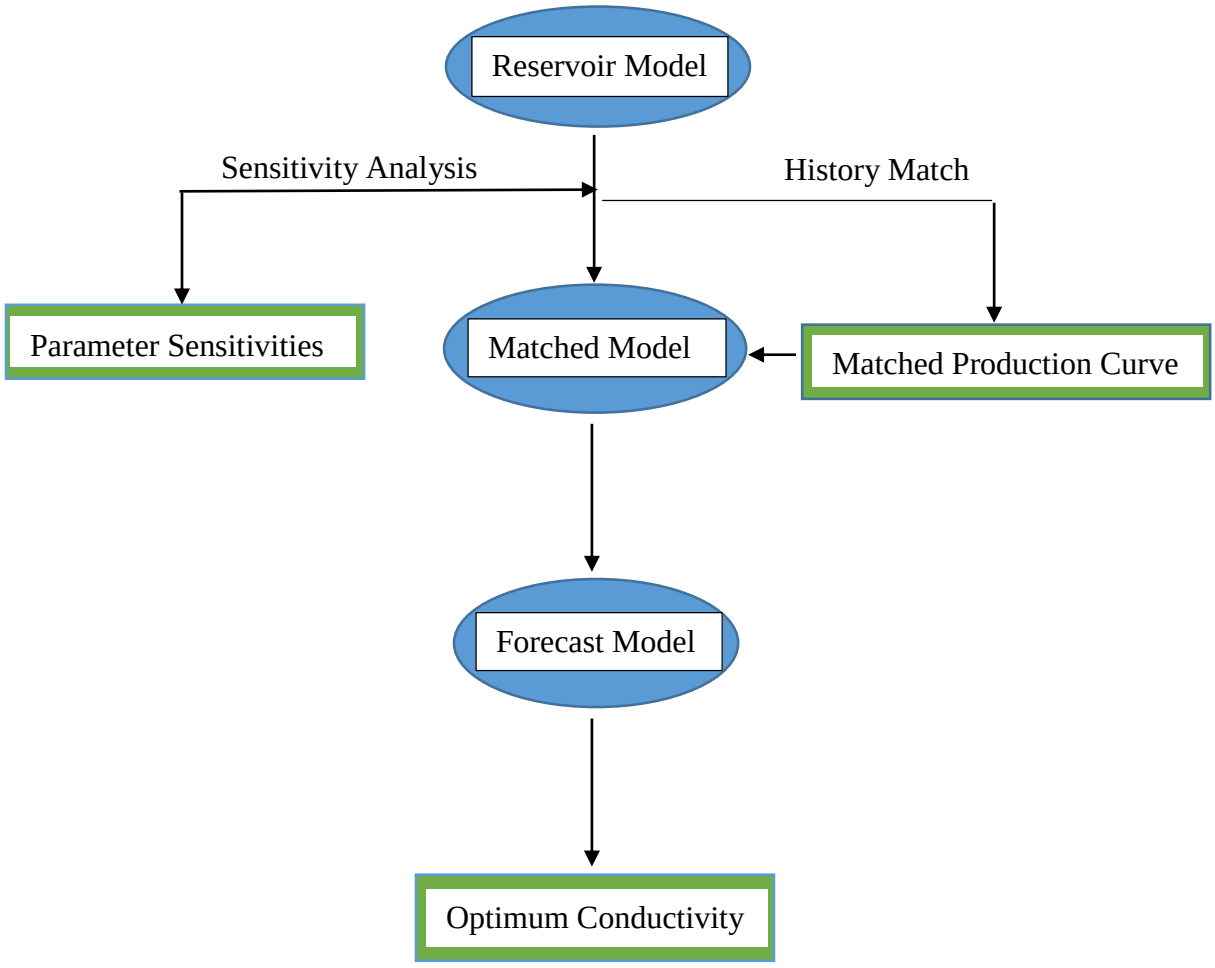

Figure 2-1: Hydraulic fracture conductivity optimization workflow

2.1 Reservoir Model

The Horn River Basin is located in northeastern British Columbia, and the Horn River shales are estimated to contain 372 – 529 Tcf of probabilistic gas in place (GIP) (Johnson et al., 2011), which has great potential for unconventional resource development. The shale gas consists primarily of methane. The Horn River shales have a high degree of natural fracturing due to a complex basin history and a high quartz content, which makes the shales very brittle (Novlesky et al., 2011). The shales are divided into the Evie, Otter Park, and Muskwa formation. Typical reservoir data from a horizontal well C-096-H/094-O-08 completed in Muskwa and Otter Park formation was selected to execute the workflow.

Figure 2-2 is the production history of this horizontal well. The fracking for the well was completed in August, 2010, and the production history started in December, 2010. At the beginning of production, there was no water produced. Therefore, the flow back of fracking fluid should be done before the production. After two year production, there was a little water production which only lasted 6 months. The water saturation of the reservoir must very low according the water production. The well was hydraulically fractured in 16 stages. 15 stages have 4 clusters and one stage has 3 clusters. The cluster spacing is 25m so there were 63 transverse planar hydraulic fractures in total. A wire-mesh natural fracture network is also included in this model. Based on the well information and the average well spacing in Horn River basin, a reservoir model was set up with a dimension 1675m×400m×40m. The preliminary parameters for the reservoir model are listed in Table 2-1.

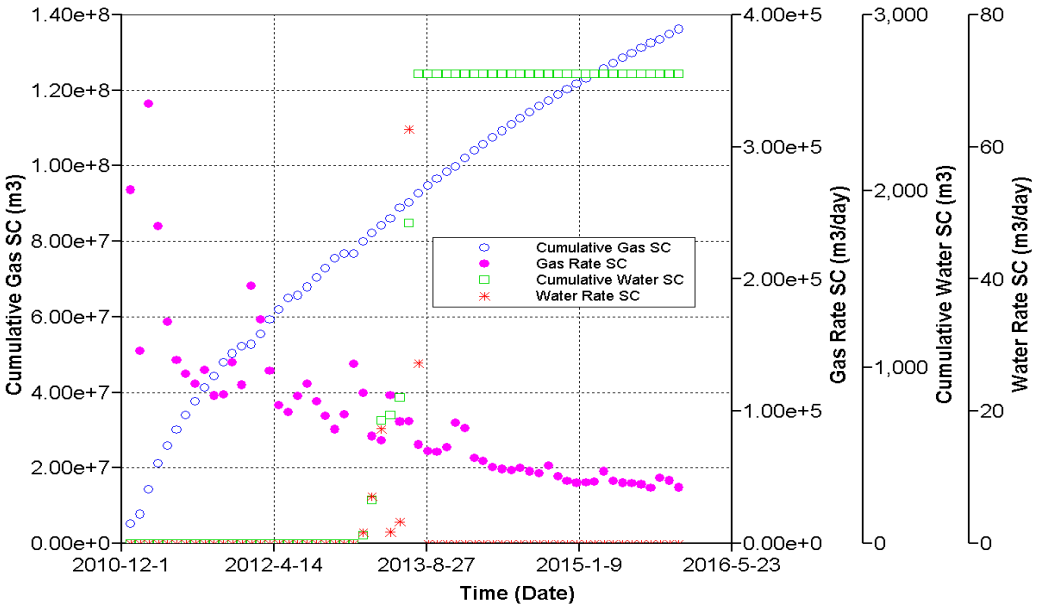

Figure 2-2: Production history of the well C-096-H/094-O-08

Table 2-1: Preliminary reservoir parameters used in sensitivity analysis

Parameters	Value
Depth	2415m
Matrix Porosity	0.05
Matrix Permeability	0.0001md
Pore Pressure Gradient	16.8 kPa/m
Initial Pore Pressure	40572kPa
Rock Compressibility	8.7e-7 1/kPa
Formation Temperature	127℃
Flowing Bottomhole Pressure(BHP)	3448kPa
Initial Water Saturation	0.2
Hydraulic Fracture Conductivity	31md-m
Hydraulic Fracture Spacing	25m
Hydraulic Fracture Half-length(x_f)	150m
Hydraulic Fracture Height	40m
Hydraulic Fracture Width	0.003m
Natural Fracture spacing	25m
Natural Fracture Conductivity	0.003md-m
Horizontal Well Length	1575m

The CMG GEM (2014) simulator is used to simulate the fluid flow in the matrix, hydraulic fractures, and natural fracture network. For this reservoir model, each grid size is 25m×25m×5m. Local refinement is used to accurately simulate the transient effect around the hydraulic fractures, while logarithmic refinement is employed to reduce refinement far away from the fractures so that runtime can be reduced. The hydraulic fractures are explicitly modeled as a part of the matrix. A dual permeability system is applied to model matrix-matrix, matrix-fracture, and fracture-fracture flow. Two different relative permeability curves for the matrix and fractures are set up. Since the study in the reference paper (Novlesky et al., 2011) focused on a well completed in Muskwa /Otter Park shale as well, the relative permeability curve k_{rg} for the matrix is used from the paper as shown in Figure 2-3. The relative permeability of gas and water vs. water saturation inside fractures still uses a linear relationship.

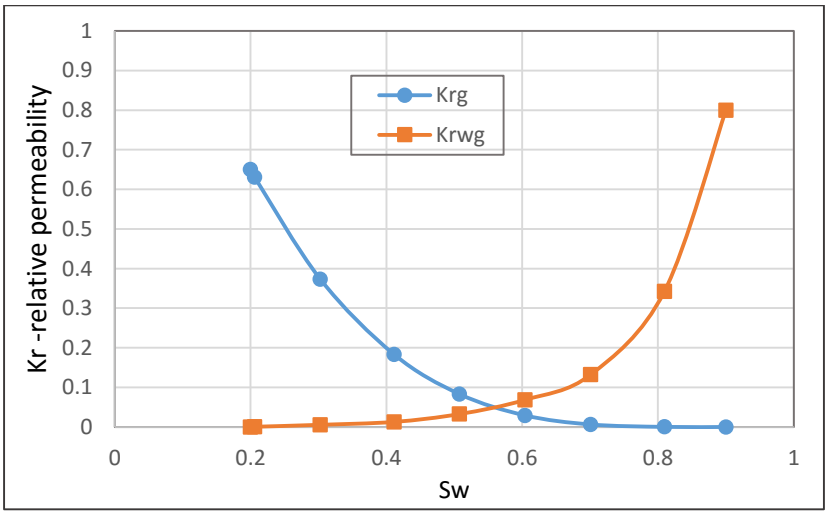

Figure 2-3: Gas and water relative permeability vs. water saturation

Shale and tight gas flow has high velocities inside the propped fractures, which can deviate from Darcy's flow, so non-Darcy's flow in fractures is considered in this shale gas reservoir. The

non-Darcy's flow can be modelled with the Forchheimer equation as below (Yu and Sepehrnoori, 2013):

$$-\nabla p = \frac{\mu}{k} v + \beta \rho v^2 \quad (2\text{-}1)$$

where p is the phase pressure, v is the velocity, μ is the viscosity, k is the permeability, ρ is the phase density, and β is the non-Darcy's flow coefficient. In this model, β is determined from a correlation by Evans and Civan (1994):

$$\beta = \frac{1.485E9}{(k)^{1.021}} \quad (2\text{-}2)$$

Since the correlation is obtained from a large variety of porous media under different conditions, it is expected to provide a reasonable estimation (CMG GEM, 2013).

Gas in shale reservoirs usually has two forms: One is free gas stored in matrix pores and natural fractures; the other one is adsorbed gas onto solid organic material in the shale. When shale gas is producing and reservoir pressure is decreasing, the adsorbed gas can be released. Thus, the gas adsorption process should be considered in this reservoir simulation as well. Langmuir isotherm is one of the most popular models used to describe this process (Yu and Sepehrnoori, 2013). The Langmuir equation is as follows (CMG GEM, 2013):

$$\omega_i = \frac{V_L p}{p_L + p} \quad (2\text{-}3)$$

where ω_i is the adsorbed gas content in moles per unit mass of rock, $V_L$is the Langmuir volume, and p_L is the Langmuir pressure corresponding to a point at the Langmuir isotherm curve at which the gas adsorption equals one half of the maximum adsorbed gas content, i.e., the Langmuir volumeV_L. The Langmuir volume and pressure can be determined from adsorption isotherm testing on core samples. In this case, the Langmuir volume equals 0.128 gmol/kg and the Langmuir pressure is 6667kPa, which are obtained from Novlesky et al. (2011) as well. Figure 2-4 is the Langmuir isotherm curve used in this simulation.

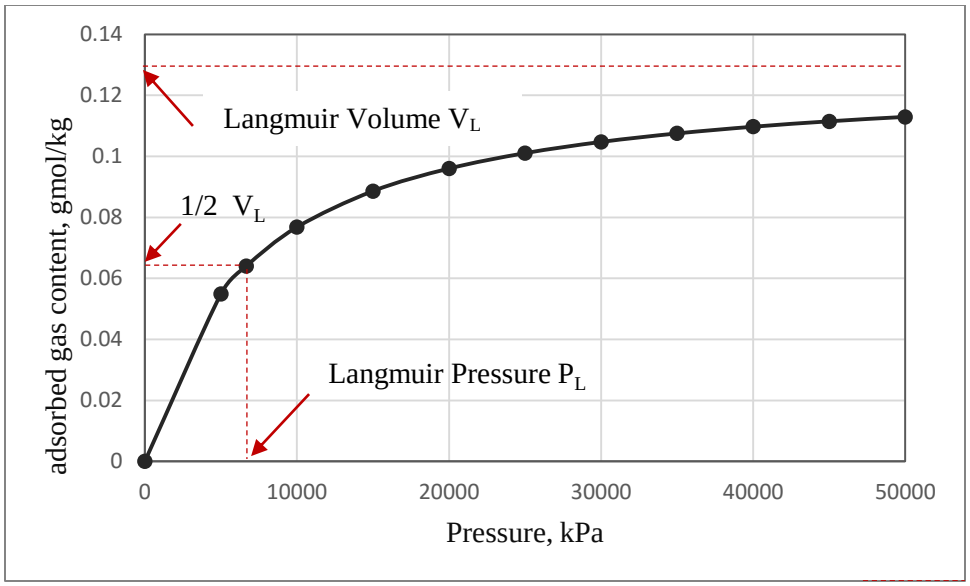

Figure 2-4: Langmuir isotherm curve for this reservoir model

As the reservoir depletes, the pore pressure drops and the effective closure stress exerting to proppants increases. Proppants inside fractures may be crushed or embedded into rock that leads to the reduction of fracture width and permeability, and, therefore, the fracture conductivity during production. Thus, the propped fracture conductivity changes with production time. Alramahi and Sundberg (2012) used different shale samples ranging from stiff to soft shales to test the variation in the propped fracture conductivity under varied effective closure pressure, as depicted in Figure 2-5. The conductivity in the *y*-axis was normalized to the fracture conductivity measured at 500psi, and the closure pressure in the *x*-axis was effective closure pressure which is the difference between minimum stress and reservoir pressure inside fractures. The pressure dependent conductivity also is considered in this study. The closure stress is 46367kPa obtained from a regional mini-frac test, and then the initial effective closure pressure can be calculated to equal 5795kPa based on the initial reservoir pressure 40572kPa. Considering the shale studied in this simulation as a stiff case (Young's modulus $\geq 6\times 10^6$psi), using the stiff case curve in Figure 2-

5, and normalizing the conductivity to the conductivity read at the initial effective closure pressure 5795kPa, we can get the conductivity multiplier vs. reservoir pressure for propped fractures in Figure 2-7, which is an input in the fracture compaction table in the simulator to see the geo-mechanical effect. Fredd et al. (2001) studied the pressure dependent conductivity of partially propped and un-propped fractures in the laboratory. Cipola et al. (2008) extrapolated those data from Fredd et al. (2001) for lower Young's modulus to see the effect of the effective closure pressure and Young's modulus on un-propped fractures as shown in Figure 2-6. In this study, the natural or secondary fractures pressure dependent conductivity multiplier in Figure 2-7 is obtained from Figure 2-6 based on the same method used for propped fracture conductivity multiplier calculation. According to Figure 2-6, shales with modulus greater than 6×10^6psi are classed as the stiff case, the medium case can be in the range of 2×10^6- 5×10^6psi, and the modulus under 2×10^6psi is the soft case. In addition to that the pressure dependent fracture conductivity is considered, varied conductivity along the length of propped fractures is also taken into account. The conductivity decreases along the length of fractures due to the proppant settling. The fracture tip conductivity is assumed as one tenth of the conductivity near the wellbore.

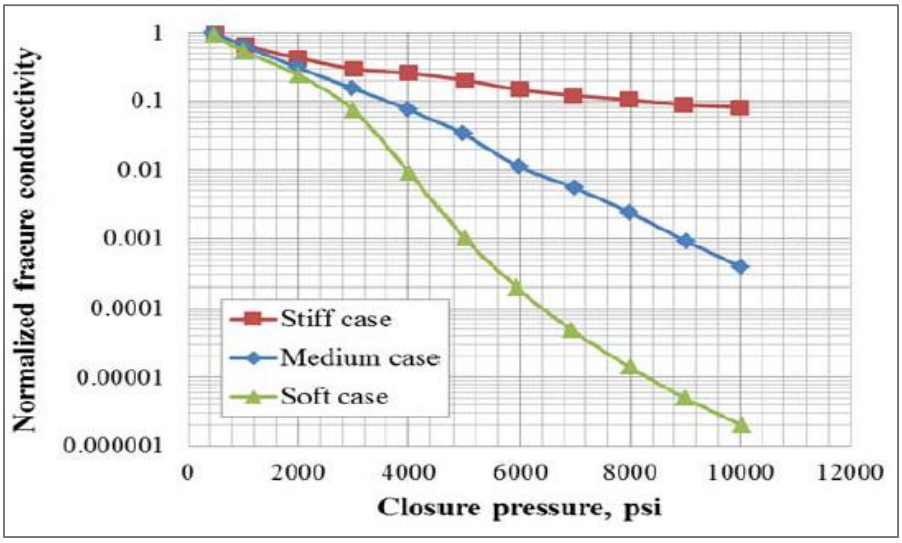

Figure 2-5: Effect of closure pressure on propped fracture conductivity for stiff to soft shale (Yu and Sepehrnoori, 2013)

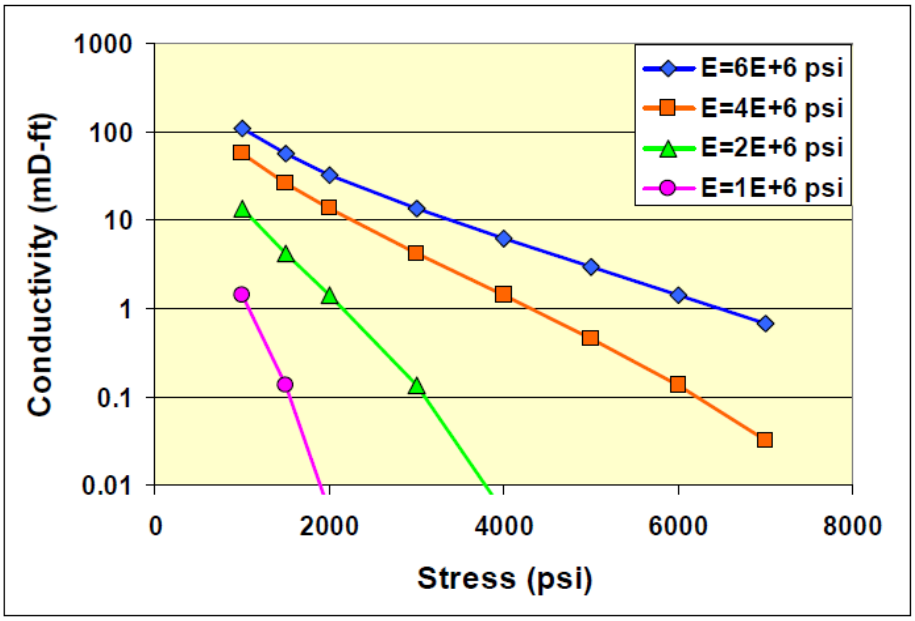

Figure 2-6: Effect of closure pressure and modulus on un-propped fractures with shear offset (Cipola et al. 2008)

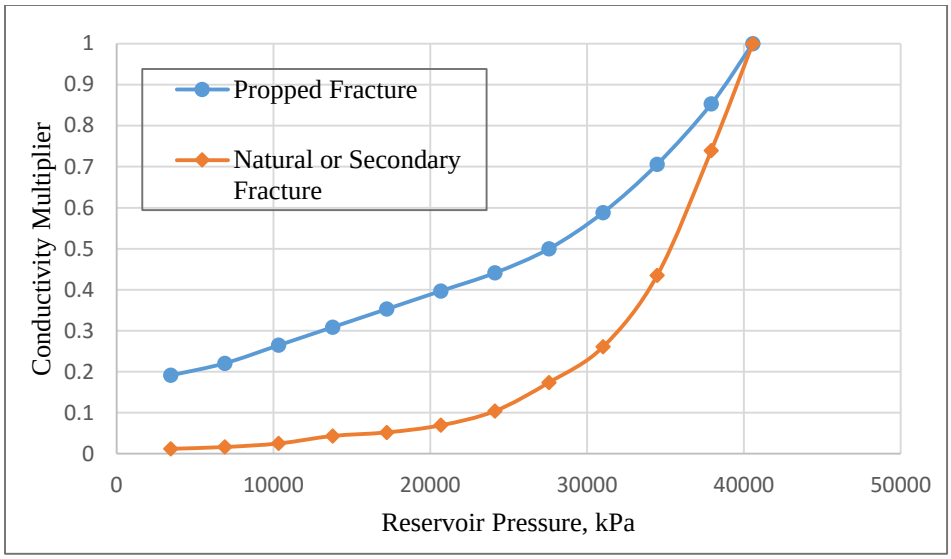

Figure 2-7: Conductivity Multiplier of stiff case in this reservoir model

Figure 2-8 is a schematic diagram of this reservoir model in the GEM simulator, and a 3D view of a bi-wing planar fracture is also shown in Figure 2-9.

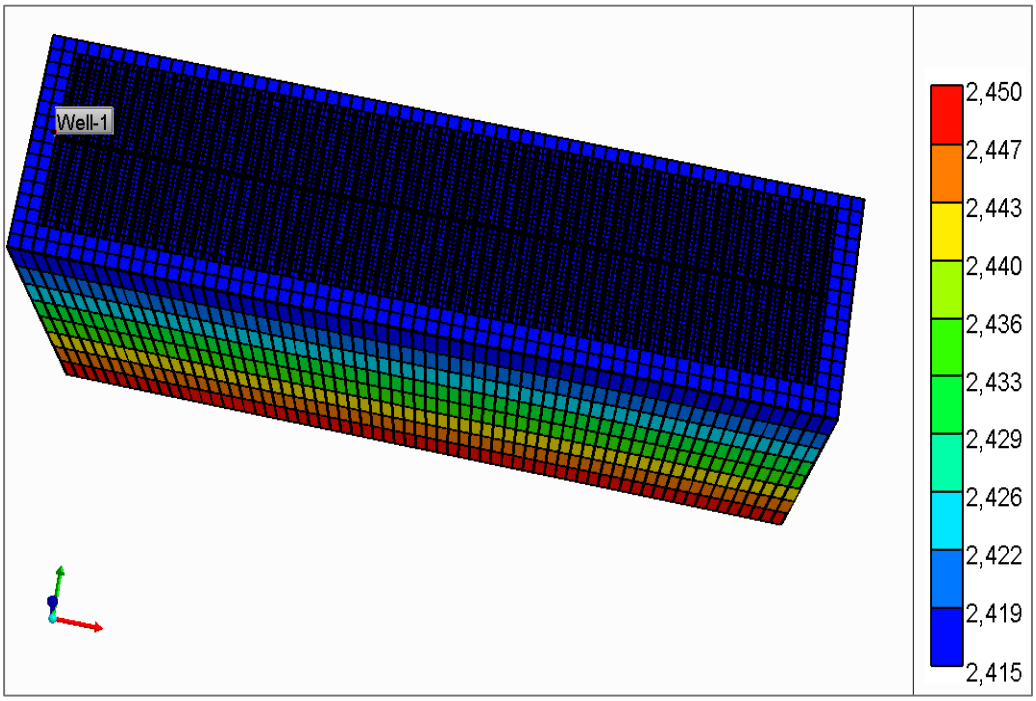

Figure 2-8: A 3D view of this reservoir model

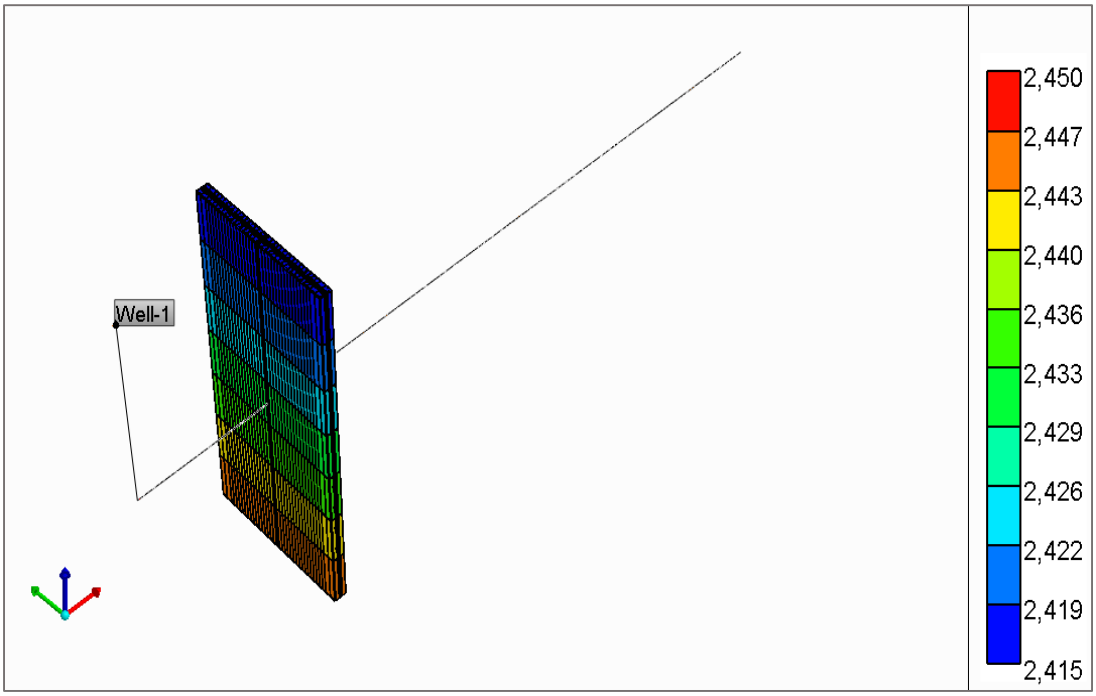

Figure 2-9: A 3D view of a bi-wing planar fracture in this model

2.2 Sensitivity Analysis

A sensitivity analysis is used to determine the effect of different parameters and their range on an objective function. We can see how each parameter impacts the production of the well by sensitivity analysis results. The most sensitive parameters have a large impact on the production of the well so the sensitivity analysis results can help to determine which parameters to be modified when we start a history matching. In this case, we want to see how sensitive the cumulative gas production is to propped fracture conductivity so the objective function is cumulative gas production. The ranges of parameters, which are analyzed in the sensitivity analysis, are listed in Table 2-2. Their ranges are selected based on the possible value for this shale gas reservoir. Some values of the parameters are continuous real numbers, and others are discrete values. For the parameters, propped fracture compaction and natural fracture compaction in Table 2-2, the numeral value 1 and 2 represent the propped fracture compaction table of stiff and medium case,

and the 3 and 4 correspond to the natural fracture compaction table of stiff and medium case, respectively. The fracture conductivity multipliers for the compaction tables for medium cases are shown in Figure 2-10.

Table 2-2: Parameters used for this sensitivity analysis

Variable	CMOST Parameter Name	Value
Matrix Permeability	Matrix_ PERM	0.00001- 0.001 md
Matrix Porosity	Matrix_ POR	0.03 – 0.1
Maximum Adsorbed Gas (the Langmuir volume)	Max_ Adsorbed_ Mass	0.042 – 0.214 gmol/kg
Flowing Bottomhole Pressure	Min_ Bottomhole_ Pressure	3448 – 10000 kPa
Pore Pressure	Pore_ Pressure	30000 – 50000 kPa
Propped Fracture Half-length	Propped_ FracHalflength	50 – 180 m
Propped Fracture Conductivity	Propped_ Frac_ Conductivity	0.0305 – 60 md.m
Propped Fracture Spacing	Propped_ Frac_ Spacing	25 – 200 m (discrete value)
Propped Fracture Width	Propped _ Frac _ Width	0.001-0.008m
Natural Fracture Spacing	Natural_ Frac_ Spacing	5 – 200 m (discrete value)
Propped Fracture Water Saturation	Frac_ SW	0.2 – 0.7
Propped Fracture Compaction	Propped_ Frac_ Compaction	1 and 2 (discrete value)
Natural Fracture Compaction	Natural_ Frac_ Compaction	3 and 4 (discrete value)

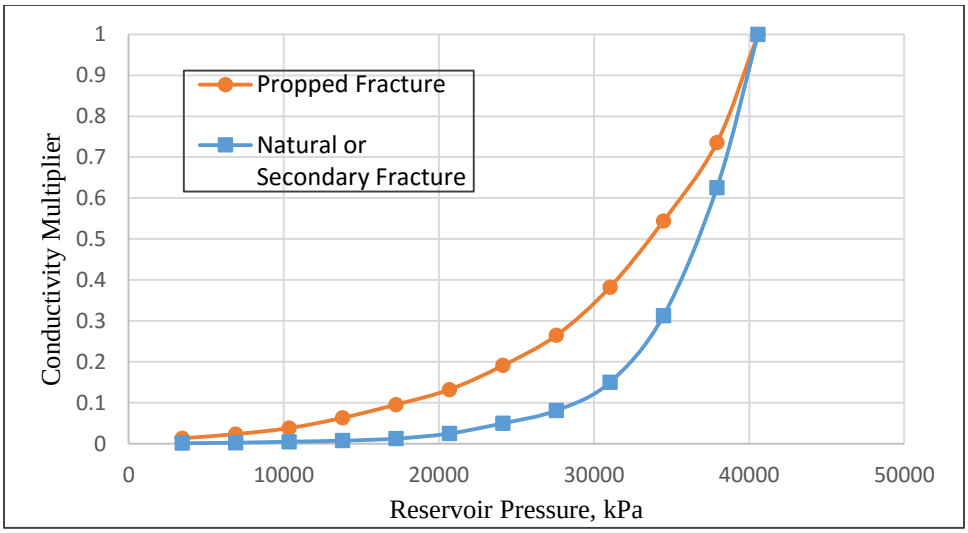

Figure 2-10: Conductivity multiplier of medium case for sensitivity analysis

A sensitivity analysis in the CMOST simulator includes two methods. One is One Parameter at a Time (OPAAT), which means each parameter is analyzed independently while the remaining parameters are set to their default value. The other method is Response Surface Methodology (RSM) that is to adjust multiple parameters simultaneously and fit a response surface (polynomial equation) to the results. The CMOST guide (2013) pointed out that although OPAAT is simple to use and its results are not complicated by effects of other parameters, the results of OPAAT can change dramatically if reference values change. Furthermore, the RSM method can analyze the interact effect of parameters on the objective functions. Hence, the RSM method is used in this sensitivity analysis. A two-level fractional factorial experimental design is chosen to create the combination of parameters values. The sensitivity analysis results are shown in a tornado plot in Figure 2-11. The tornado plot of quadratic effect estimates shows a positive or negative change in the cumulative gas as the change of each parameter occurs from the minimum value to maximum value. The statistically insignificant terms have been removed in the tornado plots.

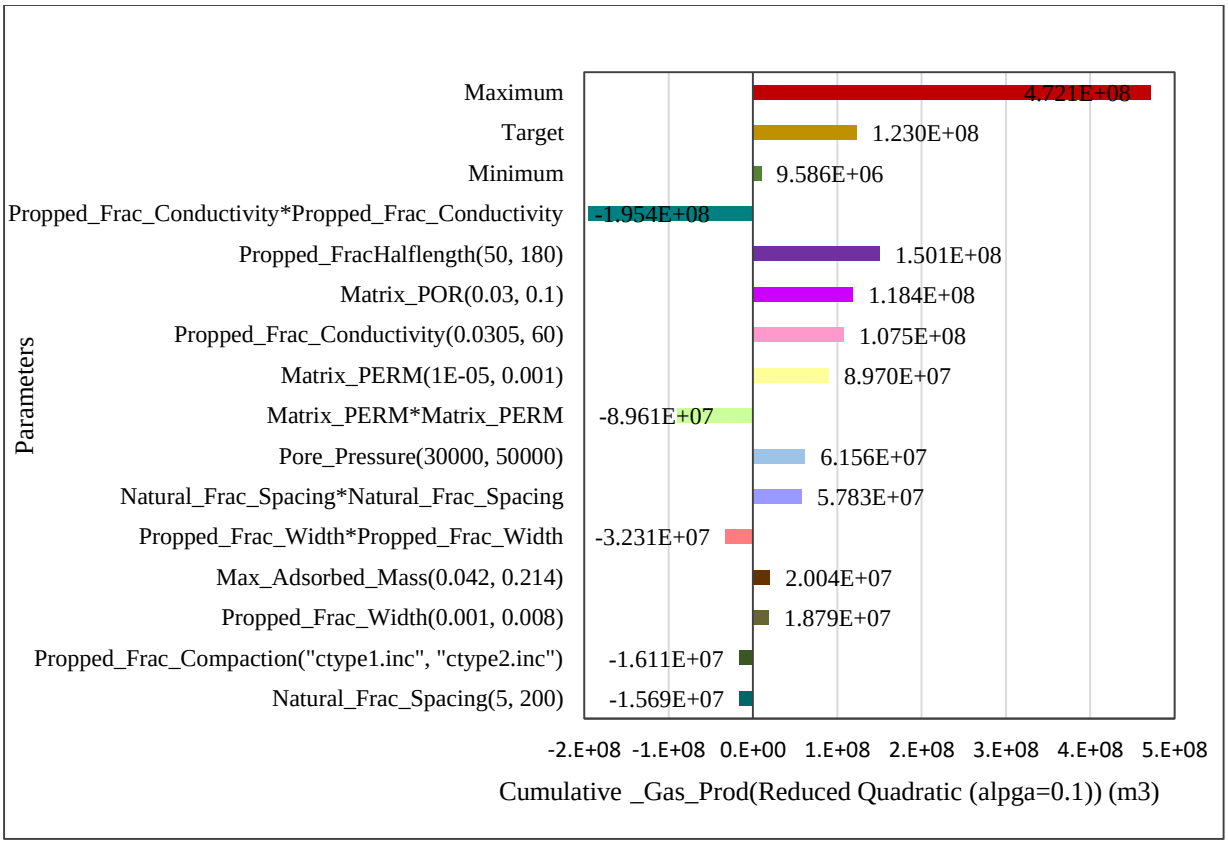

Figure 2-11: Tornado plot of quadratic effect estimates for cumulative gas production

The maximum bar and minimum bar in the tornado plot 2-11 represent the maximum and minimum cumulative gas produced of all simulation runs, respectively. The target is the value of the cumulative gas produced in the production history in Figure 2-2. The target value is between the maximum and minimum values, which indicates that it is possible to match the production history using the given set of parameters and the defined ranges. Taking the propped fracture half-length as an example, the cumulative gas produced increases 1.501E+08 m^3 when the half-length value changes from 50m to 180m. The longer bar a parameter has in the tornado plot, the more important the parameter is to the cumulative gas production. In terms of the main effect of parameters, the propped fracture half-length has the most significant effect on cumulative gas production, next is the matrix porosity, and the propped fracture conductivity and matrix

permeability come after. These results demonstrate that the post-productivity is governed by the two propped fracture properties: half-length and conductivity, as well as the two inherent reservoir properties matrix permeability and porosity which are uncontrollable by the hydraulic fracturing treatment. Thus, it can be concluded that the propped fracture conductivity occupies a very important position in a hydraulic fracturing treatment.

2.3 History Match

When building a simulation model, there are some uncertainty in the reservoir parameters such as matrix permeability, porosity, and pore pressure. History matching can help us to match this simulation model to the field data, reduce the error between the simulation results and field behavior, and, consequently, have more confidence to forecast the production of a reservoir.

It is hard to match cumulative gas history and a gas rate simultaneously because the flowing bottom-hole pressure history data is not available. Hence this study only tries to match the field gas rate since the gas rate reflects the reservoir flow behavior better. Also the study matches the cumulative water in order to determine the water saturation. The designed evolution and controlled exploration (DECE) method by CMG is used to execute the automatic history matching. From the result observers of the sensitivity analysis in Figure 2-12, it is noticeable that all the experiments (general solution) cover the field history which means the range of parameters is appropriate, and a combination of parameter values can be found to match the gas rate and cumulative water. By adjusting some sensitive parameters based on the tornado plots, the history matching of the gas rate and cumulative water is shown in Figure 2-13. The matched reservoir parameters are listed in Table 2-3, and other reservoir parameters are the same as in the preliminary reservoir model.

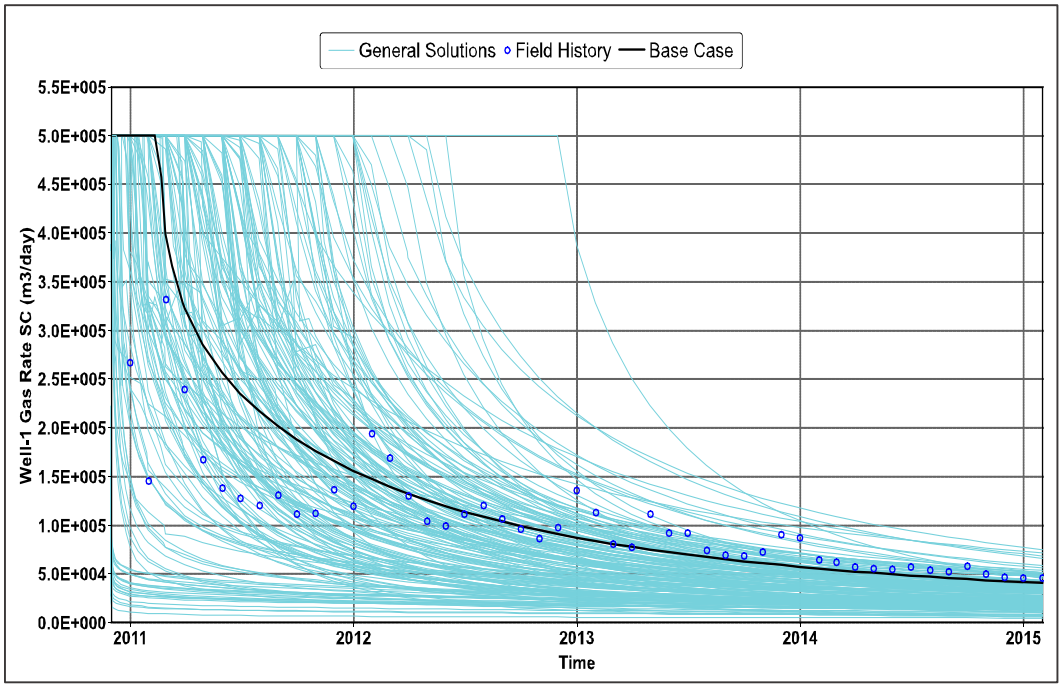

Figure 2-12: Sensitivity analysis result observation

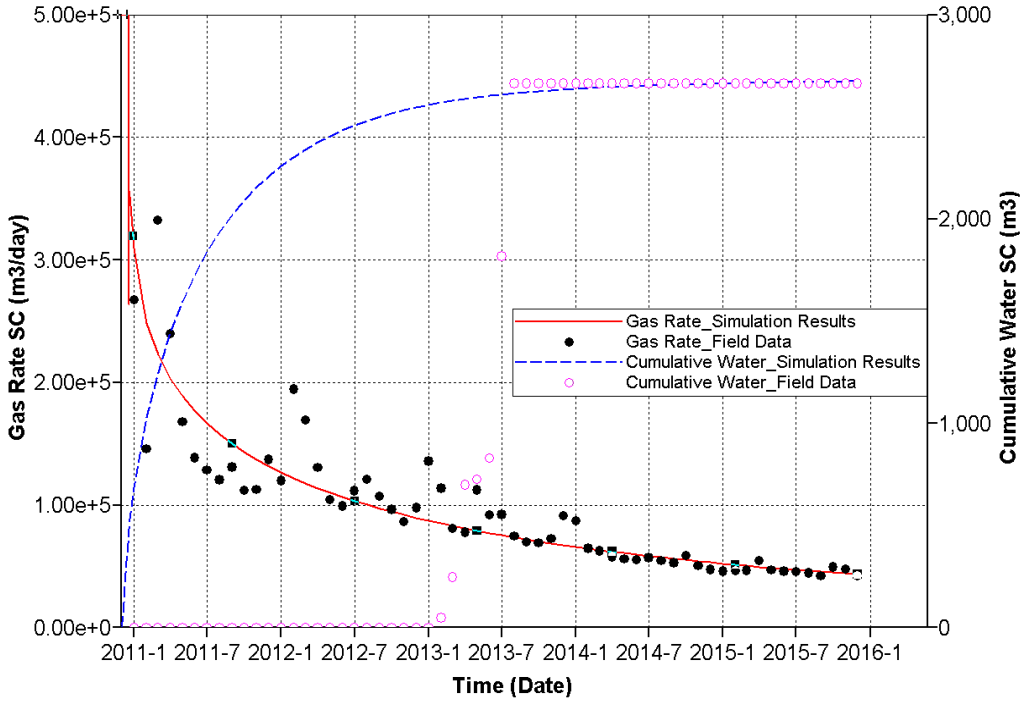

Figure 2-13: History match of gas Rate and cumulative water

Table 2-3: Matched reservoir parameters

Parameters	Value
Matrix Porosity	0.06
Matrix Permeability	0.00002 md
Fracture Half-length	165 m
Hydraulic Fracture Conductivity	4.8 md-m
Hydraulic Fracture Width	0.00206 m
Maximum Adsorbed Gas	0.2
Pore Pressure Gradient	12.5 kPa/m
Closure Pressure Gradient	14.5 kPa/m
Initial Pore Pressure	30188 kPa
Natural Fracture spacing	15 m
Natural Fracture Conductivity	0.003 md-m
Initial Water Saturation	0.15

2.4 Optimum Fracture Conductivity Forecast

The matched reservoir model can be used as a base case to forecast the optimum fracture conductivity. The prediction of optimum fracture conductivity focuses on shale and tight gas reservoirs in Western Canadian Sedimentary Basin (WCSB) with matrix permeability on four orders of magnitude from 0.00001 md to 0.01 md due to the permeability range of shale and tight reservoirs shown in Figure 2-14. It is noticeable from Figure 2-14 that the permeability range between 0.00001 to 0.0001md represents shale reservoirs, and the permeability of 0.001 to 0.01md means tight reservoirs. The simulator still uses GEM (2014). A series of reservoir simulations are conducted to find a relationship between the propped fracture conductivity and cumulative gas production of the well. With an increase in the propped fracture conductivity, the cumulative gas production increases as well. However, the cumulative gas production will become insensitive to

a further increase in fracture conductivity when the conductivity reaches a certain value. The certain value is the optimum fracture conductivity we are looking for. It is well known that the hydraulic fracture geometry is actually very complex instead of bi-wing planar fractures, so the fracture models include the planar fractures and complex fracture geometry.

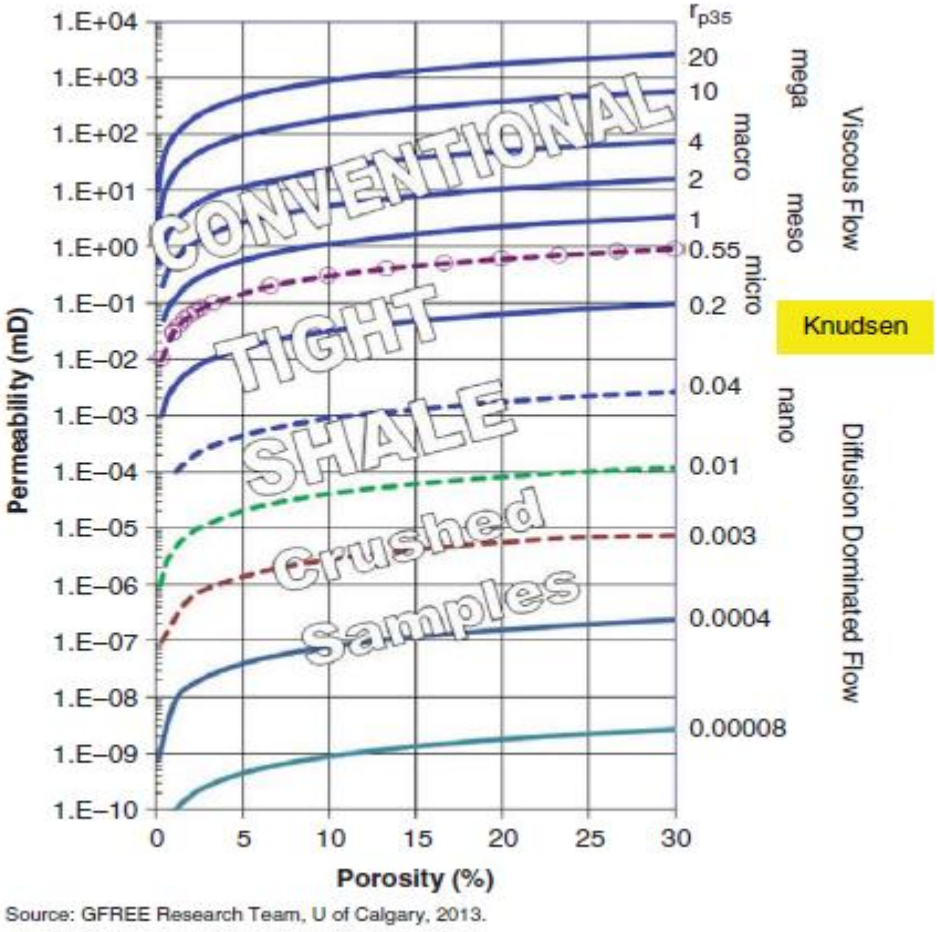

Figure 2-14: Possible range of permeability, porosity, and pore throat of conventional, shale, and tight reservoirs (Aguilera, 2013)

2.4.1 Planar Fracture Model

The planar fracture model is symmetrical and bi-wing fractures shown in Figure 2-15, and the propped fracture width is uniform along the fracture length for the simulation. Changing the

fracture conductivity is just to change the fracture intrinsic permeability. The fracture conductivity varying linearly along the fracture length is still considered through this study. In the preliminary reservoir model, the fracture tip conductivity is assumed as one tenth of the near wellbore conductivity, but it is found that one fifth works better for this history matched model. Also, the fracture conductivity changing with time is taken into account. Since the pore pressure has been changed from 40572kPa to 30188kPa, the fracture compaction table should be changed as well. The new tables will be given in the geo-mechanical effect section.

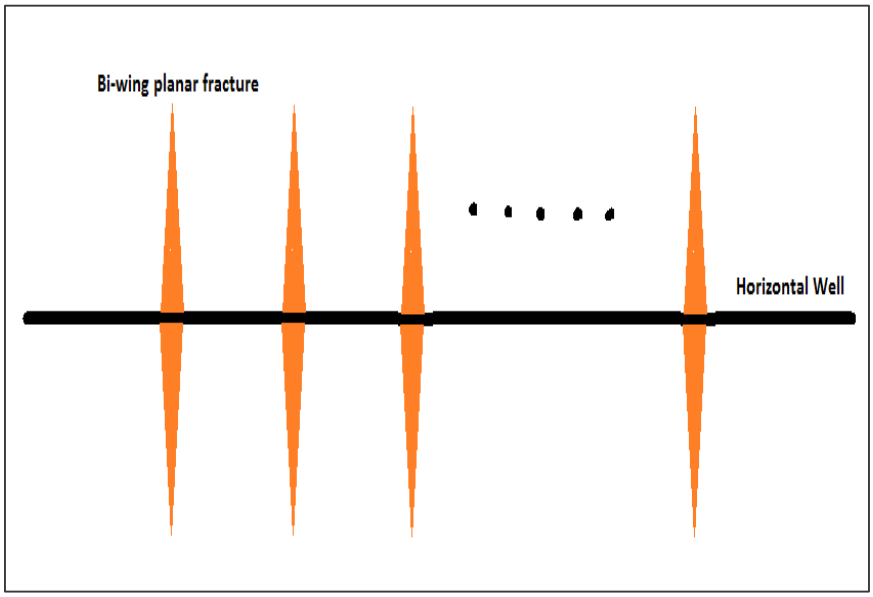

Figure 2-15: Symmetrical bi-wing planar fracture

(1) First, a number of simulations are run to find the effect of the propped fracture half-length on the optimum fracture conductivity with the constant following bottom hole pressure 3448kPa. The fracture half-length is varied from 50m to 175m, and the other reservoir parameters are the same as in the base case. The model does not have any natural fracture so that only the effect of a parameter at a time can be evaluated. The propped fracture conductivity is changed

from 0.1md-m to 1000md-m representing finite to infinite fracture conductivity, and the production time is evaluated at 1, 5, 10, and 20 years. The four production times can cover the requirement of fracture conductivity from reservoir transient flow to steady flow. Figure 2-16 depicts the relationship between the cumulative gas production and propped fracture conductivity with different fracture half-length and production time. The cumulative gas production increases with the propped fracture conductivity until it reaches an asymptotic value at a conductivity threshold. So further increase in conductivity after the threshold is not economical for a given fracture length. The start point of the asymptote in the *y*-axis is about 98% of the maximum production of each length. All cumulative gas production are normalized to the maximum production of the same length, and the normalized cumulative production are drawn against fracture conductivity in Figure 2-17. Then a cut-off line at 98% of maximum production is applied to get the quantitative value of optimum fracture conductivity for each fracture length.

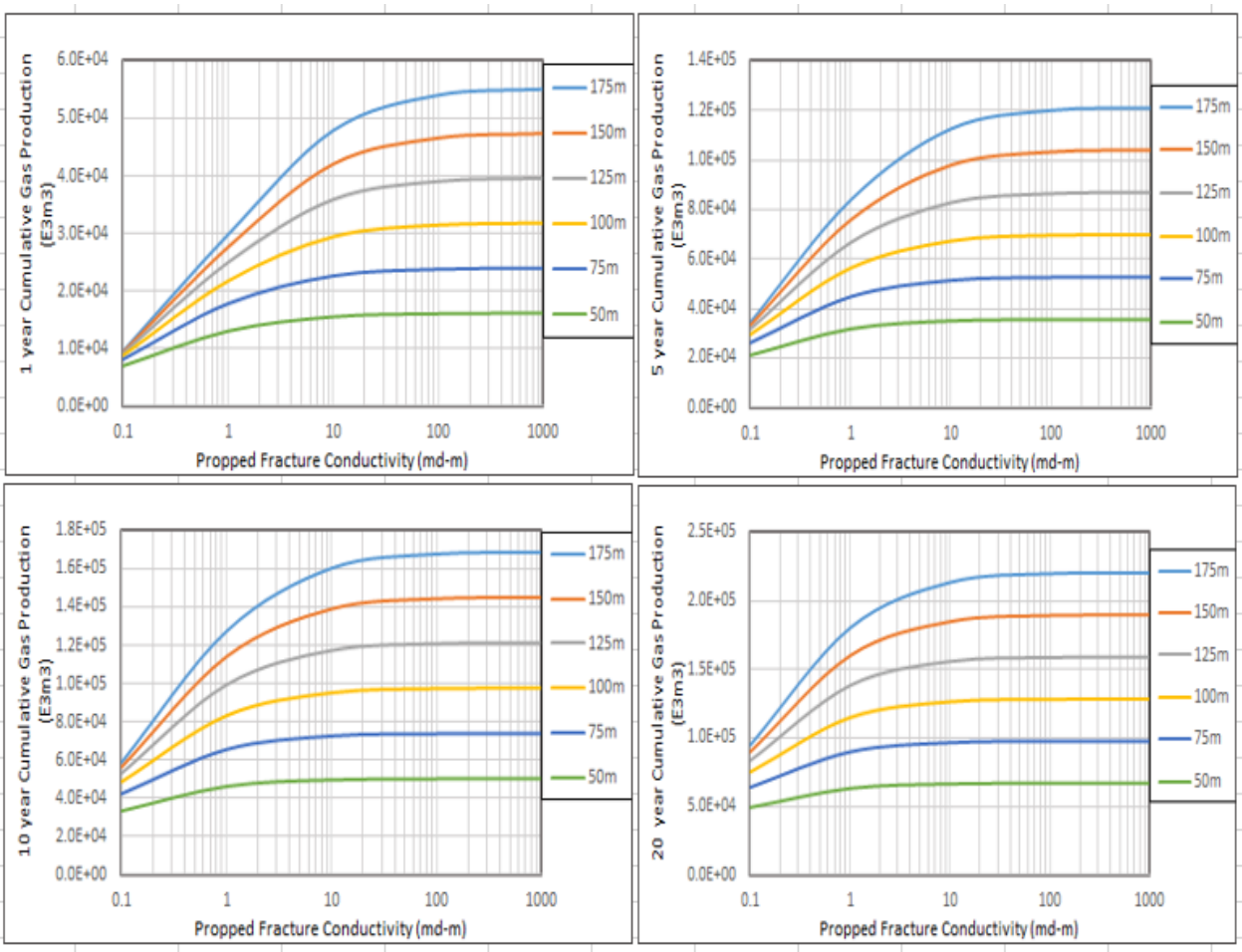

Figure 2-16: Cumulative gas production vs. propped fracture conductivity with different fracture length and production time

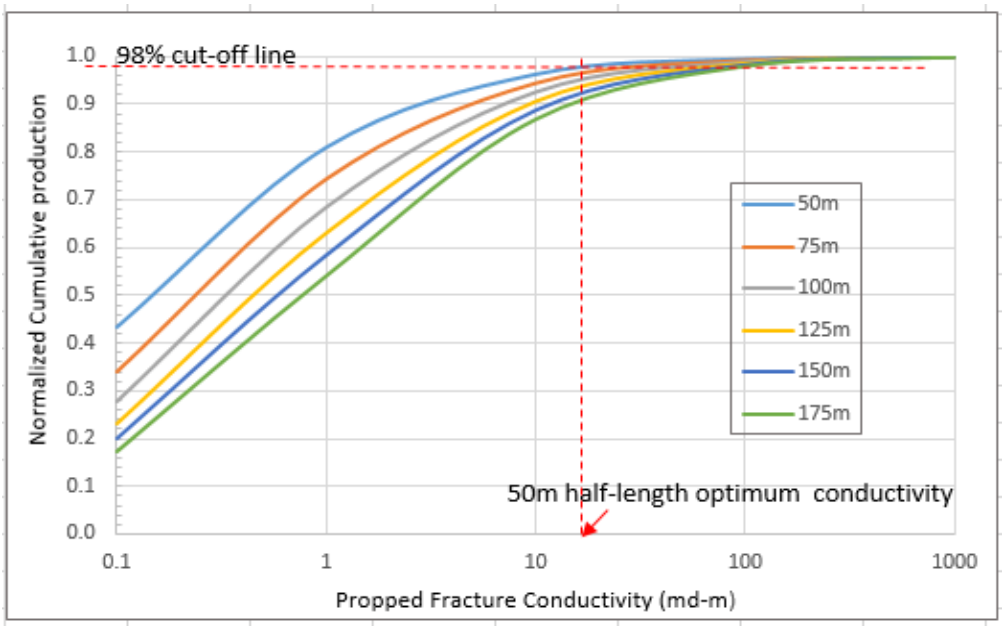

Figure 2-17: Normalized cumulative production vs. fracture conductivity

(2) Second, it is well known that the matrix permeability plays a critical role in shale or tight gas production. In this section, the matrix permeability is varied from 0.00002md to 0.01md in order to see the effect of matrix permeability on the optimum fracture conductivity. The permeability range of 0.00002md and 0.0001md represents typical shale gas reservoirs, and the mid-range permeability of 0.001md and 0.01md represents tight gas reservoirs (Figure 2-14). Only one trend can be observed from Figure 2-17 in that the optimum fracture conductivity increases with fracture half-length; therefore, it is unnecessary to refine the fracture half-length range. From now on the simulations to see the effects of other factors only consider the half-length 50, 100 and 150m for simplification.

(3) The third factor to consider is the geomechanics effect on the optimum fracture conductivity. As mentioned earlier, the hydraulic fracture conductivity is pressure dependent, and will decrease with the pore pressure dropping in fractures. One of the mechanisms causing the hydraulic fracture conductivity impairment is the embedment of proppants into rock. Alramahi

and Sundberg (2012) demonstrated using a correlation between proppant embedment and Young's modulus (Figure 2-18) that proppant embedment is largely controlled by Young's modulus. It is noticeable from Figure 2-18 that the bigger proppant embedment the lower Young's modulus, which means stiff rock has less conductivity loss than soft rock. This geomechanics difference of rock must impact the reservoir production, and also impact the optimum fracture conductivity to reach the corresponding near–maximum production. In this section, three scenarios are considered, including stiff shale with Young's modulus greater than 6×10^6psi, the medium case with Young's modulus in the range of 2×10^6- 5×10^6psi, and soft shale with Young's modulus under 2×10^6psi. To realize these three scenarios, three propped fracture compaction tables at the initial reservoir pressure 30188kPa have been built by using the raw data from Figure 2-5. The base case reservoir parameters without natural fractures are still applied to this section. The three conductivity multiplier vs. reservoir pressure plots drawn based on the three sets of compaction tables are shown in Figure 2-19, which clearly illustrates the conductivity of softer rock drops dramatically with reservoir pressure decreasing.

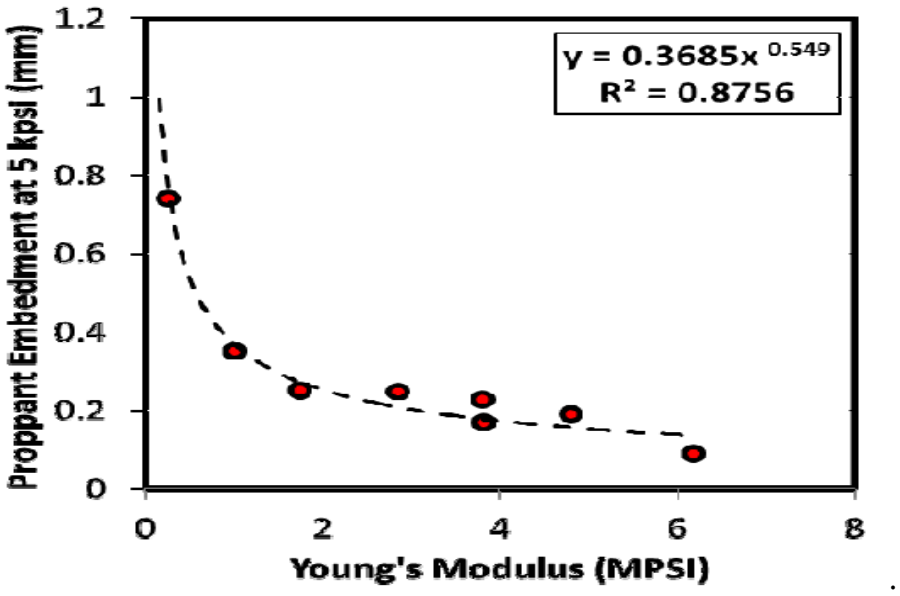

Figure 2-18: Correlation between proppant embedment and Young's Modulus (Alramahi and Sundberg, 2012)

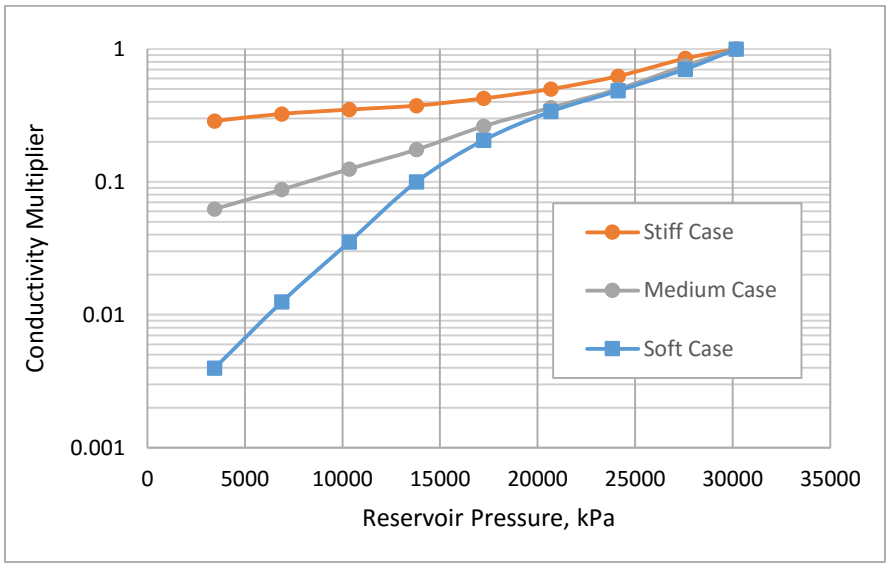

Figure 2-19: Propped fracture conductivity multiplier for three cases

(4) Aguilera (2010) pointed out that a tight gas reservoir should be represented at least by dual porosity models: matrix porosity and micro-fracture porosity. A shale gas reservoir should be

represented by at least a quadruple porosity models: matrix porosity, organic porosity, micro-fracture porosity, and hydraulic fracture porosity. This means that the existence of natural fractures in tight and shale gas reservoirs is very common. The effect of natural fractures on the optimum fracture conductivity is an important aspect to be considered. To model the natural fractures, the natural fracture inputs in the simulator are fracture porosity, fracture permeability and fracture spacing. It is known that the fracture porosity and fracture permeability are both a function of fracture width and fracture spacing. Since the fracture numbers are the same in the *I* and *J* directions and there is no fracture in the *K* direction, the fracture porosity can be calculated by the formula below (CMG GEM, 2013):

$$fracture\ porosity = \frac{volume\ of\ natural\ fractures\ in\ a\ grid}{volume\ of\ a\ grid} \quad (2\text{-}4)$$

where:

$$Volume\ of\ natural\ fractures\ in\ a\ grid\ = 2 \times\ fracture\ number\ \times$$
$$fracture\ width\ \times grid\ length\ in\ the\ I\ or\ J\ direction \times grid\ thickness \quad (2\text{-}5)$$

$$fracture\ permeability\ in\ the\ I\ or\ J\ direction = \frac{fracture\ conductivity}{fracture\ spacing} \quad (2\text{-}6)$$

$$fracture\ permeability\ in\ K\ direction = fracture\ permeability\ in\ I\ direction +$$
$$fracture\ permeability\ in\ J\ direction \quad (2\text{-}7)$$

The natural fracture width, spacing, and conductivity are not like those of hydraulic fractures, and they are beyond the engineer's control so it is hard to model natural fractures exactly. Based on the experiments to measure the natural fracture conductivity by Zhang et al. (2014) and un-propped fracture conductivity stated by Cipolla et al. (2009), the fracture conductivity is chosen to vary from 0.00003md-m to 3md-m in order to see the influence of natural fracture conductivity on the optimum fracture conductivity. The corresponding fracture width is calculated by using a cubic law (Witherspoon et al., 1980):

$$\frac{Q}{\Delta h} = \left(\frac{W}{L}\right)\left(\frac{\rho g}{12\mu}\right)e^3 \qquad (2\text{-}8)$$

where, Q is the flow rate, Δh is the hydraulic head gradient, W is the width of a fracture face, L is the fracture length, ρ and g are the fluid density and acceleration of gravity, respectively, μ is the fluid viscosity, and e is the fracture aperture. Combining Darcy's flow $Q = \frac{kA\Delta p}{\mu L}$ and equation 2-8, the relationship of fracture intrinsic permeability and fracture aperture can be got as below:

$$k = e^2/12 \qquad (2\text{-}9)$$

When the fracture conductivity is in the range of 0.0003-3md-m, the corresponding fracture aperture can be calculated as 0.71μm-33μm (see appendix A). This cubic law does not consider the fracture face roughness (Konzuk and Kueper, 2002) so it is just a rough estimation for the fracture aperture. Also, the fracture spacing is changed from 5m to 100m to examine its effect on the optimum fracture conductivity. The natural fracture compaction table is built as well by using the raw data from Figure 2-6 with the stiff case due to more common existence of natural fractures in the stiff rock. The un-propped fracture conductivity multiplier vs. reservoir pressure plot is shown in Figure 2-20. The other reservoir parameters still use the base case values.

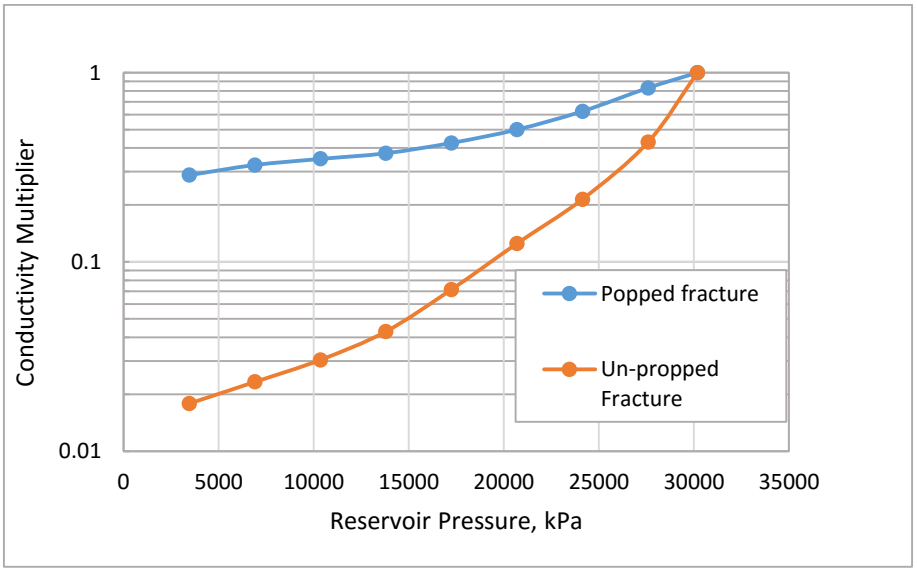

Figure 2-20: Un-propped fracture conductivity multiplier for stiff case

(5) The effect of hydraulic fracture spacing on the optimum fracture conductivity is also evaluated. The hydraulic fracture spacing is 25m in the base case. To examine the effect, the hydraulic fracture spacing is changed, respectively, to these values: 10m, 50m, and 100m.

2.4.2 Complex Fracture Model

Micro seismic mapping demonstrates that the current hydraulic fracturing technique: multiple stages with light sand and water fracking, has generated a fracture network system in shale gas reservoirs (Warpinski et al., 2008). A complex fracture model cannot be ignored to consider the optimum fracture conductivity requirement. A complex fracture network dramatically increases a surface area of fractures and stimulated volume, which significantly improves the productivity of shale gas reservoirs. It is more difficult to obtain a complex fracture network for a high viscosity fracture fluid and matrix permeability above 0.001md due to the difficulty of the high viscosity fluid penetrating into natural fractures or fissures and the excessive fluid loss in the higher permeability reservoirs (Beugelsdijk et al., 2000; Cipola et al., 2008; Warpinski et al., 2008; Cipola et al., 2011). The factors to control the propagation of complex hydraulic fractures are stress, mechanical properties such as Young's modulus and Poison's ratio, as well as the distribution and properties of natural fractures (Cipola et al., 2011). A small difference between the maximum and minimum horizontal stress more easily creates the fracture complexity. The brittleness of shales is also regarded as an important factor for developing a large fracture network compared to ductile shales (Warpinski et al., 2008). However, there is no way to precisely predict how a fracture network develops for any fracturing treatment with the current technology. The micro-seismic mapping can only show the occurrence of a complex fracture network and help us to understand the possible development of fracture geometry. Also, no reservoirs are equal, and the complex fracture geometries are different. The reservoir simulation of hydraulic fracture geometry needs to

be calibrated with the micro seismic mapping. Thus, in the case of modelling a complex fracture network, the fracture geometry is arbitrary due to the lack of the micro seismic mapping, but a general information can be provided about the different fracture conductivity requirement between the planar fracture and complex fracture models.

To evaluate the effect of complex fracture geometry on the optimum fracture conductivity, the base case reservoir parameters are still applied. Moreover, a couple of scenarios are considered. First, the matrix permeability is changed from 2e-5md up to 0.001md to see its impact with a complex fracture network since it is unlikely to have the complex fracture network with the matrix permeability above 0.001md. Next, the effect of pre-existing natural fractures is also taken into account. The natural fracture spacing and conductivity are the base case values: 15m and 0.01md-ft, respectively. The natural fractures are reactivated as the secondary fractures, which have higher conductivity than natural fractures and lower conductivity than hydraulic fractures. In this case, the width of the secondary fractures is assumed as 0.0005m, and the secondary fracture permeability is one fifth of the hydraulic fracture permeability. The hydraulic fracture conductivity is varied from 0.1md-m to 10md-m to find the optimum fracture conductivity since the conductivity of 10md-m is almost the highest conductivity which a complex fracture network can reach in this simulation.

As mentioned earlier, the complex fracture geometry is arbitrary, but its creation in the GEM reservoir simulator is referred to a micro seismic mapping in publications, such as Figure 2-21. The effect of stress shadow on fracture geometry is considered as well. Basically the stress shadow describes the interaction among adjacent hydraulic fractures. The stress shadow means that when a hydraulic fracture is opened under a certain net pressure, it exerts an extra compressive stress on the surrounding region. If a second hydraulic fracture is created parallel to the first

existing open fracture and if it falls within the stress shadow, the second fracture will require a higher net pressure to propagate, and /or it has a narrower width because the second fracture is experiencing a higher closure stress than the original in-situ stress, which is exerted by the first open hydraulic fracture. A well-known effect of stress shadow is that the fractures in the middle region have a smaller width due to the increased compressive pressure from the neighboring fractures (Wu et al., 2012). An example of stress shadow effects was demonstrated by Wu et al. (2012) in Figure 2-22. Figure 2-22 (a) has four stages of hydraulic fractures without stress shadow effects. When taking into account the influence of stress shadow on the propagation of hydraulic fracture network, Figure2-22 (b) shows that stage 1 (red color) is the same as in Figure 2-22 (a), stage 2 (green color) and stage 3 (purple) cannot propagate too far and are narrower compared to stages 1 and 4 (blue) due to stress shadow, and stage 4 moves away from stage 3 towards the heel section where there is no stress shadow. After referring to the micro seismic mapping and stress shadow, the plane view of the complex fracture network in this simulator is shown in Figure 2-23. Also, Figure 2-24 is a 3D view of the fracture network.

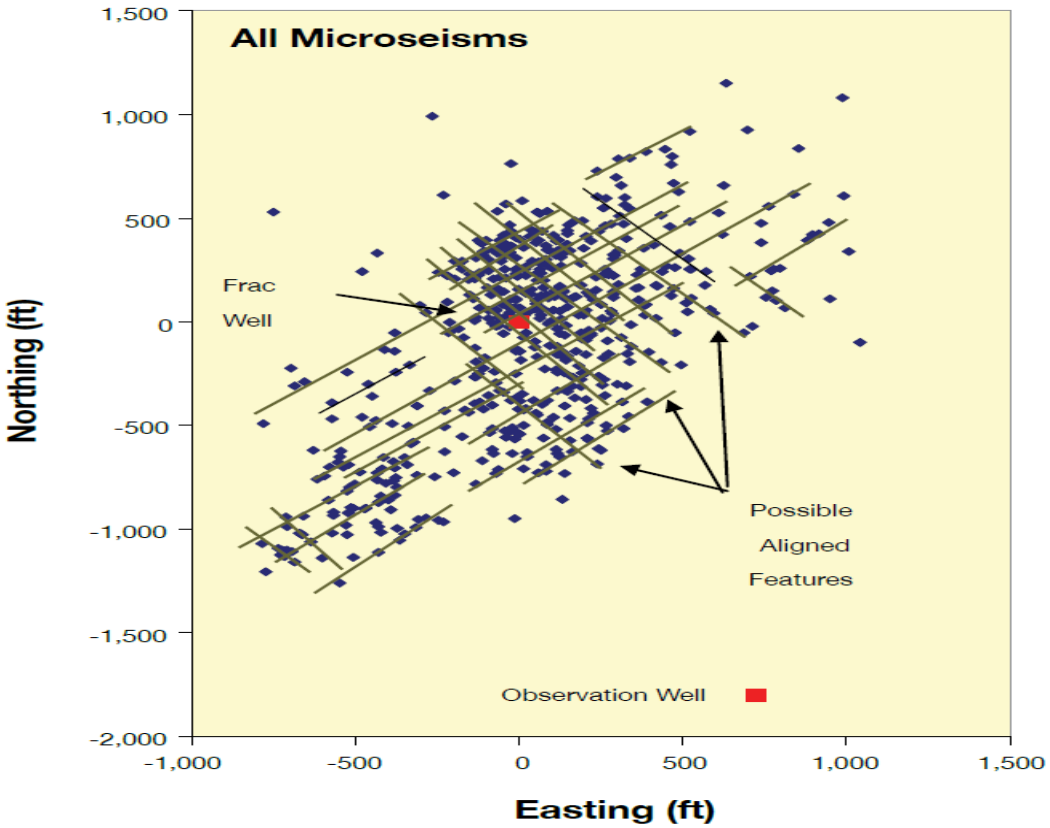

Figure 2-21: An example of micro-seismic mapping for a complex fracture network (Warpinski et al., 2008)

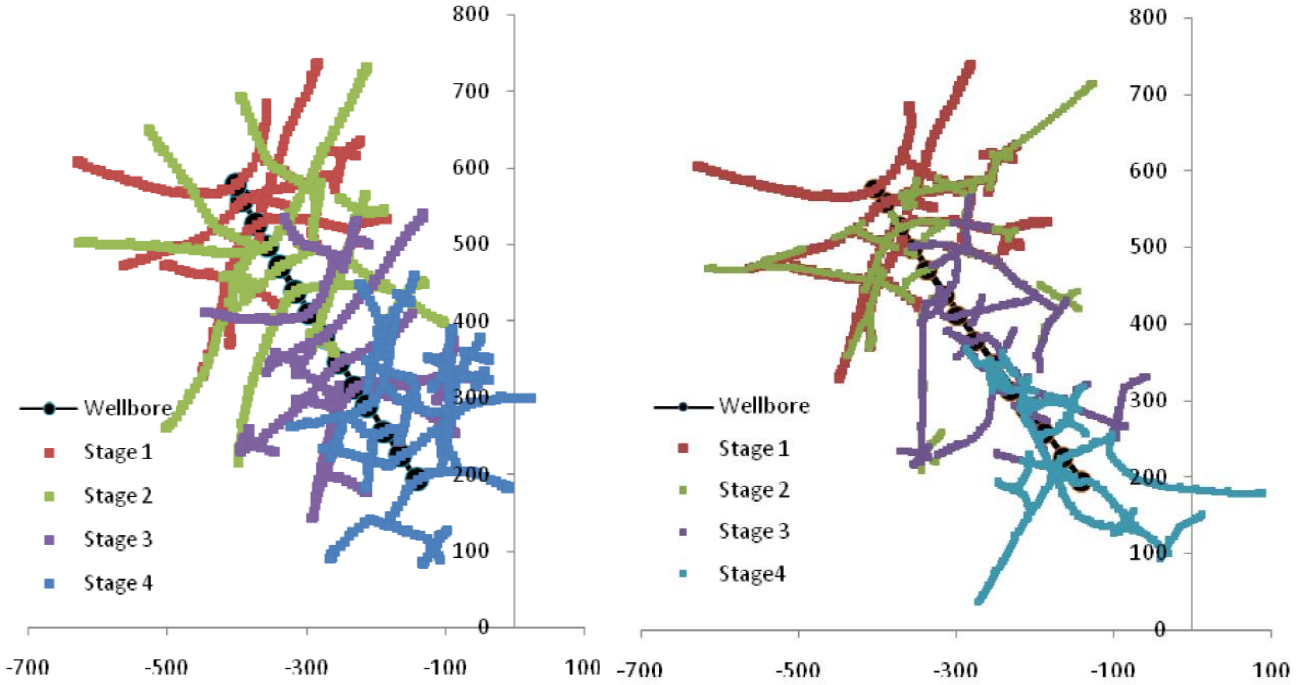

(a) Hydraulic fracture without stress shadow (b) Hydraulic fracture with stress shadow

Figure 2-22: Propagation of hydraulic fracture network without and with stress shadow (Wu et al., 2012)

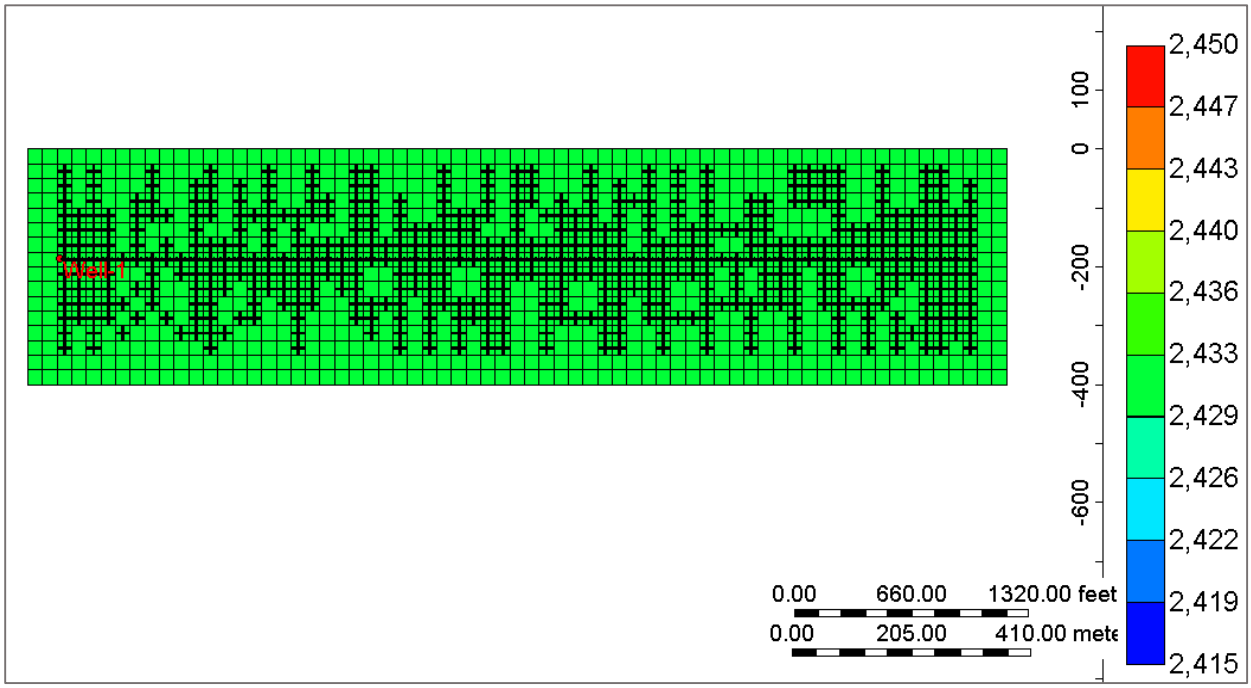

Figure 2-23: Plane view of a complex fracture network

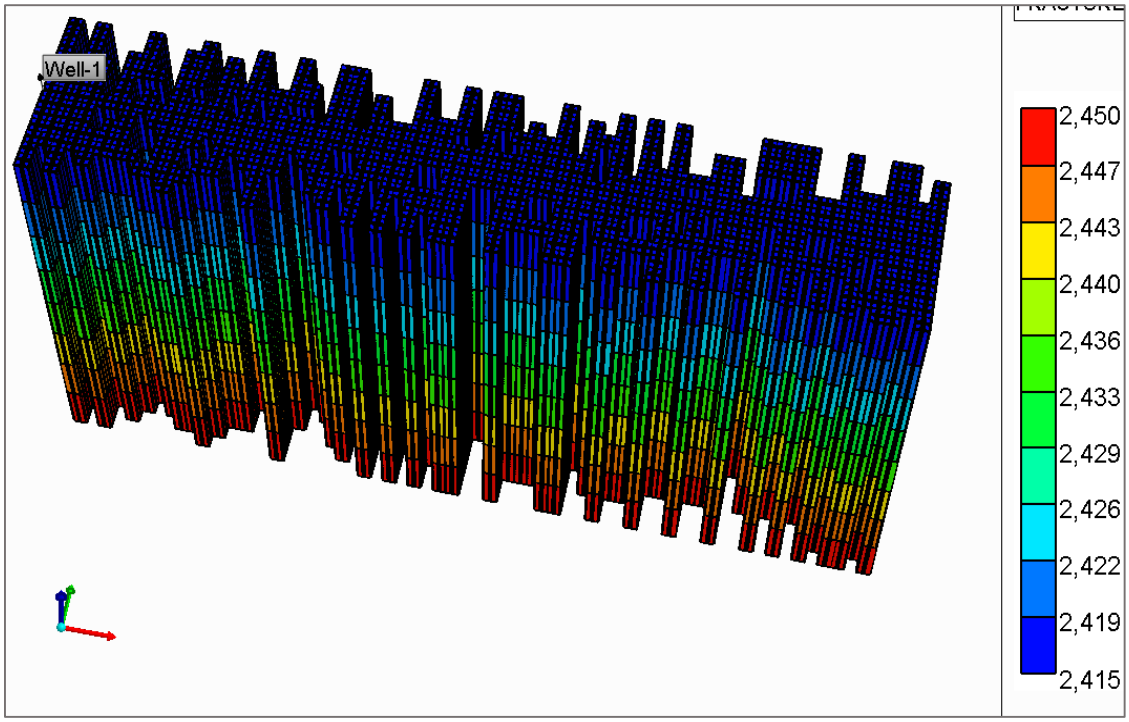

Figure 2-24: 3D view of a complex fracture network

Chapter 3 : Results and Discussion

In this chapter, the results of optimum fracture conductivity for two fracture geometry models are presented, and the optimum fracture conductivity under different scenarios are compared.

3.1 Effects of Hydraulic Fracture Length

Using a 98% cut-off line to normalized cumulative gas production for different hydraulic fracture length (Figure 2-17), the optimum fracture conductivity of short-term and long- term can be obtained in Figure 3-1. It can be observed that the optimum fracture conductivity increases with hydraulic fracture length at each production time. The short-term production (1 year) requires the highest fracture conductivity to get the near-maximum production at the same fracture propped length. The optimum fracture conductivity decreases with an increase in production time. The reason for an optimum fracture conductivity increase with fracture length is that longer hydraulic fractures penetrated deeper in the reservoir, which leads to more production compared to shorter hydraulic fractures and needs higher flow capacity of fractures to deliver more fluid to the wellbore. The conclusion of higher optimum fracture conductivity for the first year production is consistent with the high way theory of Economides et al. (2000) which likened the hydraulic fractures to a high way. There is more traffic during a peak hour (transient period) than a steady–flow traffic condition for a high way. Thus, for the transient flow period, i.e., the first year production, hydraulic fractures need to have high fracture conductivity to carry the high inflow of gas. The transient flow changes to steady- flow as a result of reservoir production, and the optimum fracture conductivity reduces due to the less and less inflow of gas.

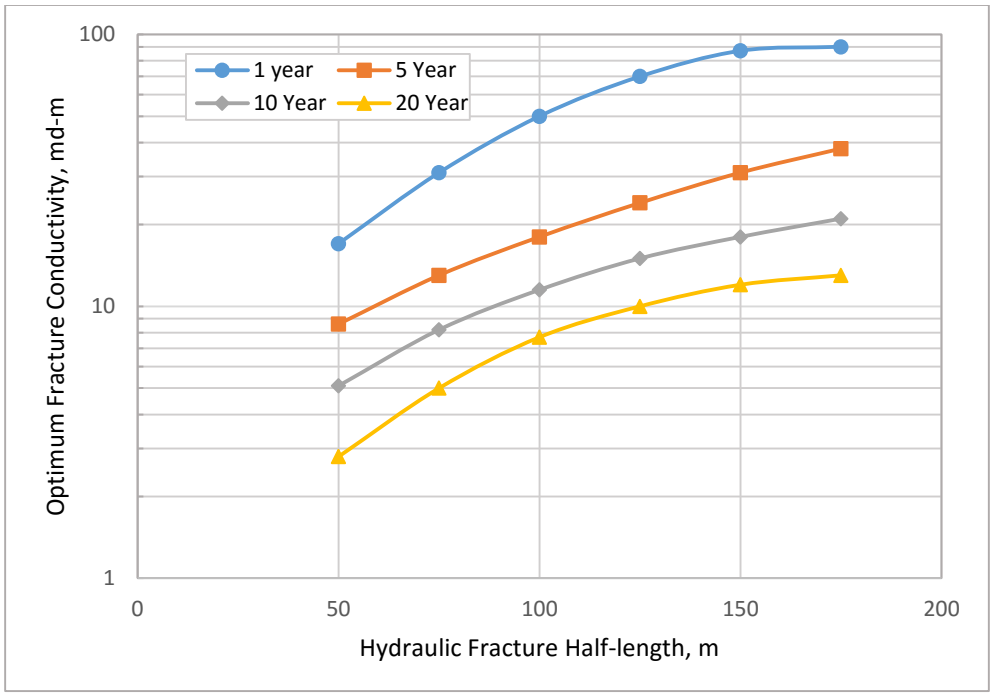

Figure 3-1: Optimum fracture conductivity vs hydraulic fracture half-length

Figure 3-2 compares the first year optimum fracture conductivity from this study with that from Gu et al. (2014). Their results are based on a shale gas reservoir with matrix permeability 2e-5 md and without natural fractures, which is the same as the case in this section. The main trends of the two curves in Figure 3-2 are similar, but it can be observed that the optimum fracture conductivity obtained from this study is about 5 times higher than that from Gu et al. (2014) at the same fracture length. There are two reasons for that. One is that the production from this reservoir is far more than the production in a reservoir from Gu et al. (2014) so higher inflow of gas needs higher fracture conductivity. The other reason is that they only considered constant propped fracture conductivity with time and along the hydraulic fractures. Because the propped fracture conductivity reduces with reservoir depletion and it also decreases from the near-wellbore to a fracture tip, these conditions require higher initial fracture conductivity to make up for the conductivity loss in order to carry the high inflow of gas.

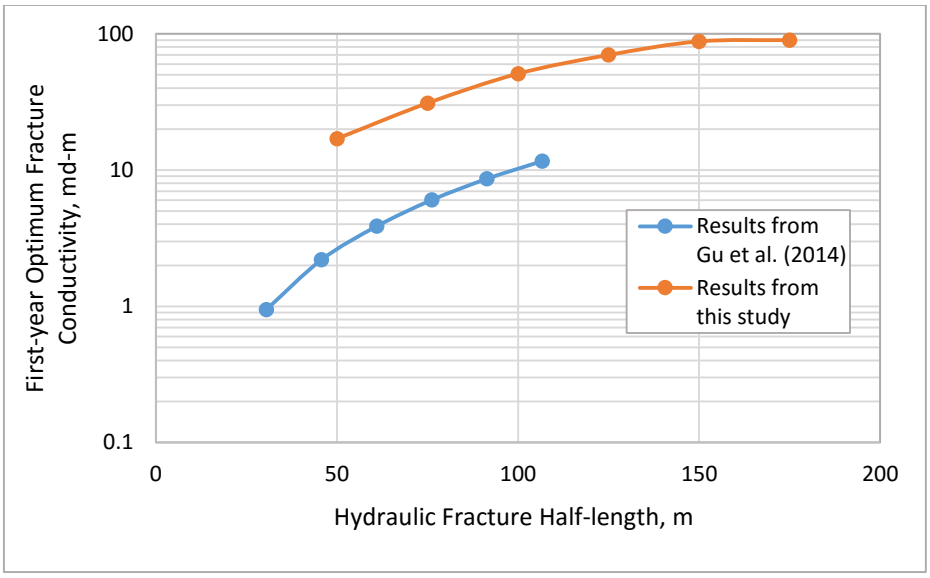

Figure 3-2: Comparison of first year optimum fracture conductivity from this study and Gu et al. (2014)

The dimensionless fracture conductivity (F_{CD}) of 30 for a constant fracture length is usually regarded as an optimum value for conventional tight reservoirs. Warpinski et al. (2008) pointed out that this approach may not apply to horizontal wells because it does not consider the intersection between a wellbore and fractures and the associated flow convergence. F_{CD} = 30 could be used in this case to see if it is valid here. Taking a fracture half-length 100m as an example, the required fracture conductivity is calculated as 0.06md-m based on equation (1-1). The first year production is less than 28% of the maximum achievable production at the propped fracture conductivity of 0.06md-m according to Figure 2-17. The 5-year, 10-year, and 20-year production is less than 42%, 50%, and 58% of the maximum achievable production, respectively. Table 3-1 lists the optimum fracture conductivity for four production times at different fracture length and the optimum fracture conductivity obtained from F_{CD} = 30. These results illustrate the limitation

of applying the conventional dimensionless fracture conductivity theory to a shale gas reservoir with horizontal wells.

Table 3-1: Comparison of optimum fracture conductivity

Fracture Half-length(m)	Optimum Fracture Conductivity from the Study (md-m)				Optimum Fracture Conductivity from F_{CD} =30 (md-m)
	1 -year	5-year	10 -year	20-year	
50	17	8.6	5.1	2.7	0.03
75	31	13	8.2	5	0.05
100	51	18	11.5	7.7	0.06
125	70	24	15	10	0.08
150	88	31	18	12	0.09
175	90	38	21	13	0.11

3.2 Effects of Matrix Permeability on Optimum Fracture conductivity

Figure 3-3 is the plots of optimum fracture conductivity vs. matrix permeability at propped half-length 50m. It is obvious that the optimum fracture conductivity goes up with the matrix permeability and the first-year production requires the highest fracture conductivity to carry flow. This demonstrates that there is larger inflow of gas from the reservoir into hydraulic fractures with a higher matrix permeability reservoir, which needs higher flow capacity of fractures, and the first year has the peak flow; therefore, the highest optimum fracture conductivity is required.

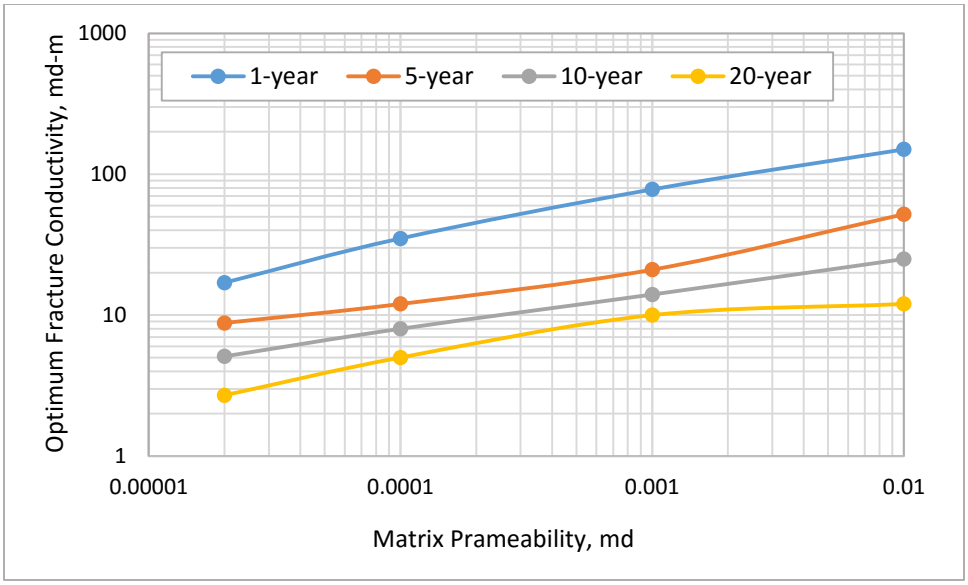

Figure 3-3: Optimum fracture conductivity vs. matrix permeability (xf =50m)

Figure 3-4 is the optimum fracture conductivity for popped half-length 100m. It can be observed that the trend of the plot with 100m at a production time of 20 years is somewhat different from that of the plot with 50m. When it is 20 years, the optimum fracture conductivity increases with matrix permeability up to *k*=1E-3md, and it starts to reduce until 1E-2md. Why the 20-year optimum fracture conductivity has a different trend can be explained from Figure 3-5, which shows the pressure decline of a grid vs. production time for three fracture lengths with fracture conductivity 100md-m and *k* =0.01md, and 20-year normalized cumulative production vs. hydraulic fracture conductivity at xf=100m. The plots show that the 20-year production can achieve nearly 60% of the maximum production even with low flow capacity of fractures (0.1md-m) because the reservoir with 1E-2md (yellow curve) has drained fast at propped fracture half-length 100m compared to the half-length 50m. This low reservoir pressure in the later period due to fast drainage leads to a low inflow of gas, so it generates a lower fracture conductivity

requirement for the later period (20-year), but the optimum fracture conductivity requirement is still higher than that in the reservoir with permeability 2E-5md and 1E-4md.

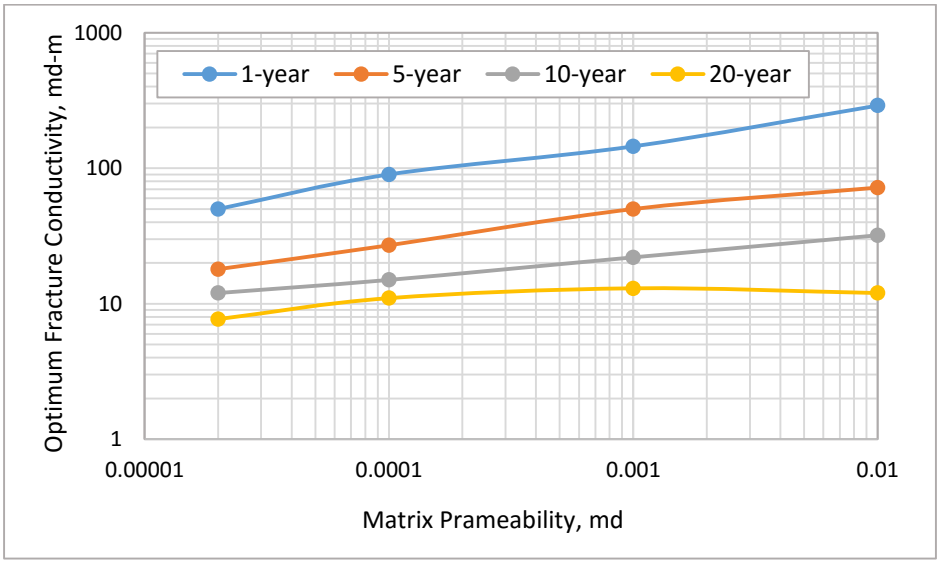

Figure 3-4: Optimum fracture conductivity vs. matrix permeability (xf =100m)

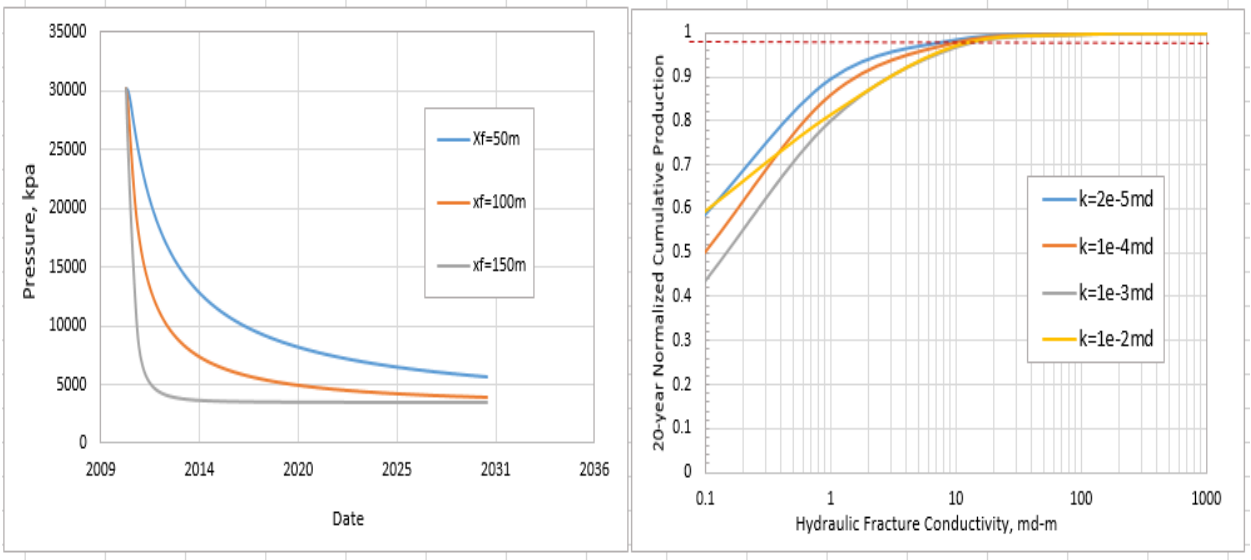

Figure 3-5: Pressure curve of a grid and normalized cumulative production vs. hydraulic fracture conductivity (xf =100m)

Figure 3-6 contains the simulation results for fracture half-length 150m. The trend of the first–year optimum fracture conductivity vs. matrix permeability is the same as that of the plots with 50m and 100m. The optimum fracture conductivity of 5-year and 10-year start decreasing from *k*= 0.001md, whereas that of 20-year starts decreasing from k= 0.0001md. The reduction of optimum fracture conductivity happens 15 years earlier than that at fracture half-length 100m. This is because the reservoir with higher permeability and 150m of fracture half-length has faster drainage than that with fracture half-length 100m. It lowers the fracture conductivity requirement after 5-year production due to the less and less inflow of gas. The fast drainage even makes the optimum fracture conductivity of 20-year to start decreasing from *k*=0.0001md. Figure 3-7 is a comparison of optimum fracture conductivity of fracture half-length100m and 150m. The dash lines represent optimum fracture conductivity of fracture half-length150m. This comparison shows that the optimum fracture conductivity of fracture half-length 150m under higher matrix permeability may be lower than that of fracture half-length 100m at later period of the production time. Last, Table 3-2 lists the optimum fracture conductivity values at different matrix permeability.

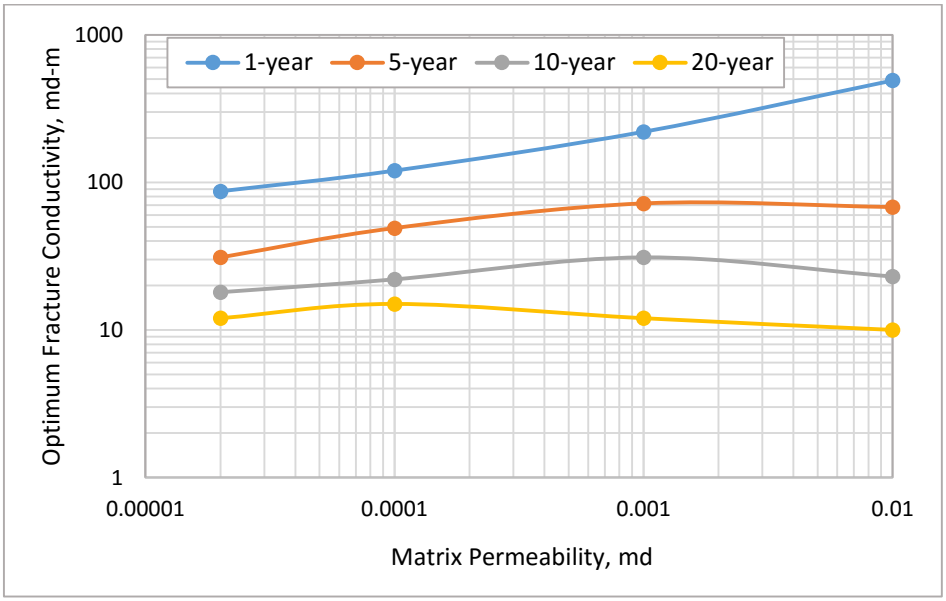

Figure 3-6: Optimum fracture conductivity vs. matrix permeability (xf =150m)

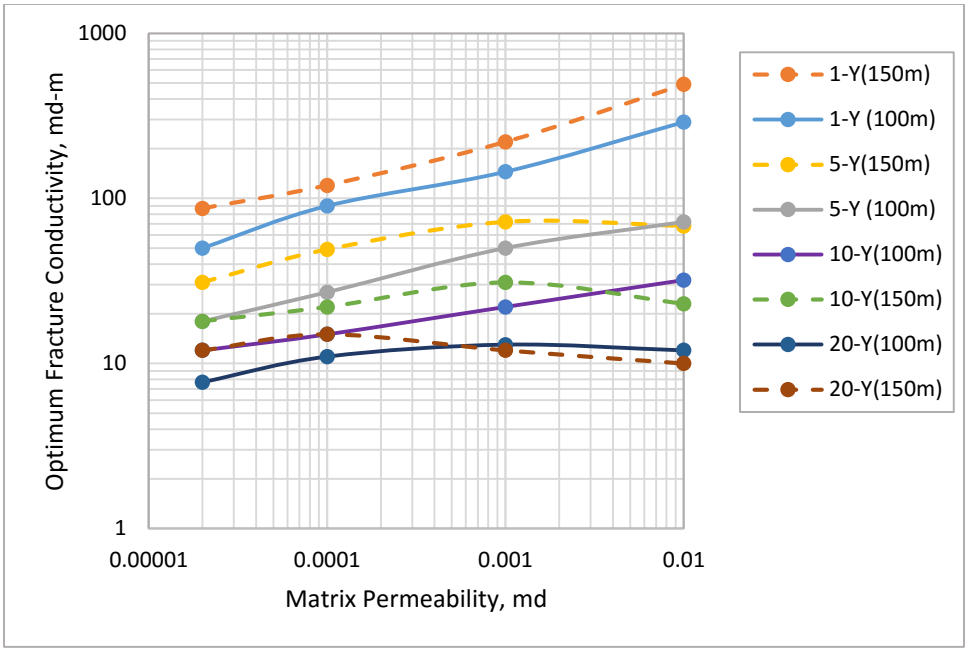

Figure 3-7: Comparison of optimum fracture conductivity between fracture length 100m and 150m

Table 3-2; Optimum fracture conductivity value at different matrix permeability

Matrix Permeability (md)	Optimum Fracture Conductivity at x_f=50m (md-m)				Optimum Fracture Conductivity at x_f=100m (md-m)				Optimum Fracture Conductivity at x_f=150m (md-m)			
	1-Y	5-Y	10-Y	20-Y	1-Y	5-Y	10-Y	20-Y	1-Y	5-Y	10-Y	20-Y
0.00002	17	8.8	5.1	2.7	50	18	11.5	7.7	87	31	18	12
0.0001	35	12	8	5	90	27	15	11	120	49	22	15
0.001	78	21	21	10	145	50	22	13	220	72	31	12
0.01	150	52	25	12	290	72	32	12	490	68	23	10

3.3 Geomechanics Effect on the Optimum Fracture Conductivity

The normalized cumulative production vs. hydraulic fracture conductivity (Figure 3-8) illustrates that the soft case needs higher fracture conductivity to achieve near-maximum production. Figure 3-9 compares the optimum fracture conductivity of three cases at different

production times with propped fracture half-length 50m, 100m and 150m, respectively. These plots have similar trends: optimum fracture conductivity reducing with production time and longer fracture length requiring higher fracture conductivity, which has been explained earlier. Also, it shows the optimum fracture conductivity of three cases in order of decreasing: soft case, medium case, and stiff case. The first-year optimum fracture conductivity for the medium and soft cases with half-length 100m and 150m is over 100md-m. It can be concluded that the softer rock the higher optimum fracture conductivity requirement. The reason is that the softer rock is more prone to proppant embedment, and therefore, the higher fracture conductivity for softer rock is required to overcome proppant embedment. Again, Table 3-3 lists the optimum fracture conductivity values for the three cases.

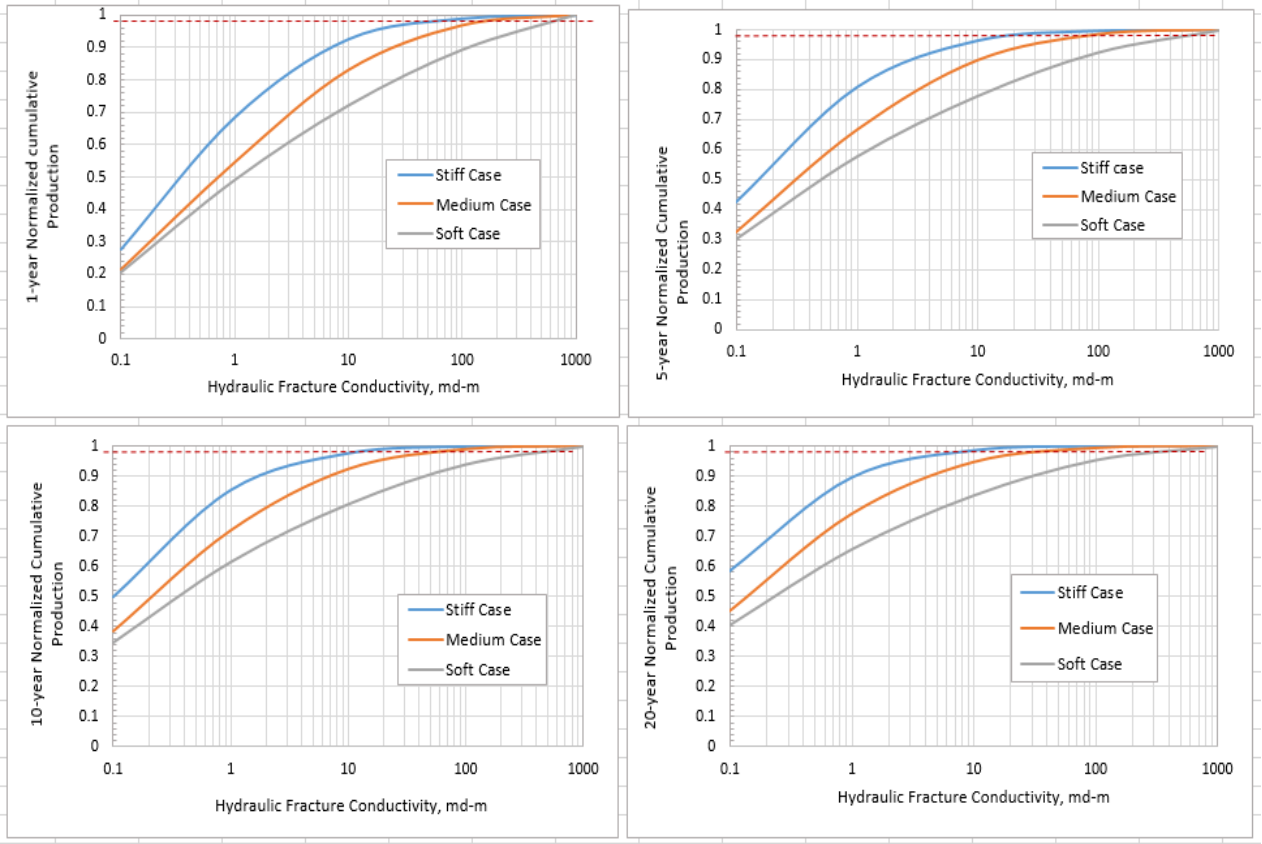

Figure 3-8: Normalized cumulative production vs. hydraulic fracture conductivity with different stiffness (xf =100m)

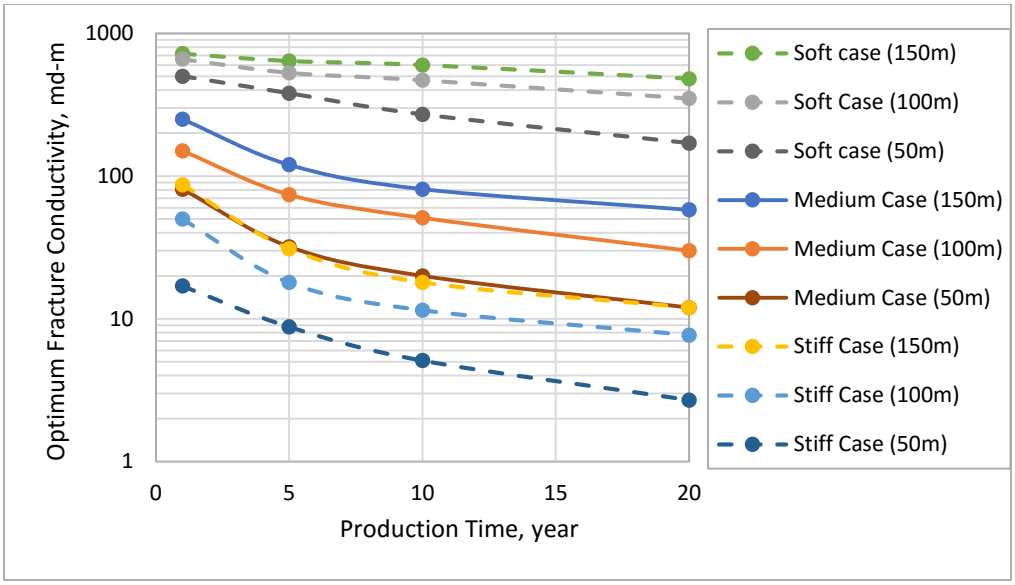

Figure 3-9: Comparison of optimum fracture conductivity for three cases

Table 3-3: Optimum fracture conductivity value for three cases

Stiffness	Optimum Fracture Conductivity at x_f=50m (md-m)				Optimum Fracture Conductivity at x_f=100m (md-m)				Optimum Fracture Conductivity at x_f=150m (md-m)			
	1-Y	5-Y	10-Y	20-Y	1-Y	5-Y	10-Y	20-Y	1-Y	5-Y	10-Y	20-Y
Stiff Case	17	8.8	5.1	2.7	51	18	11.5	7.7	88	31	18	12
Medium Case	81	32	20	12	150	74	51	30	250	120	81	58
Soft Case	500	380	270	170	660	530	470	350	720	640	600	480

3.4 Impact of Natural Fracture on Optimum Fracture Conductivity

Natural fracture spacing and conductivity are varied to see natural fractures impact on optimum fracture conductivity. When holding natural fracture spacing (NFS) to the base case 15m, the effect of natural fracture conductivity (NFC) can be examined by changing its value from 3e-

5md-m to 3md-m. Also, holding natural fracture conductivity to 0.03md-m, the effect of NFS on optimum fracture conductivity can be evaluated. Figure 3-10 shows a result of changing NFC for fracture half-length 150m. Both the 1-year and 10-year plots illustrate that when natural fracture conductivity is smaller than 3e-2md-m, the optimum fracture conductivity is getting close, which means the impact of NFC becomes small. The comparison of optimum fracture conductivity with different fracture length at production time 1-year and 10-year is shown in Figure 3-11. First, it can be concluded that longer fractures require higher optimum fracture conductivity, and the first-year production (transient flow) needs the highest fracture conductivity as in the previous simulation results. Furthermore, for the first-year production, the optimum fracture conductivity goes down with NFC decreasing and it is reaching a plateau after 3e-5md-m. This is because high natural fracture conductivity increases the effective permeability of reservoirs, and, therefore, larger inflow of gas needs higher fracture conductivity. NFC 3e-5 generates an effective horizontal permeability 2e-6md in terms of equation (2-6), which is smaller than the matrix permeability 2e-5md, so NFC less than 3e-5md does not impact reservoir depletion, and then the optimum fracture conductivity, which leads to the curve tending to a plateau. With the 10-year production (steady flow), the optimum fracture conductivity gradually decreases with NFC when NFC is greater than 3e-3 md-m, and then it slightly increases with NFC reducing after NFC 3e-3md-m. This difference from the 1-year production after NFC 3e-3md-m is due to the pressure dependence of natural fracture conductivity. Low NFC (< 3e-3md-m) drops dramatically after 10 years due to reservoir depletion, and it needs the higher primary fracture conductivity to make up for the loss of NF conductivity, in order transport the relative high remaining influx of gas to the wellbore.

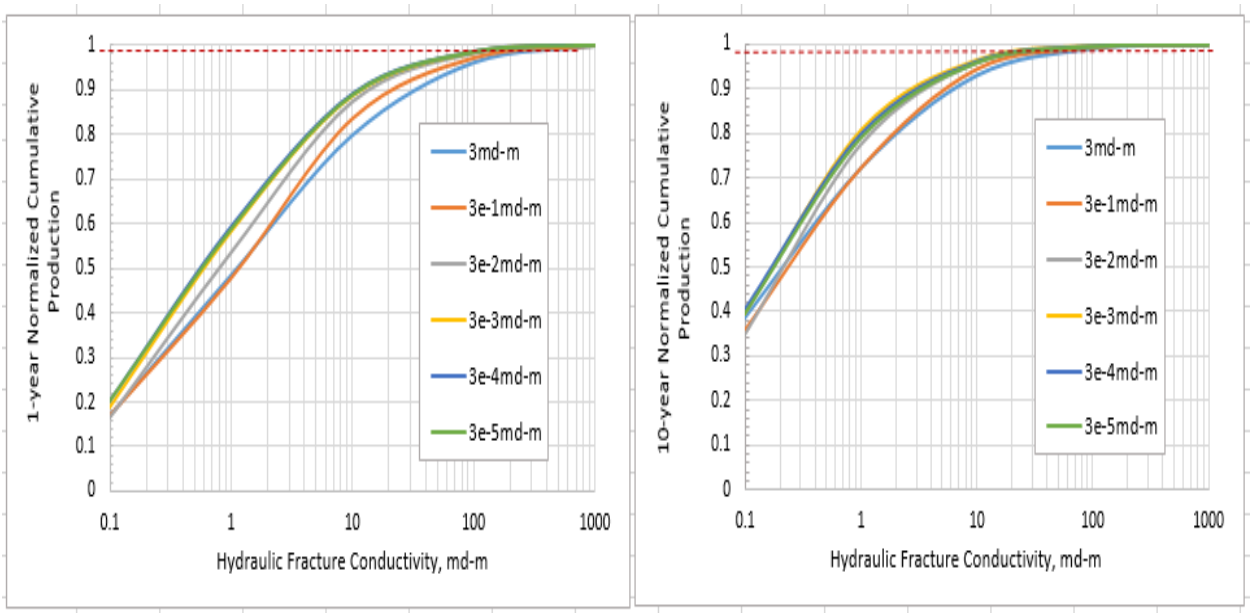

Figure 3-10: Normalized production vs. propped fracture conductivity with different NFC

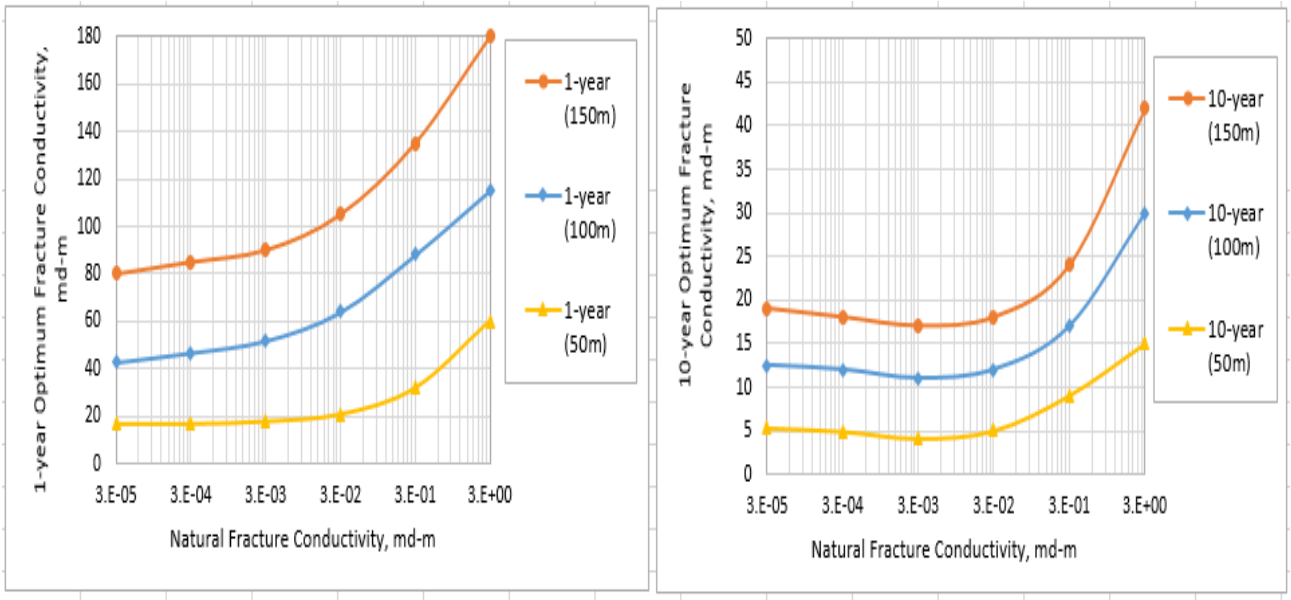

Figure 3-11: Comparison of optimum fracture conductivity for NFC effects

The relationship between normalized cumulative production and hydraulic fracture conductivity with different natural fracture spacing (NFS) for fracture half-length 150m can be

seen in Figure 3-12. It is observed that for the 1-year production, the impact of NFS on optimum fracture conductivity is small when NFS is greater than 20m, while changing NFS has insignificant effects on optimum fracture conductivity for the 10-year production due to the reduced natural fracture conductivity with time. Figure 3-13 illustrates the optimum fracture conductivity with three fracture half-lengths and two production times. The results of reducing NFS are similar with increasing NFC because reducing NFS also has improved the reservoir effective permeability. The first-year optimum fracture conductivity goes to a plateau after NFS 100m, which means that natural fracture spacing does not impact the optimum fracture conductivity much when NFS is greater than 100m. For the 10-year production, it can be seen that the optimum fracture conductivity at each fracture half-length is very close, which means that NFS has a small impact on the optimum fracture conductivity. As said earlier, the NFC less than 3e-2md-m has a small impact on optimum fracture conductivity in this study so even changing NFS still has very small impact when the NFC has reduced less than 3e-2md-m after 10 years due to pressure dependent conductivity.

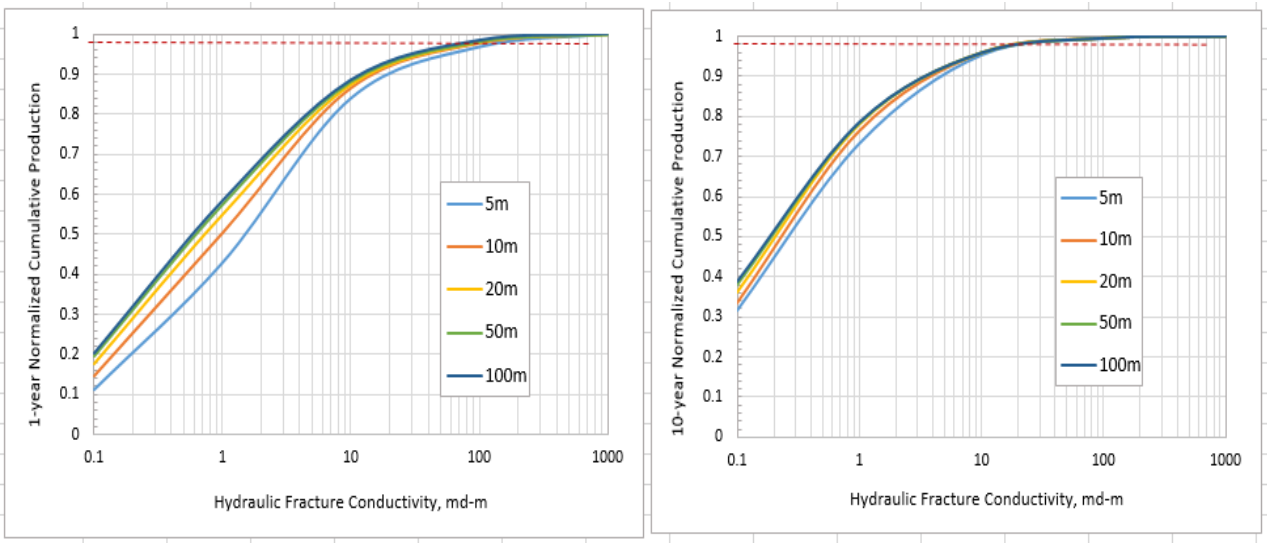

Figure 3-12: Normalized production vs. propped fracture conductivity with different NFS

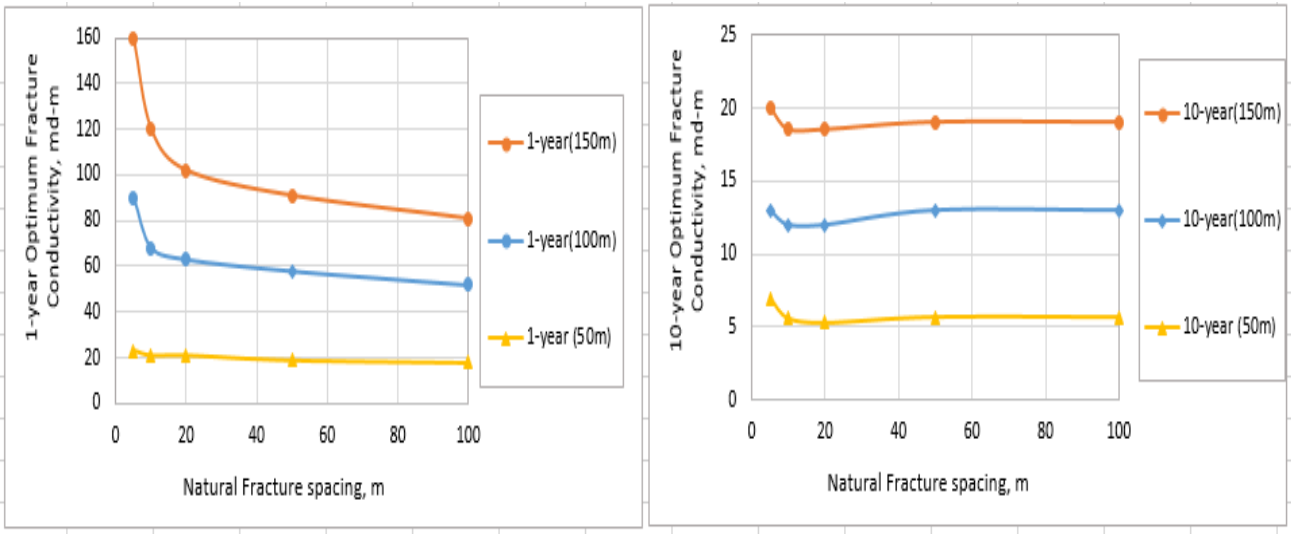

Figure 3-13: Comparison of optimum fracture conductivity for NFS effects

Comparing the effects of NFC and NFS (Figures 3-11 and 3-13) to plots obtained from Gu et al. (2014) as shown in Figure 3-14, it can be observed that the main trends of the firs-year optimum fracture conductivity with NFS and NFC changing are similar, but there is a difference existing in the 10-year optimum fracture conductivity plots due to two reasons. One is that this simulation considers varied natural fracture conductivity with time, so the decline of natural fracture conductivity after the 10-year production results in the different effects. The other reason is the reservoir in Figure 3-14 having matrix permeability 2e-4md, which is one order of magnitude greater than the base case permeability in this study, but the NFS and NFC ranges are the same for both simulations. Therefore, the effective permeability produced by natural fractures has a different impact. The difference also demonstrates that the optimum fracture conductivity requirement may come up with different results for different reservoirs and well completions. Last, Tables 3-4 and 3-5 summarize the optimum fracture conductivity values for the NFC and NFS effects.

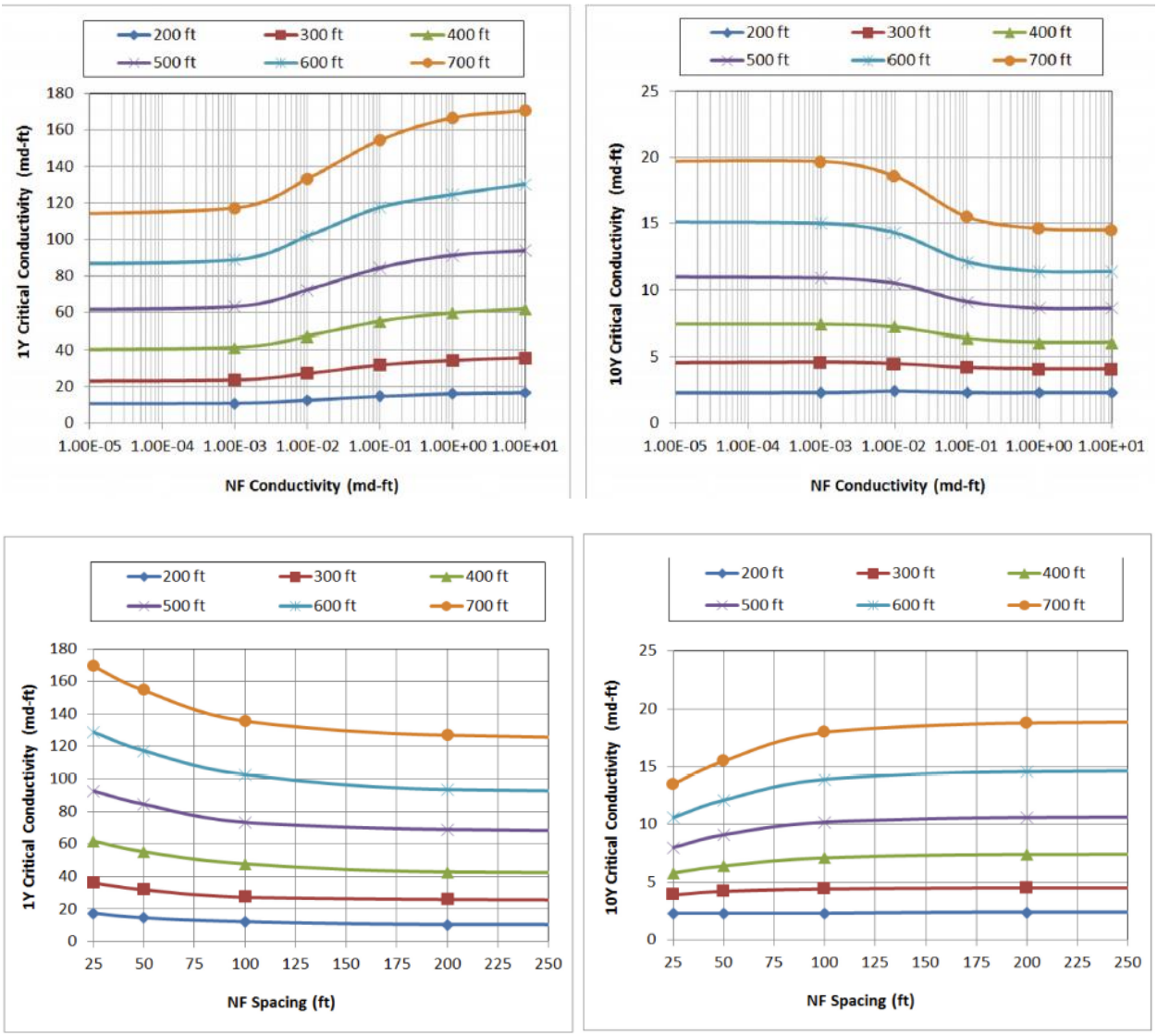

Figure 3-14: Effects of NFS and NFC on optimum fracture conductivity (Gu et al. 2014)

Table 3-4: Optimum fracture conductivity values for different NFC

Conductivity (md-m)	1-year Optimum Fracture Conductivity (md-m)			10-year Optimum Fracture Conductivity (md-m)		
	x_f =50m	x_f =100m	x_f =150m	x_f =50m	x_f =100m	x_f =150m
0.00003	17	43	80	5.4	12.5	19
0.0003	17	47	85	5	12	18
0.003	18	52	90	4.2	11	17
0.03	21	64	105	5.1	12	18
0.3	32	88	135	9.1	17	24
3	60	115	180	15	30	42

Table 3-5: Optimum fracture conductivity values for different NFS

NF spacing (m)	1-year Optimum Fracture Conductivity (md-m)			10-year Optimum Fracture Conductivity (md-m)		
	x_f =50m	x_f =100m	x_f =150m	x_f =50m	x_f =100m	x_f =150m
5	23	90	160	7	13	20
10	21	68	120	5.6	12	18.5
20	21	63	102	5.3	12	18.5
50	19	58	91	5.7	13	19
100	18	52	81	5.7	13	19

3.5 Impact of Hydraulic Fracture Spacing

The effects of hydraulic fracture spacing (HFS) on fracture conductivity for fracture half-length 100m are shown in Figure 3-15. It is noticeable that the four different HFS curves of the 1-year production almost overlap. This means that the optimum fracture conductivity of four different HFS is close for the 1-year production, and the impact of HFS on the optimum fracture conductivity is small. Also, it shows a bigger distance between the HFS 10m curve and other three curves with the longer production time, which means that the percentage increase of optimum fracture conductivity from HFS 10m to HFS 25m becomes larger as the production time gets

longer. Furthermore, Figure 3-16 depicts the comparison of the optimum fracture conductivity of four production times with different HFS at fracture half-length 100m and 150m. First, it follows the same trend that the optimum fracture conductivity decreases as production time increases for the same hydraulic fracture length, and longer fracture length requires higher optimum fracture conductivity at different HFS. The reasons for the above conclusions have been given in Section 3.1. Second, optimum fracture conductivity increases with hydraulic fracture spacing getting larger for all the cases until it gradually reaches a plateau after HFS 25m. This can be explained from the highway theory (Economides et al., 2000). For a certain feeder system, if there are two or even more highways to carry the same traffic compared to only one highway, the ability of carrying traffic of each highway is not necessary to be high due to traffic diversion. The same principle applies to hydraulic fracture conductivity. Small hydraulic fracture spacing means more hydraulic fractures to drainage the reservoir so the requirement of each hydraulic fracture conductivity for small HFS is lower than that of large HFS. In this case, HFS 10m has the lowest optimum fracture conductivity. With the number of hydraulic fractures reducing, each hydraulic fracture needs higher conductivity to transport the flow. When the conductivity reaches a certain value (a plateau), even larger HFS (fewer hydraulic fractures) can still meet the needs of carrying the flow. Lastly, the slope of each curve from point HFS 10m to point HFS 25m increases with production time, which is actually the same conclusion from Figure 3-15. Gu et al. (2014) pointed out that hydraulic spacing represents a drainage boundary, which is impacted by the long-term production more than the short term production. The optimum fracture conductivity values are summarized in Table 3-6.

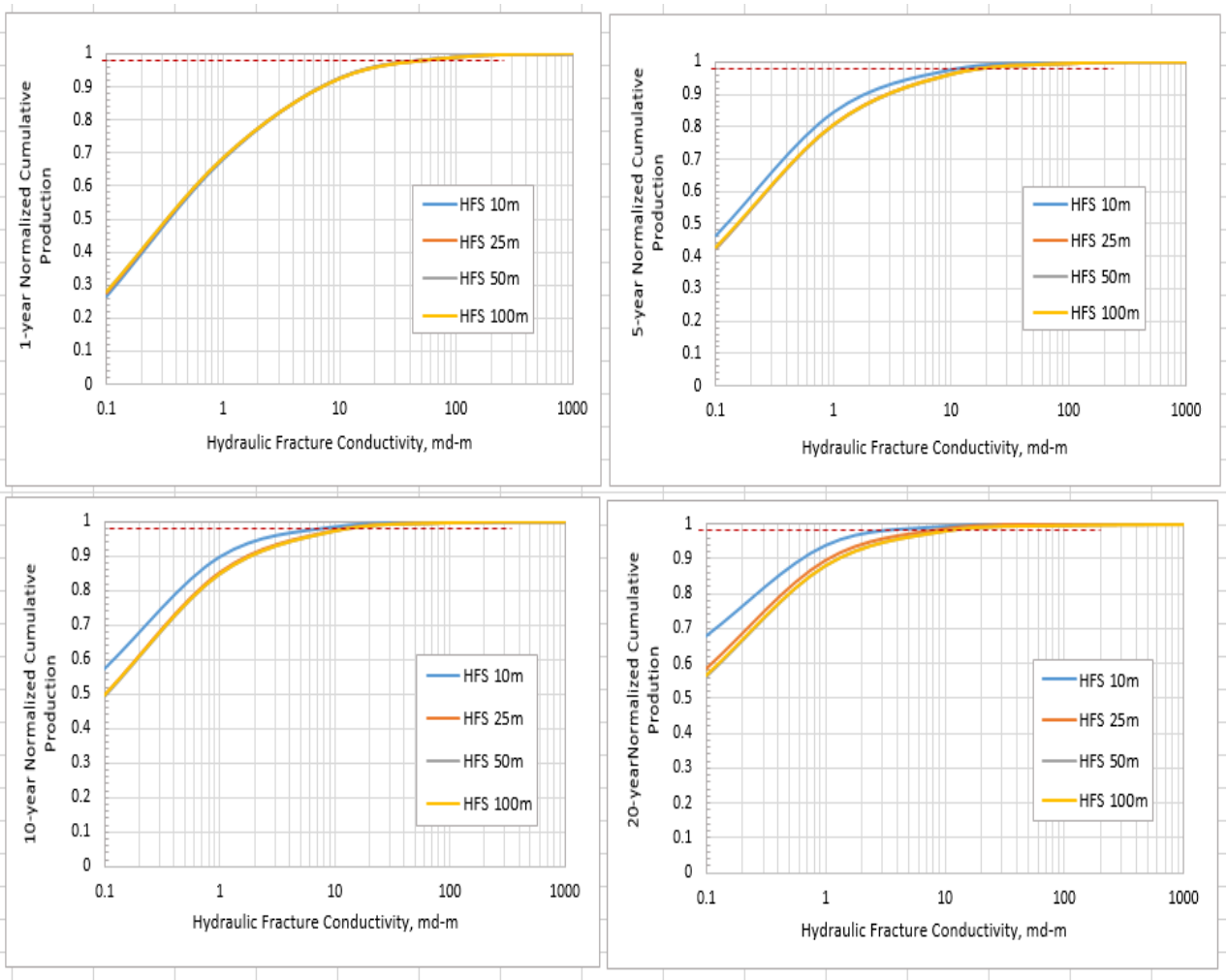

Figure 3-15: Normalized production vs. propped fracture conductivity with different HFS (xf =100m)

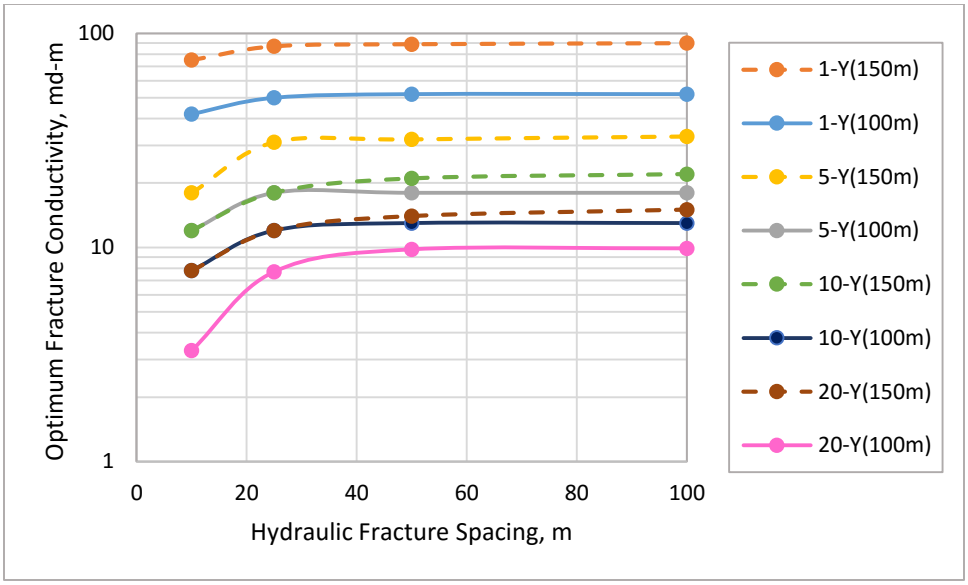

Figure 3-16: Comparison of optimum fracture conductivity for HFS effects

Table 3-6: Optimum fracture conductivity values for different HFS

HFS (m)	1-year Optimum Fracture Conductivity (md-m)		5-year Optimum Fracture Conductivity (md-m)		10-year Optimum Fracture Conductivity (md-m)		20-year Optimum Fracture Conductivity (md-m)	
	x_f=100m	x_f=150m	x_f=100m	x_f=150m	x_f=100m	x_f=150m	x_f=100m	x_f=150m
10	42	75	12	18	7.8	12	3.3	7.8
25	50	87	18	31	12	18	7.7	12
50	52	89	18	32	13	21	9.8	14
100	52	90	18	33	13	22	9.9	15

3.6 Effects of Complex Hydraulic Fractures

Figure 3-17 shows the relationship of normalized cumulative production vs. hydraulic fracture conductivity at matrix permeability 2e-5md with different production time. It depicts the same trend as with planar fractures that the short-term production (1 year) requires the highest fracture conductivity to get the near-maximum production. The optimum fracture conductivity decreases with an increase in production time.

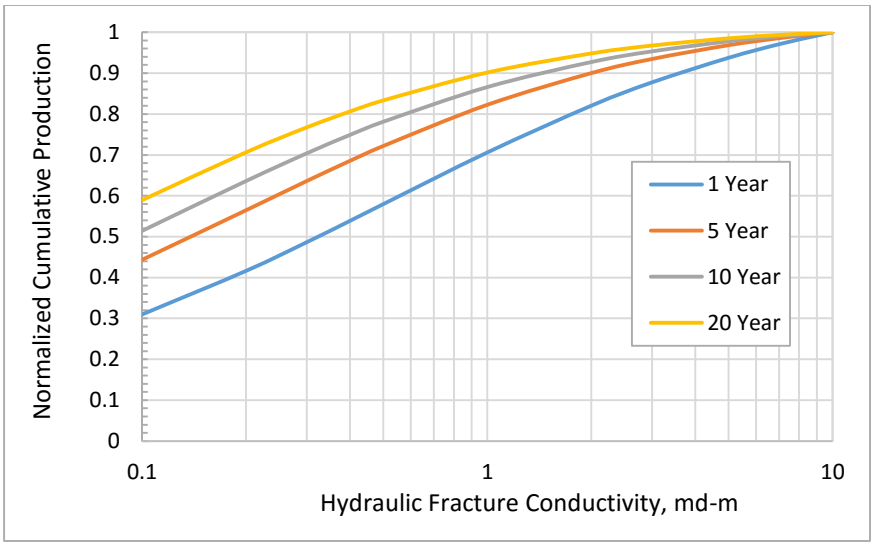

Figure 3-17: Normalized production vs. propped fracture conductivity with different production time for complex fractures (k=2e-5md)

The effect of a complex fracture network for different matrix permeability has also been considered, and the results are shown in Figures 3-18 and 3-19, respectively. Again, the effects of complex fractures on optimum fracture conductivity with different matrix permeability follow the same trend as with planar fractures that the optimum fracture conductivity increases with matrix permeability. The reason for this has been stated in the planar fracture section.

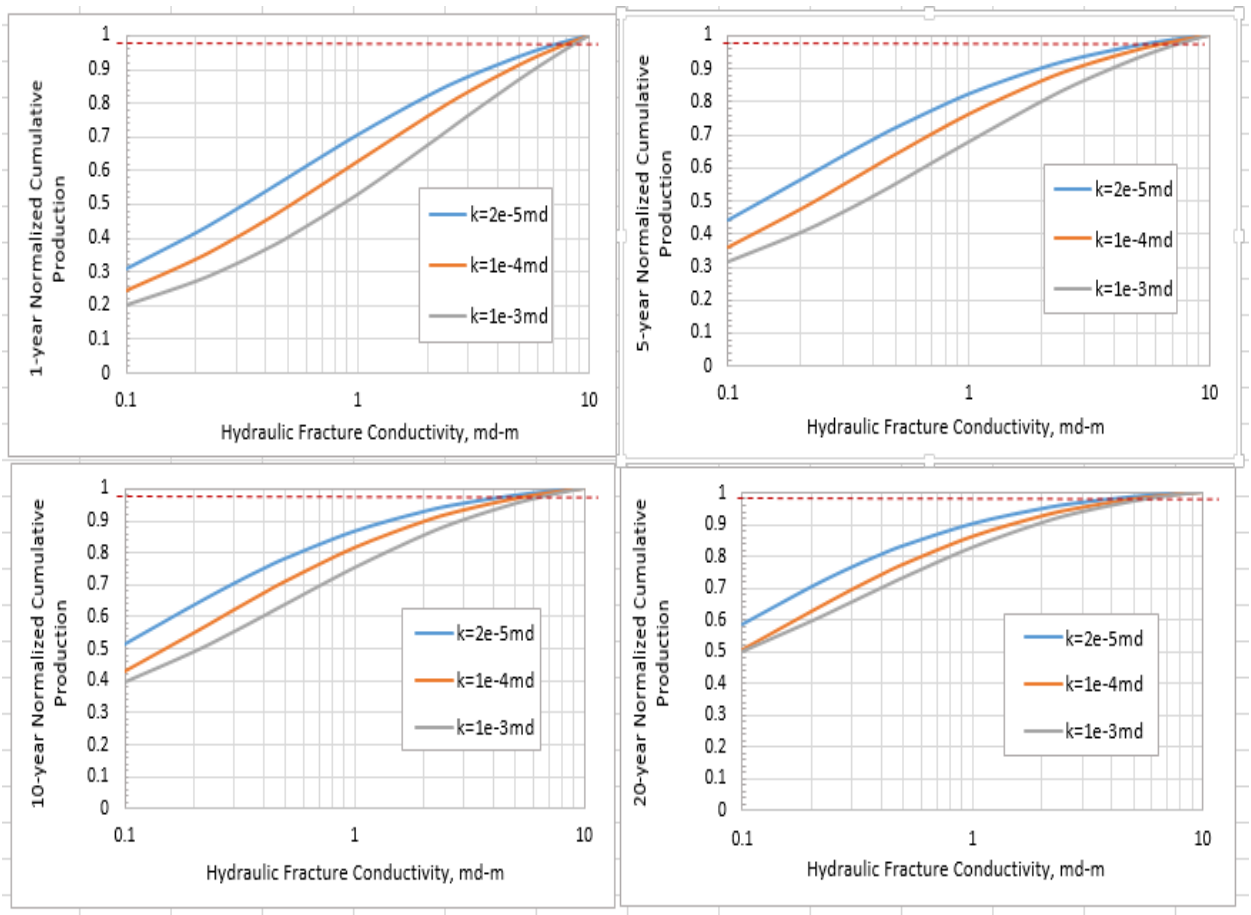

Figure 3-18: Normalized production vs. propped fracture conductivity with different permeability and production time

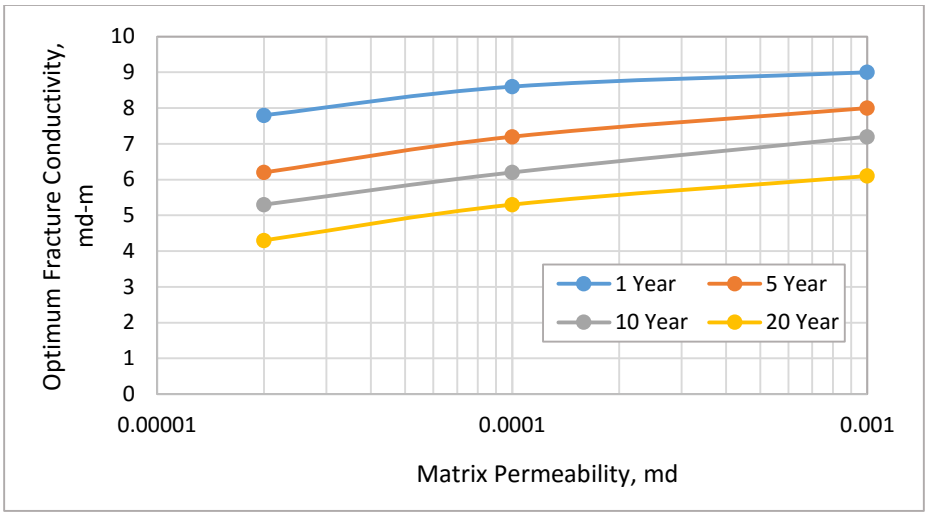

Figure 3-19: Comparison of optimum fracture conductivity with different permeability and production time

Additionally, the impact of complex fractures on reservoirs without and with natural fractures (NF) has been compared in Figure 3-20. The optimum fracture conductivity with NF is higher than that without NF. It can be understood easily that the existence of NF increases the effective permeability so higher inflow of gas requires larger optimum fracture conductivity.

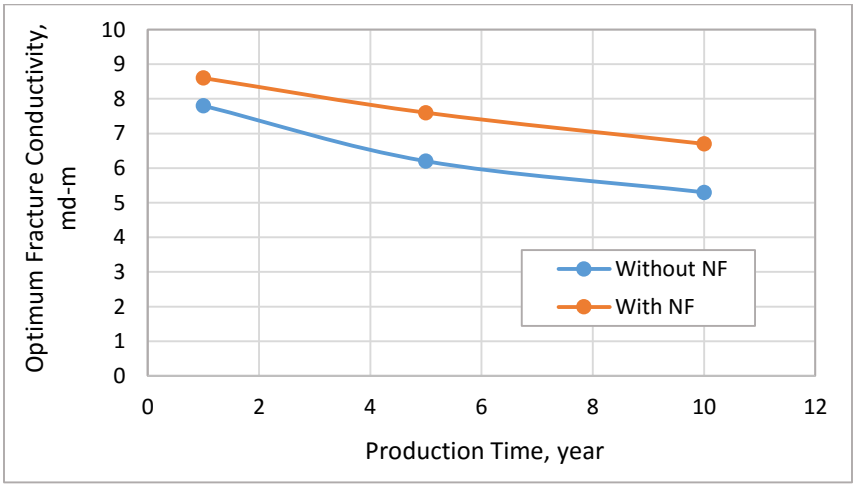

Figure 3-20: Comparison of optimum fracture conductivity without and with NF (k=2e-5md)

Last, the effects of planar fractures and a complex fracture network on optimum fracture conductivity are compared as well. Starting from the wellbore, the extent of the complex fractures in this study reaches 150m (Figure 2-23), so the complex fractures are compared to the planar fractures with 150m half-length. First, the cumulative production of the well with planar fractures at conductivity 1000md-m and complex fractures at conductivity 10md-m for various reservoir permeability is compared in Figure 3-21, in order to see if the two fracture geometries result in similar productivity, so the optimum fracture conductivity could be compared at the same level. The comparison indicates that for permeability 2e-5md, the productivity from complex fractures is better than that from planar fractures in the first 5 years. With an increase in permeability, the productivity from planar fractures is getting better than that from complex fractures but the difference of productivity is not big. These results demonstrate that exploiting the fracture complexity is more beneficial for a lower permeability reservoir, given that producing complex fractures by using slick water fracking has lower costs. Whether to exploit or control fracture complexity is dependent on reservoir permeability, which is also in accordance with the conclusion from Cipola et al. (2008).

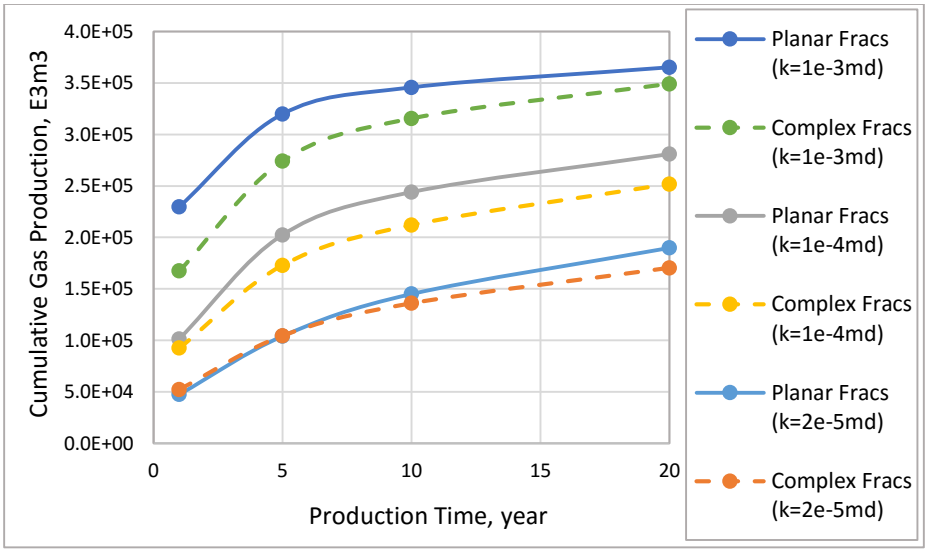

Figure 3-21: Comparison of productivity for planar and complex fractures

The comparison of optimum fracture conductivity for the two fracture geometries is shown in Figure 3-22. It is observed that the optimum fracture conductivity of planar fractures is far higher than that of complex fractures. This is because the complex fractures form an extensive interconnected network which reduces the fracture conductivity requirement according to the high-way theory. The optimum fracture conductivity of planar fractures for the first-year production can be over 10 times greater than that of complex fractures. With an increase in production time, the difference of optimum fracture conductivity between planar and complex fractures becomes smaller. Moreover, the influence of production time on the optimum fracture conductivity for the complex fractures is small. A comparison of optimum fracture conductivity in a reservoir of permeability 2e-5md with NF is shown in Figure 3-23, which presents the same trend as in Figure 3-22. The optimum fracture conductivity values for complex fractures are listed in Table 3-7.

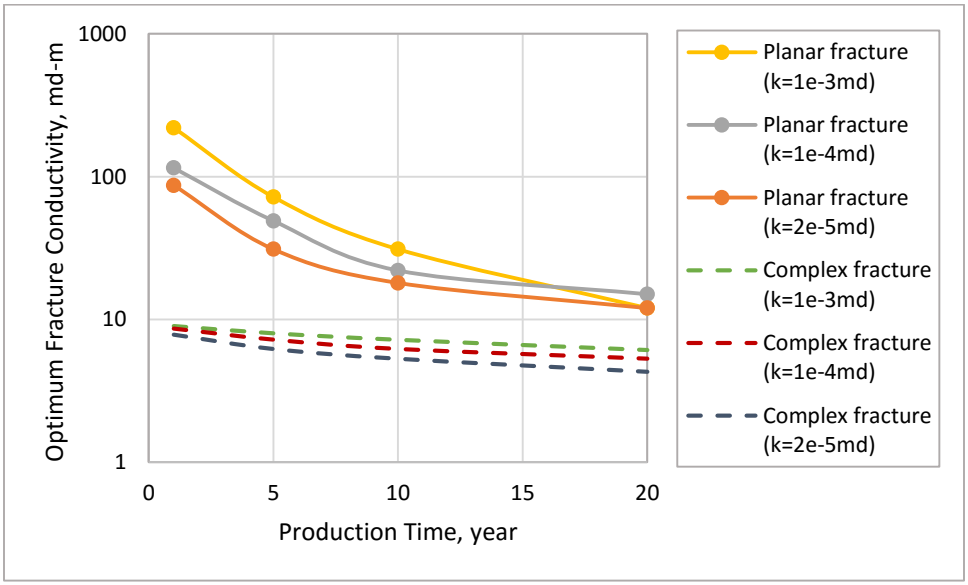

Figure 3-22: Comparison of optimum fracture conductivity with planar and complex fractures without NF

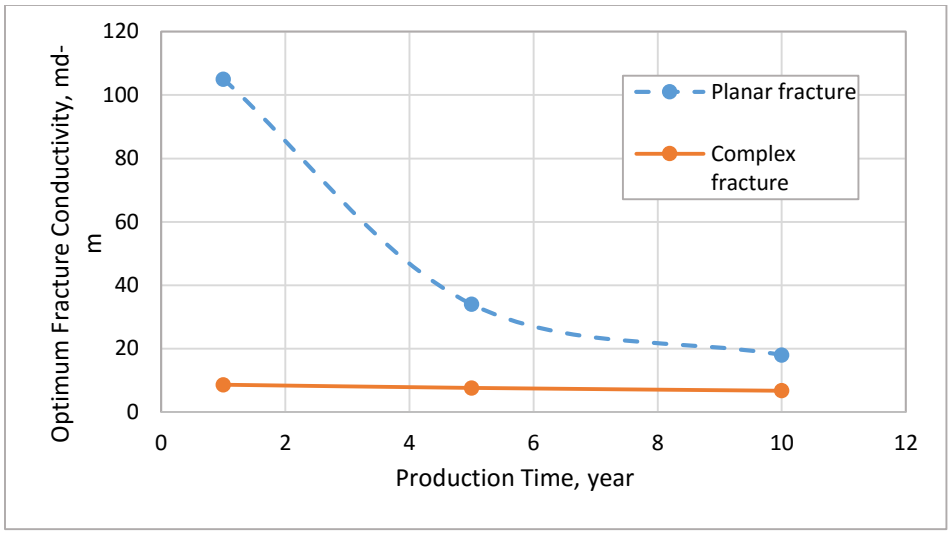

Figure 3-23: Comparison of optimum fracture conductivity with planar and complex fractures with NF (k=2e-5md)

Table 3-7: Optimum fracture conductivity values for complex fractures

Production Time (year)	Optimum fracture conductivity without NF (md-m)			Optimum fracture conductivity with NF (md-m)
	k=2e-5md	k=1e-4md	k=1e-3md	k=2e-5md
1	7.8	8.6	9	8.6
5	6.2	7.2	8	7.6
10	5.3	6.2	7.2	6.7
20	4.3	5.3	6.1	N/A

3.7 Proppant and Fracking Fluid Selection

The selection of proppants and a fracking fluid can be based on the optimum fracture conductivity. An example to choose the proppants and fluid will be presented in this section.

Four types of proppants are commonly used in hydraulic fracture treatments for unconventional reservoirs: sand, ceramic, resin-coated sand (RCS), and resin coated ceramic (RCC). Proppants with resins are more resistant to crush by distributing a load more evenly and

trapping the fines in the resin coating (Al-Sadhan, 2014). The proppants are ranked in order of low to high strength: sand, RCS, ceramic and RCC (Kullman, 2011). Furthermore, sand is generally divided into white and brown sand, and white sand is stronger than brown sand. Ceramic proppants have three kinds in terms of their density: lightweight, intermediate density, and high density ceramics. The higher density has the higher strength, but lightweight ceramics can be transported further into fractures by a low viscosity fluid like slick water. The proppant size is also important in fracture treatments. Proppant sizes are generally between 140 to 8 mesh (105μm to 2.38mm); for example, 40/70 mesh is 420μm to 210μm and 20/40 mesh is 841μm to 420μm (Liang et al., 2015). Typically, proppants with a larger size provide higher conductivity. An evaluation for overall performance of proppant is the proppant conductivity testing. International Organization for Standardization (ISO) has released a standard procedure ISO13503-5 for long-term baseline conductivity tests. The service companies and proppant suppliers provide the baseline conductivity values obtained under the ISO 13503-5 condition for their proppants. However, the baseline conductivity does not account for the downhole reservoir situation such as the detrimental effects of multi-phase flow, non-Darcy's flow, reduced proppant concentration, and fines migration. As stated in the literature review, the effective conductivity could be over 90% reduction from the baseline conductivity after accounting for a realistic situation (Palisch et al., 2007; Vincent, 2009).

In the example for the proppant selection, three cases of the first-year optimum fracture conductivity obtained from previous sections are chosen: high Young's modulus formation with planar fractures, medium Young's modulus with planar fractures, and complex fractures with natural fractures. These optimum fracture conductivity values from simulation results are effective conductivity, which account for the downhole reservoir situation, so these values are multiplied by 10 since they have the 90% reduction from the baseline conductivity. The modified optimum

fracture conductivity under fracture half-length 50m to 150m (solid lines) is plotted in Figure 3-24, as well as the baseline conductivity of some proppants at different sizes and concentration (dash lines). Carbolite is a lightweight ceramic, and Carborop is an intermediate density ceramic. These baseline conductivities of proppants are obtained from the Carbo website, Al-Sadhan (2014), Pearson et al. (2014), Vincent (2010), and Barree et al. (2016), respectively. These conductivity tests are under closure pressure 34474kPa and temperature 121˚C which match the reservoir conditions in the study.

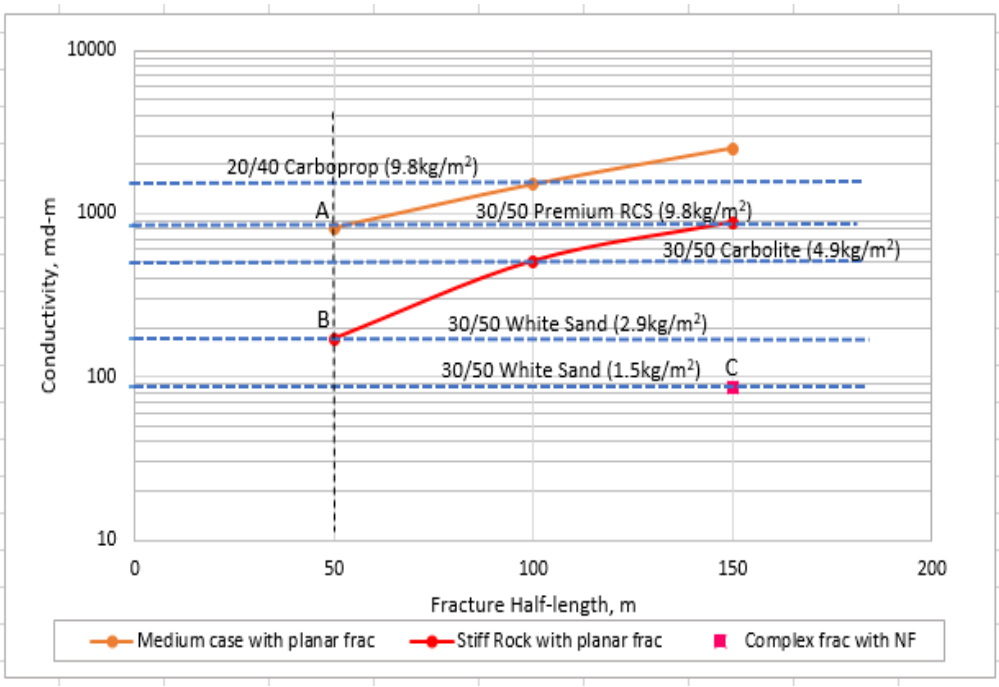

Figure 3-24: Three cases of optimum fracture conductivity along with the baseline conductivity of some proppants

If the hydraulic fracture treatments want to achieve propped half-length 50m, the modified optimum conductivity is 810md-m for the medium case with planar fractures (point A) and 170md-m for stiff rock with planar fractures (point B) in Figure 3-24, respectively. It can be seen that the conductivity of 30/50 premium RCS at 9.8kg/m^2 and 30/50 White Sand at 2.9kg/m^2 passes point

A, B, repectively, so the two proppants meet the optimum conductivity requirements. The base reservoir model in this study assumes fracture height 40m and 16 stages. Therefore, for the planar fracture cases, each fracture has a 100m × 40m× 2 = 8000m^2 fracture area. The amount of proppants can be calculated by the product of the fracture area and proppant concentration per unit fracture area. Then, each fracture needs 78,400kg 30/50 premium RCS for the medium case, and 23,200kg 30/50 White Sand for the stiff case. If each stage has average 4 fractures in this study, it comes to 313,600kg per stage for the medium case and 92,800kg per stage for the stiff case. As the complex fracture case, the conductivity of 30/50 White Sand at 1.5kg/m^2 passes point C and it can meet the optimum conductivity requirement. It is hard to estimate the fracture area of complex fractures due to the irregular geometry of complex fracutures. Here is an approximate method used according to the simulation of Cipolla, and Wallace (2014), which shows that the fracture area of planar fractures has 20% more than that of a complex fracture network under the same microcosmic mapping events. The total fracture area of planar fractures with half-length 150m is 1.5 million m^2 so the fracture area of complex fractures in this case is 1.2 million m^2. Then, the amount of 30/50 White Sand for this well is about 1.8 million kg for the complex fracture case, and each stage needs about 112,500kg 30/50 White Sand if the hydraulic fracturing treatment has 16 stages.

A fracture fluid system contains the common types as follows: slickwater, linear gel, crosslinked fluid, and hybrid. The hybrid is either crosslinked/slickwater or linear gel/slickwater. The low viscosity of slickwater makes it little ability to suspend or transport proppants. Moreover, a slickwater fracking typically creates narrower pumping fracture width than its crosslinked fluid counterpart. Hence, it is difficult to place higher proppant concentration and large size proppants in sickwater fracturing. Generally, proppant concentration less than 2 PPA (lbm/gal) and smaller

sized proppants are used in slickwater fracturing, including 30/50, 40/70, and in some cases 100 mesh (Palisch et al., 2010). Sometimes, larger size or high quality proppants such as 20/40 ceramics are pumped in a "tail in" stage to increase the near-wellbore conductivity. Handren and Palisch (2009) compared the slickwater and hybrid fracturing, and summarized that most slickwater jobs have proppant concentration 1 PPA, while hybrid jobs generally have average concentration of 2 PPA. Fredd et al. (2001) pointed out that proppant concentration of 0.1 and 1.0lb/ft^2 in a fracture corresponded to a slickwater fracturing with 0.5 PPA proppants and a conventional fracturing with 4 PPA proppants.

In this example, 30/50 premium RCS at 9.8kg/m^2 (equals 2lb/ft^2) is selected for the medium case. The concentration of 9.8kg/m^2 can be equivalent to over 4 PPA proppants in a fracturing treatment. Thus, a crosslinked fluid is chosen for the fracture design due to the high proppant concentration. With 30/50 White Sand at 2.9 kg/m^2 (equals 0.6lb/ft^2) which is equivalent to about 2 PPA, the hybrid fluid can be an option for the stiff rock case. Last, for the complex fracture case, it is obvious that a slickwater system should be chosen to transport the 30/50 White Sand at 1.5 kg/m^2 (equals 0.3lb/ft^2). These fluid selections demonstrate that for softer shale, a viscous fracture fluid is needed to satisfy the high optimum conductivity requirement.

The example above illustrates a simple workflow to choose t proppants and a fluid in terms of the optimum fracture conductivity. It accounts for neither the safety factor, which considers the loss of proppants during the downhole operation, nor the economic aspects of proppants and hydraulic fractures. The workflow can be a preliminary selection method. In practice, a fracture simulator should be employed to give the pumping schedule based on the preliminary selection and model the propagation of fractures to see if the optimum fracture conductivity has been

reached. The example shows that the fracture design should be different for different property of shale formations.

Chapter 4 : Conclusions and Future Work

In this thesis, a workflow is established and applied to shale/tight gas reservoirs with characteristics from Horn River basin. First, a sensitivity analysis and history match are conducted by using CMOST to see the importance of fracture conductivity on the well productivity and ensure the reliability of the reservoir model. Then a planar hydraulic fracture model and a complex fracture network are built and explicitly modeled, respectively, in the GEM reservoir simulator. A complex fluid flow in a matrix, hydraulic fractures, and natural fractures is simulated by GEM. A parametric study is executed to examine the relationship between the optimum fracture conductivity and the reservoir and treatment design parameters such as fracture half-length, production time, matrix permeability, rock stiffness, natural fracture properties (conductivity and spacing), and hydraulic fracture spacing. The optimum fracture conductivity obtained by reservoir simulations are compared and analyzed. A procedure to determine the type and amount of proppants as well as the fracture fluid type based on the optimum fracture conductivity is presented.

This work leads to the following conclusions:

- Fracture conductivity is very important to the well productivity for shale gas plays.
- The optimum fracture conductivity increases with hydraulic fracture length. Also the optimum fracture conductivity increases with hydraulic fracture spacing; however, the effect of hydraulic fracture spacing on the optimum fracture conductivity becomes insignificant when HFS is greater than a certain value (25m in this study).
- The transient flow period (short-term production) needs higher fracture conductivity compared to a steady flow period. If operators want high initial production and fast pay back, the short-term optimum fracture conductivity should be considered.

- The reservoir simulation results indicate that the higher optimum fracture conductivity is required to make up for the conductivity loss during production after considering the varied conductivity with time and along fractures.
- Reservoirs with higher permeability require higher fracture conductivity for short-term production, but for long-term production the higher fracture conductivity may not be needed due to fast drainage.
- The softer a formation the higher the optimum fracture conductivity so a hybrid or gelled fracture fluid can be appropriate for hydraulic fracturing in a softer formation.
- The short-term optimum fracture conductivity is proportional to NFC but inversely proportional to NFS. When NFC is smaller than a certain value (3e-3md-m in this study), the long-term optimum fracture conductivity is inversely proportional to NFC. All in all, the impacts of NFC and NFS on the optimum fracture conductivity are small as NFC is smaller than or NFS is greater than a certain value.
- The requirement of optimum fracture conductivity for a complex fracture network is far lower than that for planar fractures. Due to the large interconnected network produced, the impact of production time on the optimum fracture conductivity is small for a complex fracture network.
- The simulation results demonstrate that a complex fracture network is more beneficial in an ultra-low permeability reservoir with a stiff formation given a low cost of slick-water fracking.
- By comparing the optimum fracture conductivity results in this study with others' results, we can conclude that the results are dependent on the chosen reservoir properties as well as the completion designs, and they are not generalized to other reservoirs.

- This thesis shows that there are different optimum fracture conductivity requirements for different properties of shale /tight plays so we should apply the workflow to an individual reservoir in order to optimize hydraulic fracturing designs.

The workflow provided in this study is helpful to the hydraulic fracture design optimization. The relationship between the optimum fracture conductivity and the reservoir/treatment design parameters, and the range of the optimum fracture conductivity values can be a reference to engineers who are involved in the hydraulic fracturing designs. There are not many references about the complex fracture simulation currently so the simulation of a complex fracture network provides a good basis for future research of complex fractures. This study still has a lot of room for improvement. The recommendations for future work are below:

- Add the economical consideration and determine if the optimum fracture conductivity is practical, because the optimum fracture conductivity results in this study only cover the technical aspects, and some conductivity results may be idealized given the realistic operation conditions and operational costs.
- Incorporate the micro-seismic mapping events into the building of complex fracture network models, which makes the complex facture models more realistic.
- Improve the reservoir models built, such as more realistic natural fracture distribution other than wire-mesh natural fractures.
- Improve the procedure of selecting the proppants and fracking fluid by using a fracture simulator to simulate the fracture propagation and the proppant placement, and combining the economical evaluation for the proppants and fracking fluid.
- Extend the subjects of this study to tight oil and shale liquid rich gas plays.

References

Agarwal, R. G., Carter, R. D., & Pollock, C. B. (1979, March 1). Evaluation and Performance Prediction of Low-Permeability Gas Wells Stimulated by Massive Hydraulic Fracturing. Society of Petroleum Engineers. doi:10.2118/6838-PA.

Aguilera, R. (2010, January 1). Flow Units: From Conventional to Tight Gas to Shale Gas Reservoirs. Society of Petroleum Engineers. doi:10.2118/132845-MS.

Aguilera, R. (2013, April 19). Flow Units: From Conventional to Tight Gas to Shale Gas to Tight Oil to Shale Oil Reservoirs. Society of Petroleum Engineers. doi:10.2118/165360-MS.

Alramahi, B., & Sundberg, M. I. (2012, January 1). Proppant Embedment and Conductivity of Hydraulic Fractures in Shales. American Rock Mechanics Association.

Al-Sadhan, N. (2014). Prediction of Short-term and Long-term Baseline Conductivity Degradation for Proppants of Different Types and Sizes. Colorado School of Mines. Department of Petroleum Engineering:http: //dspace.library.colostate.edu/webclient/DeliveryManager/digitool_items /csm01_storage/2014/12/02/file_1/419426.

Awoleke, O. O., Romero, J. D., Zhu, D., & HIll, D. (2012). Experimental Investigation of Propped Fracture Conductivity in Tight Gas Reservoirs Using Factorial Design. Paper SPE 151963 Presented at SPE Hydraulic Fracturing Conference, Woodlands, Texas, USA, 6-8 Feb.

Barree, R. D., Miskimins, J. L., Conway, M. W., & Duenckel, R. (2016, February 1). Generic Correlations for Proppant Pack Conductivity. Society of Petroleum Engineers. doi:10.2118/179135-MS

Bazan, L. W., Brinzer, B. C., Meyer, B. R., & Brown, E. K. (2013, August 20). Key Parameters Affecting Successful Hydraulic Fracture Design and Optimized Production in Unconventional Wells. Society of Petroleum Engineers. doi:10.2118/165702-MS.

Bennett, C. O., Rosato, N. D., Reynolds, A. C., & Raghavan, R. (1983, April 1). Influence of Fracture Heterogeneity and Wing Length on the Response of Vertically Fractured Wells. Society of Petroleum Engineers. doi:10.2118/9886-PA.

Besler, M. R., Steele, J. W., Egan, T., & Wagner, J. (2007, January 1). Improving Well Productivity and Profitability in the Bakken--A Summary of Our Experiences Drilling, Stimulating, and Operating Horizontal Wells. Society of Petroleum Engineers. doi:10.2118/110679-MS.

Beugelsdijk, L. J. L., de Pater, C. J., & Sato, K. (2000, January 1). Experimental Hydraulic Fracture Propagation in a Multi-Fractured Medium. Society of Petroleum Engineers. doi:10.2118/59419-MS.

Britt, L. K., & Bennett, C. O. (1985, January 1). Determination of Fracture Conductivity in Moderate-Permeability Reservoirs Using Bilinear Flow Concepts. Society of Petroleum Engineers. doi:10.2118/14165-MS.

Carbo Website: http://www.carboceramics.com/products-and-services/fracture-technologies /ceramic-proppant.

Cinco L., H., Samaniego V., F., & Dominguez A., N. (1978, August 1). Transient Pressure Behavior for a Well with a Finite-Conductivity Vertical Fracture. Society of Petroleum Engineers. doi:10.2118/6014-PA.

Cinco-Ley, H., & Samaniego-V., F. (1981, September 1). Transient Pressure Analysis for Fractured Wells. Society of Petroleum Engineers. doi:10.2118/7490-PA.

Cipolla, C. L., Lolon, E. P., Erdle, J. C., & Rubin, B. (2010, August 1). Reservoir Modeling in Shale-Gas Reservoirs. Society of Petroleum Engineers. doi:10.2118/125530-PA.

Cipolla, C. L., Lolon, E., Mayerhofer, M. J., & Warpinski, N. R. (2009, January 1). Fracture Design Considerations in Horizontal Wells Drilled in Unconventional Gas Reservoirs. Society of Petroleum Engineers. doi:10.2118/119366-MS.

Cipolla, C., & Wallace, J. (2014, February 4). Stimulated Reservoir Volume: A Misapplied Concept? Society of Petroleum Engineers. doi:10.2118/168596-MS

Cipolla, C. L., Warpinski, N. R., Mayerhofer, M. J., Lolon, E., & Vincent, M. C. (2008, January 1). The Relationship between Fracture Complexity, Reservoir Properties, and Fracture Treatment Design. Society of Petroleum Engineers. doi:10.2118/115769-MS.

Cipolla, C. L., Weng, X., Mack, M. G., Ganguly, U., Gu, H., Kresse, O., & Cohen, C. E. (2011, January 1). Integrating Microseismic Mapping and Complex Fracture Modeling to Characterize Hydraulic Fracture Complexity. Society of Petroleum Engineers. doi:10.2118/140185-MS.

CMG: CMOST User's Guide, Computer Modeling Group Ltd., 2013.

CMG: GEM Tutorial, Computer Modeling Group Ltd., 2013.

Cobb, S. L., & Farrell, J. J. (1986, January 1). Evaluation of Long-Term Proppant Stability. Society of Petroleum Engineers. doi:10.2118/14133-MS.

Cooke, C. E. (1973, September 1). Conductivity of Fracture Proppants in Multiple Layers. Society of Petroleum Engineers. doi:10.2118/4117-PA.

Cooke, C. E. (1975, October 1). Effect of Fracturing Fluids on Fracture Conductivity. Society of Petroleum Engineers. doi:10.2118/5114-PA.

Coulter, G. R., Benton, E. G., & Thomson, C. L. (2004, January 1). Water Fracs and Sand Quantity: A Barnett Shale Example. Society of Petroleum Engineers. doi:10.2118/90891-MS.

Economides, M., Deimbachor, F. X., Brand, C. W., & Heinemann, Z. E. (1991, December 1). Comprehensive -Simulation of Horizontal-Well Performance. Society of Petroleum Engineers. doi:10.2118/20717-PA.

Econnomides, M.J., Nolte, K.G., Reservoir Stimulation, Third Edition, Wiley Publishing, 2000.

Elbel, J. L. (1988, August 1). Considerations for Optimum Fracture Geometry Design. Society of Petroleum Engineers. doi:10.2118/13866-PA.

Evans, R.D., and Civan, F. 1994. Characterization of Non-Darcy Multiphase Flow in Petroleum Bearing Formations. Report, U.S. DOE Contract No. DE-AC22-90BC14659, School of Petroleum and Geological Engineering, University of Oklahoma.

Fan, L., Thompson, J. W., & Robinson, J. R. (2010, January 1). Understanding Gas Production Mechanism and Effectiveness of Well Stimulation in the Haynesville Shale Through Reservoir Simulation. Society of Petroleum Engineers. doi:10.2118/136696-MS.

Fisher, M. K., Heinze, J. R., Harris, C. D., Davidson, B. M., Wright, C. A., & Dunn, K. P. (2004, January 1). Optimizing Horizontal Completion Techniques in the Barnett Shale Using Microseismic Fracture Mapping. Society of Petroleum Engineers. doi:10.2118/90051-MS.

Fisher, M. K., Wright, C. A., Davidson, B. M., Goodwin, A. K., Fielder, E. O., Buckler, W. S., & Steinsberger, N. P. (2002, January 1). Integrating Fracture Mapping Technologies to Optimize Stimulations in the Barnett Shale. Society of Petroleum Engineers. doi:10.2118/77441-MS.

Fredd, C.N., McConnell S.B., Boney C.L. and England K.W. 2001. Experimental Study of Fracture Conductivity for Water-Fracturing and Conventional Fracturing Application. SPE Journal (September 2001).

Gringarten, A. C., Ramey, H. J., & Raghavan, R. (1974, August 1). Unsteady-State Pressure Distributions Created by a Well With a Single Infinite-Conductivity Vertical Fracture. Society of Petroleum Engineers. doi:10.2118/4051-PA.

Gringarten, A. C., Ramey, H. J., & Raghavan, R. (1975, July 1). Applied Pressure Analysis for Fractured Wells. Society of Petroleum Engineers. doi:10.2118/5496-PA.

Gidley, J. L. (1991, November 1). A Method for Correcting Dimensionless Fracture Conductivity for Non-Darcy Flow Effects. Society of Petroleum Engineers. doi:10.2118/20710-PA.

Gu, M., Kulkarni, P. M., Rafiee, M., Ivarrud, E., & Mohanty, K. K. (2014, September 30). Understanding the Optimum Fracture Conductivity for Naturally Fractured Shale and Tight Reservoirs. Society of Petroleum Engineers. doi:10.2118/171648-MS.

Guppy, K. H., Cinco-Ley, H., Ramey, H. J., & Samaniego-V., F. (1982, October 1). Non-Darcy Flow in Wells With Finite-Conductivity Vertical Fractures. Society of Petroleum Engineers. doi:10.2118/8281-PA.

Handren, P. J., & Palisch, T. T. (2009, August 1). Successful Hybrid Slickwater-Fracture Design Evolution: An East Texas Cotton Valley Taylor Case History. Society of Petroleum Engineers. doi:10.2118/110451-PA.

Holditch, S.A. (Jan. 1979). Criteria of Propping Agent Selection. Norton Co., Dallas.

Holditch, S. A., & Blakeley, D. M. (1992, February 1). Flow Characteristics of Hydraulic Fracture Proppants Subjected to Repeated Production Cycles. Society of Petroleum Engineers. doi:10.2118/19091-PA.

Holditch, S. A., & Morse, R. A. (1976, October 1). The Effects of Non-Darcy Flow on the Behavior of Hydraulically Fractured Gas Wells (includes associated paper 6417). Society of Petroleum Engineers. doi:10.2118/5586-PA.

Johnson, M. F., Walsh, W., Budgell, P. A., & Davidson, J. A. (2011, January 1). The Ultimate Potential for Unconventional Gas in the Horn River Basin: Integrating Geological Mapping with Monte Carlo Simulations. Society of Petroleum Engineers. doi:10.2118/148976-MS.

Kim, C. M., & Willingham, J. R. (1987, January 1). Flow Response of Propped Fracture to Repeated Production Cycles. Society of Petroleum Engineers. doi:10.2118/16912-MS.

King, G. E. (2010, January 1). Thirty Years of Gas Shale Fracturing: What Have We Learned? Society of Petroleum Engineers. doi:10.2118/133456-MS.

Konzuk, J. and Kueper, B.H., 2002. A study on the use of cubic-law based models for simulating flow through discrete rough-walled fractures. Proceedings, Fractured Rock Aquifers, National Ground Water Association, Denver, CO, March 13 – 15. Retrieve from http://info.ngwa.org/gwol/pdf/020773508.PDF.

Kullam, J. (2011). The Complicated World of Proppant Selection. http://images.sdsmt.edu/learn/speakerpresentation/Kullmam.pdf.

Liang, F., Sayed, M., Al-Muntasheri, G., & Chang, F. F. (2015, March 8). Overview of Existing Proppant Technologies and Challenges. Society of Petroleum Engineers. doi:10.2118/172763-MS

Mayerhofer, M. J., Lolon, E. P., Youngblood, J. E., & Heinze, J. R. (2006, January 1). Integration of Microseismic-Fracture-Mapping Results with Numerical Fracture Network Production Modeling in the Barnett Shale. Society of Petroleum Engineers. doi:10.2118/102103-MS.

McDaniel, B. W. (1986, January 1). Conductivity Testing of Proppants at High Temperature and Stress. Society of Petroleum Engineers. doi:10.2118/15067-MS.

McDaniel, B. W. (2011, January 1). How "Fracture Conductivity is King" and "Waterfracs Work" Can both be Valid Statements in the Same Reservoir. Society of Petroleum Engineers. doi:10.2118/148781-MS.

McDaniel, B. W. (2012, January 1). Can We Achieve Acceptable Hydraulic Fracture Conductivity Using Waterfracs? Society of Petroleum Engineers. doi:10.2118/152910-MS.

McGuire, W. J., & Sikora, V. J. (1960, October 1). The Effect of Vertical Fractures on Well Productivity. Society of Petroleum Engineers. doi:10.2118/1618-G.

Mullen, J., Lowry, J. C., & Nwabuoku, K. C. (2010, January 1). Lessons Learned Developing the Eagle Ford Shale. Society of Petroleum Engineers. doi:10.2118/138446-MS.

Nolte, K. G., & Economides, M. J. (1991, September 1). Fracture Design and Validation With Uncertainty and Model Limitations. Society of Petroleum Engineers. doi:10.2118/18979-PA.

Novlesky, A., Kumar, A., & Merkle, S. (2011, January 1). Shale Gas Modeling Workflow: From Microseismic to Simulation -- A Horn River Case Study. Society of Petroleum Engineers. doi:10.2118/148710-MS.

Parker, M. A., & McDaniel, B. W. (1987, January 1). Fracturing Treatment Design Improved by Conductivity Measurements Under In-Situ Conditions. Society of Petroleum Engineers. doi:10.2118/16901-MS.

Palisch, T. T., Duenckel, R. J., Bazan, L. W., Heidt, J. H., & Turk, G. A. (2007, January 1). Determining Realistic Fracture Conductivity and Understanding its Impact on Well Performance - Theory and Field Examples. Society of Petroleum Engineers. doi:10.2118/106301-MS.

Palisch, T. T., Vincent, M., & Handren, P. J. (2010, August 1). Slickwater Fracturing: Food for Thought. Society of Petroleum Engineers. doi:10.2118/115766-PA

Pearson, C. M., Griffin, L., & Chikaloff, J. (2014, February 4). Measuring Field Supplied Proppant Conductivity: Issues Discovered in an Operator. Society of Petroleum Engineers. doi:10.2118/168641-MS

Penny, G. S., & Jin, L. (1995, January 1). The Development of Laboratory Correlations Showing the Impact of Multiphase Flow, Fluid, and Proppant Selection Upon Gas Well Productivity. Society of Petroleum Engineers. doi:10.2118/30494-MS.

Poe, B. D., Shah, P. C., & Elbel, J. L. (1992, January 1). Pressure Transient Behavior of a Finite-Conductivity Fractured Well With Spatially Varying Fracture Properties. Society of Petroleum Engineers. doi:10.2118/24707-MS.

Pope, C. D., Palisch, T., & Saldungaray, P. (2012, January 1). Improving Completion And Stimulation Effectiveness In Unconventional Reservoirs- Field Results In The Eagle Ford Shale Of North America. Society of Petroleum Engineers. doi:10.2118/152839-MS.

Prats, M. (1961, June 1). Effect of Vertical Fractures on Reservoir Behavior-Incompressible Fluid Case. Society of Petroleum Engineers. doi:10.2118/1575-G.

Raghavan, R., & Joshi, S. D. (1993, March 1). Productivity of Multiple Drainholes or Fractured Horizontal Wells. Society of Petroleum Engineers. doi:10.2118/21263-PA.

Raghavan, R. S., Chen, C.-C., & Agarwal, B. (1997, September 1). An Analysis of Horizontal Wells Intercepted by Multiple Fractures. Society of Petroleum Engineers. doi:10.2118/27652-PA.

Roberts, B. E., van Engen, H., & van Kruysdijk, C. P. J. W. (1991, January 1). Productivity of Multiply Fractured Horizontal Wells in Tight Gas Reservoirs. Society of Petroleum Engineers. doi:10.2118/23113-MS.

Russell, D. G., & Truitt, N. E. (1964, October 1). Transient Pressure Behavior in Vertically Fractured Reservoirs. Society of Petroleum Engineers. doi:10.2118/967-PA.

Scott, J. O. (1963, December 1). The Effect of Vertical Fractures on Transient Pressure Behavior of Wells. Society of Petroleum Engineers. doi:10.2118/729-PA.

Soliman, M. Y., Hunt, J. L., & El Rabaa, A. M. (1990, August 1). Fracturing Aspects of Horizontal Wells. Society of Petroleum Engineers. doi:10.2118/18542-PA.

Sun, J., & Schechter, D. (2015, December 1). Investigating the Effect of Improved Fracture Conductivity on Production Performance of Hydraulically Fractured Wells: Field-Case Studies and Numerical Simulations. Society of Petroleum Engineers. doi:10.2118/169866-PA.

Veatch, R. W. (1983, April 1). Overview of Current Hydraulic Fracturing Design and Treatment Technology--Part 1. Society of Petroleum Engineers. doi:10.2118/10039-PA.

Vincent, M. C. (2002, January 1). Proving It - A Review of 80 Published Field Studies Demonstrating the Importance of Increased Fracture Conductivity. Society of Petroleum Engineers. doi:10.2118/77675-MS.

Vincent, M. C. (2009, January 1). Examining Our Assumptions -- Have Oversimplifications Jeopardized Our Ability to Design Optimal Fracture Treatments? Society of Petroleum Engineers. doi:10.2118/119143-MS

Vincent, M. C. (2010, January 1). Restimulation of Unconventional Reservoirs: When are Refracs Beneficial? Society of Petroleum Engineers. doi:10.2118/136757-MS

Vincent, M. C. (2012, March 1). The Next Opportunity To Improve Hydraulic-Fracture Stimulation. Society of Petroleum Engineers. doi:10.2118/144702-JPT.

Warpinski, N. R., Mayerhofer, M. J., Vincent, M. C., Cipolla, C. L., & Lolon, E. (2008, January 1). Stimulating Unconventional Reservoirs: Maximizing Network Growth While Optimizing Fracture Conductivity. Society of Petroleum Engineers. doi:10.2118/114173-MS.

Weng, X., Kresse, O., Cohen, C.-E., Wu, R., & Gu, H. (2011, November 1). Modeling of Hydraulic-Fracture-Network Propagation in a Naturally Fractured Formation. Society of Petroleum Engineers. doi:10.2118/140253-PA.

Witherspoon, P. A., J. S. Y. Wang, K. Iwai, and J. E. Gale (1980), Validity of Cubic Law for fluid flow in a deformable rock fracture, Water Resource Research, 16(6), 1016–1024, doi:10.1029/WR016i006p01016.

Wong, D. W., Harrington, A. G., & Cinco-Ley, H. (1986, October 1). Application of the Pressure Derivative Function in the Pressure Transient Testing of Fractured Wells. Society of Petroleum Engineers doi: 10.2118/13056-PA.

Wu, R., Kresse, O., Weng, X., Cohen, C.-E., & Gu, H. (2012, January 1). Modeling of Interaction of Hydraulic Fractures in Complex Fracture Networks. Society of Petroleum Engineers. doi:10.2118/152052-MS.

Yu, W., & Sepehrnoori, K. (2013, April 19). Simulation of Gas Desorption and Geomechanics Effects for Unconventional Gas Reservoirs. Society of Petroleum Engineers. doi:10.2118/165377-MS.

Zhang, J., Kamenov, A., Hill, A. D., & Zhu, D. (2014, August 1). Laboratory Measurement of Hydraulic-Fracture Conductivities in the Barnett Shale. Society of Petroleum Engineers. doi:10.2118/163839-PA.

Appendix A: Calculation of Natural Fracture Width

As mentioned in chapter 2, the natural fracture width is calculated by the cubic law (Witherspoon et al., 1980) in this study. The cubic law is expressed as below:

$$\frac{Q}{\Delta h} = \left(\frac{W}{L}\right)\left(\frac{\rho g}{12\mu}\right)e^3 \qquad \text{(A-1)}$$

Where, Q is flow rate, Δh is the hydraulic head gradient, W is the width of fracture face, L is fracture length, $\rho\, and g$ are fluid density and acceleration of gravity respectively, μ is fluid viscosity, and e is fracture aperture. Actually, the fracture aperture e is the natural fracture width we are looking for, and Figure A-1 shows the relationship of the fracture geometry parameters.

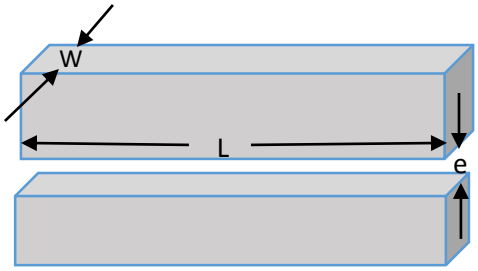

Figure A-1: Schematic of a natural fracture

Darcy's flow can be applied to flow behavior in the natural fractures.

$$\text{Darcy's flow } Q = \frac{kA\Delta p}{\mu L} \qquad \text{(A-2)}$$

Then, combine equation (A-1) and (A-2):

$$Q = \left(\frac{W}{L}\right)\left(\frac{\rho g}{12\mu}\right)e^3\Delta h = \frac{kA\Delta p}{\mu L}$$

From Figure A-1, we can get W$\times e$ =A, and$\rho g \Delta h = \Delta p$. Cross out the equal parts, the final equation becomes

$$k = e^2/12 \qquad \text{(A-3)}$$

This is the relationship between fracture intrinsic permeability and fracture aperture, i.e. fracture width. By applying the equation A-3, the fracture conductivity can be equal to:

$$k \times e = \frac{e^2}{12} \times e = \frac{e^3}{12}$$

The natural fracture conductivity in this study is from 0.0003-3md-m. Taking conductivity 3 md-m as an example, we can have 3md-m= $3\times 9.8692 \times 10^{-16} m^2 . m = 2.96 \times 10^{-15} m^3 = e^3/12$. Then, e = 33μm from the expression above. Applying the same method, the natural fracture width corresponding to each conductivity can be got in table A-1.

Table A-1: Natural fracture width values

Natural Fracture Conductivity (md-m)	Natural Fracture Width (μm)
0.00003	0.71
0.0003	1.5
0.003	3.3
0.03	7.1
0.3	15
3	33